

The Biosynthesis of Ascarosides  
in *Caenorhabditis elegans*

Thesis by  
Allison Emi Akagi

In Partial Fulfillment of the Requirements for  
the degree of  
Doctor of Philosophy in Chemistry

The logo for the California Institute of Technology (Caltech), featuring the word "Caltech" in a bold, orange, sans-serif font.

CALIFORNIA INSTITUTE OF TECHNOLOGY  
Pasadena, California

2018  
(Defended July 6, 2017)

© 2017

Allison Emi Akagi  
ORCID: 0000-0002-7233-6190

## ACKNOWLEDGEMENTS

Although the majority of what is written on the following pages represents the scientific work completed over my graduate experience, I cannot take all of the credit. The last six years have been a marathon, and I would be remiss if I failed to acknowledge the people who trained me, carried me, and cheered me along the way.

First and foremost, I would like to offer my deepest gratitude to my advisor, Paul Sternberg. When I needed a research home, he took me in. When I was in a rut, he opened countless doors for me to explore. He asked the hard questions and never let me hide in a corner. Over five years, he has pushed me to think critically and creatively, and I will forever strive to be as wonderful of a mentor for my future students.

Thank you to the members of my committee for providing focused feedback and direction on my projects. Despite having many commitments and responsibilities as Dean of Graduate Students, Doug Rees was always approachable as a committee chair and supported me through a bumpy first-year transition. Sarah Reisman was one of the faculty who convinced me to join the Caltech community during my recruitment trip and always asked thoughtful questions. Without fail, Carl Parker was always the first to arrive at every meeting and pumped me up with positive comments.

I thank my undergraduate advisor, Louis Kuo, for pushing me to succeed when I lacked the courage. Whether applying for scholarships, submitting abstracts, conducting independent research for my senior thesis, or traveling to make oral presentations at conferences, when I thought I couldn't, he said I could. I would not be where I am today without his support.

Without the collaborative efforts of the Schroeder Lab, these projects would not have progressed to this point. I would like to thank Joshua Judkins, Oishika Panda, and Alex Artyukhin for teaching me the ropes of mass spectrometry-based metabolomics and for their insightful feedback.

I could not imagine a better lab environment than the Sternberg Lab. I will forever be grateful to my labmates for patiently answering every single one of my Biology-related questions that I never learned in my training as a chemist. I have never worked in an environment filled with such overflowing support and generosity. Jonathan Liu ate lunch with me almost every day, and helped me with cloning methods, microinjection, microscopy, and countless other tasks. He is the absolute best friend in lab I could imagine. Thanks to Han and Sandy for helping me get a grasp on CRISPR, David with statistical analyses, James and Pei for their vast knowledge of dauers, and Cynthia for her expertise in behavioral analysis. I know the future of science is bright because I have worked with the best scientists and teachers.

At Caltech, I have had the opportunity to meet some truly amazing people. Shannon Stone comprised a significant portion of my safety net as a friend and roommate, and was always there when I needed a pick-me-up or honest opinion. Michael Post took me on adventures around Los Angeles and made the best homemade meals and desserts. I would also like to thank JJ Kang, Abby Pulsipher, Young In Oh, and Chithra Krishnamurthy for their advice and laughter during the hardest of times. I am fortunate to be able to call these strong, amazing women my friends.

I am extremely grateful to my extended family of aunts, uncles, and cousins for inviting me to every holiday dinner, lunch, and/or barbecue so that I felt at home. It was

comforting to know that my family is nearby. Although we have not lived in the same state in almost a decade, I also need to thank my blonde-haired, blue-eyed twin sister, Brittany Joachims. Every text message and every phone call cheered me up and pushed me to keep going.

Owen Dennis was the one who was there at the end of every day. Thank you for the back massages, the weekend excursions away from the city, the food adventures, and for standing up for me even at times when I was my own worst enemy. Thank you for helping me find laughter and joy every day.

Finally, I will never be able to sufficiently thank my family for everything they have done for me. My sister Erin gave me a leg up at an early age by teaching me how to read, write, and apply basic arithmetic which allowed to me to expand beyond the basic curriculum on my first day of school. My parents have given me everything that a parent can give a child: a home filled with love, guidance in times of need, and the freedom and resources to make choices. They have taught me to try my best to succeed, learn everything I can from my failures, and to have fun along the way. Everything I am, I owe to them, and I will be forever grateful.

## ABSTRACT

Ascarosides comprise a family of small signaling molecules that have been shown to regulate important events and behaviors in the life history of the nematode *Caenorhabditis elegans*. Although the different roles of individual ascarosides appear to be determined by the variances in chemical structure, the mechanisms by which ascarosides are synthesized as well as the locations in which ascarosides are produced within the worm are largely unknown. In this thesis, we examined ascaroside production in the intestine, hypodermis, and body wall muscle of the worm by driving the expression of the protein DAF-22 under different tissue-specific gene promoters. While the body wall muscle and hypodermis are capable of synthesizing ascarosides, the intestine appears to be the major site of pheromone production. Additionally, we found through transgenic rescue and HPLC-MS analysis, that the acyl-CoA synthetase ACS-7 plays a significant role in the addition of moieties derived from primary metabolic pathways to the 4'-position of the ascarylose sugar core of ascr#9.

Thesis Supervisor: Paul W. Sternberg

Committee Chair: Doug C. Rees

Committee Member: Sarah E. Reisman

Committee Member: Carl S. Parker

## PUBLISHED CONTENT AND CONTRIBUTIONS

Panda, O.; Akagi, A.E.; Artyukhin, A.B.; Judkins, J.C.; Le, H.H.; Mahanti, P.; Cohen, S. M.; Sternberg, P.W.; Schroeder, F.C. (2017). “Biosynthesis of modular ascarosides in *C. elegans*.” In: *Angewandte Chemie International Edition English* 56.17, pp. 4729-4733.  
doi: 10.1002/anie.201700103

The work presented in this chapter represent a collaboration between the Sternberg Lab (California Institute of Technology, Pasadena, CA) and the Schroeder Lab (Cornell University, Ithaca, NY). Allison Akagi (AA), Joshua Judkins (JJ), and Oishika Panda (OP) designed the mutant screens, cultured strains, and generated exometabolome extracts. JJ and OP acquired all HPLC-MS data. The data was analyzed by AA, OP, and JJ. Tiglic supplementation feeding assays were conducted by JJ and OP. AA performed *oac-50* mutant outcrossing. Genetic rescue of *acs-7* was performed by AA and ACS-7 localization studies were performed by AA and OP.

## TABLE OF CONTENTS

Acknowledgements .....	iii
Abstract .....	vi
Published Content and Contributions .....	vii
Table of Contents .....	viii
List of Figures and/or Tables .....	x
Nomenclature .....	xii
Chapter 1: Introduction to Ascaroside Signaling.....	1
1.1 <i>Caenorhabditis elegans</i> .....	1
1.2 Ascaroside Biosynthesis .....	2
1.3 Ascarosides in Dauer Formation.....	5
1.4 Ascarosides in Mate Attracting Behavior.....	6
1.5 Ascarosides in Social Behaviors.....	7
1.6 Ascaroside Perception.....	8
1.7 Mass Spectrometry-Based Ascaroside Profiling .....	11
1.8 Thesis Summary.....	11
1.9 Figures .....	13
1.10 References .....	24
Chapter 2: A Localization Study of Ascaroside Production.....	30
2.1 Abstract .....	30
2.2 Introduction .....	30
2.3 Results and Discussion.....	32
2.4 Conclusions .....	39
2.5 Figures .....	42
2.6 Materials and Methods.....	50
2.7 References .....	55
Chapter 3: Identifying Genes Involved in the Biosynthesis of Modular Ascarosides in <i>Caenorhabditis elegans</i> .....	58
3.1 Abstract .....	58
3.2 Introduction .....	59
3.3 Results and Discussion.....	60
3.4 Conclusions .....	66
3.5 Figures .....	68
3.6 Tables .....	82
3.7 Materials and Methods.....	83
3.8 References .....	88
Appendix A: Mitochondrial $\beta$ -Oxidation of the Ascaroside Side Chain.....	93
A.1 Introduction .....	93
A.2 Results and Discussion.....	94
A.3 Figures .....	95
A.4 References .....	97

Appendix B: Additional Mutants Screened for Biosynthetic Defects .....	98
B.1 Introduction .....	98
B.2 Results and Discussion .....	98
B.3 Figures .....	100
B.4 References .....	105
Appendix C: Strains, Plasmids, and Primers .....	107

## LIST OF ILLUSTRATIONS AND/OR TABLES

<i>Figure</i>	<i>Page</i>
1.1 The <i>C. elegans</i> Life Cycle .....	13
1.2 Modular Ascaroside Structure .....	14
1.3 Peroxisomal $\beta$ -Oxidation of Ascaroside Lipid Side Chains .....	15
1.4 4'-Modification of Ascarosides .....	16
1.5 The Dauer Larva .....	17
1.6 Ascarosides Involved in Dauer Formation .....	18
1.7 Hermaphrodite vs. Male Worm Morphology.....	19
1.8 Ascarosides Involved in Mate Attraction.....	20
1.9 Ascarosides Involved in Aggregation and Repulsion .....	21
1.10 Ciliated Sensory Neurons Involved in Ascaroside Perception ....	22
1.11 MS/MS Fragmentation of Ascarosides .....	23
2.1 The Role of DAF-22 in Short-Chain Ascaroside Biosynthesis .....	42
2.2 Tissue-Specific GFP::DAF-22 Expression .....	43
2.3 Tissue-Specific Ascaroside Profiles .....	44
2.4 Dauer Formation Activity is Restored by GFP::DAF-22 Rescue..	45
2.5 Male Retention Bioassay .....	46
2.6 Male Attraction is Restored by GFP::DAF-22 Rescue .....	47
2.7 Hermaphrodite Repulsion Assay .....	48
2.8 Hermaphrodites Neither Attract nor Repel Each Other .....	49
3.1 Simple Ascaroside Structures .....	68
3.2 Modular Ascaroside Structures.....	69
3.3 Ascaroside Structure Determines Biological Function .....	70
3.4 Specificity in Ascaroside Modification .....	71
3.5 Tiglic Acid Feeding Assay with <i>oac</i> Mutants .....	72
3.6 The Mutant <i>acs-7(tm6781)</i> Lacks <i>ascr#9</i> Derivatives .....	73
3.7 The <i>oac-50(gk402144)</i> Mutant.....	74

<i>Figure</i>	<i>Page</i>
3.8 Feeding Tiglic Acid to an Outcrossed <i>oac-50(-)</i> Mutant .....	75
3.9 ACS-7::GFP Rescue Restores <i>ascr#9</i> Derivatives .....	76
3.10 Rescuing Production of <i>ascr#9</i> Derivatives .....	77
3.11 ACS-7::GFP Does Not Localize to the Peroxisomes.....	78
3.12 ACS-7::GFP Localizes to the LROs.....	79
3.13 LRO Mutants Do Not Produce 4'-Modified Ascarosides.....	80
3.14 The <i>acs-10</i> Gene Does Not Play a Role in 4'-Modification.....	81
A.1 Examining the Role of <i>ech-2</i> .....	95
A.2 Examining the Role of Acyl-CoA Dehydrogenases .....	96
B.1 The <i>icas</i> Ascarosides .....	100
B.2 Indole-3-carboxylic Acid Biosynthesis in <i>A. thaliana</i> .....	101
B.3 The <i>cyp</i> Gene Family .....	102
B.4 Decarboxylases.....	103
B.5 The <i>elo</i> Gene Family.....	104
<i>Table</i>	<i>Page</i>
3.1 <i>O</i> -acyltransferase mutant strains.....	82
C.1 Strains.....	107
C.2 Plasmids.....	108
C.3 Primers.....	109

## NOMENCLATURE

**Ascaroside.** (ascr) A glycoside of the dideoxysugar ascarylose.

**icas.** A simple ascaroside modified at the 4'-position with an indole-3-carbonyl head group

**hbas.** A simple ascaroside modified at the 4'-position with a *p*-hydroxybenzoyl head group

**mbas.** A simple ascaroside modified at the 4'-position with an (*E*)-2-methyl-2-butenoic acid head group.

**osas.** A simple ascaroside modified at the 4'-position with an *N*-succinylated octopamine head group.

**tsas.** A simple ascaroside modified at the 4'-position with an *N*-succinylated tyramine head group.

**Dauer.** A stress-resistant alternative L3 larval stage induced during times of low food, high population density, and high temperatures.

**Excretome.** The collection of metabolites and molecules excreted by *C. elegans*.

**Gut granules.** Lysosome-related organelles found in the intestine of *C. elegans* necessary for the production of 4'-modification of ascarosides.

**High performance liquid chromatography tandem mass spectrometry.** (HPLC-MS) An analytical chemistry technique that first separates chemical components in mixtures using liquid chromatography and then subjects them to mass spectrometry for identification.

**Peroxisomal  $\beta$ -oxidation.** A four-step process that iteratively truncates the lipid carbon chain by two carbons in the form of acetyl-CoA within the peroxisomes.

## INTRODUCTION TO ASCAROSIDE SIGNALING

**1.1 *Caenorhabditis elegans***

*Caenorhabditis elegans* is a free-living soil nematode that is approximately one millimeter in length at full maturity.<sup>1</sup> First introduced as a model organism by Sydney Brenner in 1963, the genes of this multicellular organism are homologous to those of many vertebrates and have been used to uncover breakthroughs in numerous phenomena such as Alzheimer's disease, aging, diabetes, host-pathogen relationships, and metabolism.<sup>2-6</sup>

Several attributes make *C. elegans* a prime target for study. The nematode has a short reproductive cycle and can be cultured easily on agar plates or in liquid cultures when supplied with an *Escherichia coli* food source.<sup>7-8</sup> The worm is also transparent, allowing the cell lineage to be characterized by light microscopy.<sup>9</sup> All hermaphrodite worms contain exactly 959 somatic cells and males contain 1033, yet despite the small number of cells compared to other animals, *C. elegans* contains a number of distinct tissues and organs including an intestine, a hypodermis, muscle tissue, a fully mapped nervous system of 302 neurons, and gonads. Furthermore, with a genome fully sequenced for over a decade, many tools exist for genetic manipulation including RNA interference, tissue-specific promoter expression systems, and CRISPR/Cas9 gene editing.<sup>10-12</sup>

In the typical *C. elegans* life cycle, the worm begins as an embryo encased by a resilient shell and hatches into the first larval stage called L1. Under favorable environmental conditions, the worm will molt and progress through the L2, L3 and L4 larval stages before

finally reaching its reproductive adult form. The entire process spans approximately three days (Figure 1.1).<sup>13</sup> In the normal life cycle, the adult worm can live between two to three weeks; however, under stressful conditions, *C. elegans* exits the L2 larval stage and enters an alternative, developmentally-arrested larval stage called the dauer. Entry and exit into this stress-resistant stage was found to be regulated by a family of small molecules known as the ascarosides.<sup>14</sup>

The term ascaroside was first created to describe a novel lipid detected in the intestinal parasite *Ascaris lumbricoides* over 100 years ago.<sup>15</sup> These lipophilic molecules, containing long aliphatic side chains, formed a layer around *Ascaris* eggs to protect against harsh environmental conditions.<sup>16</sup> More recently, a larger collection of more hydrophilic ascarosides has been identified in *C. elegans* and other related nematodes and has been shown to regulate a multitude of behaviors and aspects of the life history of the worm including development, mate attraction, aggregation, and repulsion.

## 1.2 Ascaroside Biosynthesis

Ascarosides are defined as glycosides of the dideoxysugar ascarylose (Figure 1.2). At the first position of the sugar core is a lipid side chain that can vary in length, level of saturation, and level of oxidation. Furthermore, this lipid can be joined at either the ultimate (oscr) or penultimate carbon (ascr). Ascarosides can be further modified at the second and fourth positions of the sugar core as well as at the terminal end of the fatty acid side chain. While the biosynthetic machinery of many microorganisms has been deeply studied and characterized, more complex animals were thought to be deficient in their ability to

produce molecule signals with complex structures.<sup>17</sup> This makes ascaroside biosynthesis in *C. elegans* a surprising and interesting topic of study.

The biologically active short-chain ascarosides are derived from long-chain ascaroside precursors through peroxisomal  $\beta$ -oxidation of the lipid side chain, a process that truncates fatty-acids by two carbons in a series of four steps (Figure 1.3).<sup>18-19</sup> Mass spectrometry-based analyses of mutant excretomes, the collection of metabolites and molecules excreted by the animal, revealed that the first step of ascaroside peroxisomal  $\beta$ -oxidation in *C. elegans* is carried out by ACOX-1, an acyl-CoA oxidase, which introduces a site of unsaturation between the  $\alpha$  and  $\beta$  carbons of the fatty acid side chain. MAOC-1, a peroxisomal 2-enoyl-CoA hydratase, hydrates the double bond introduced by ACOX-1. The  $\beta$ -hydroxyacyl-CoA intermediate is then converted into a  $\beta$ -ketoacyl-CoA ester by DHS-28, a homolog of the dehydrogenase domain of mammalian peroxisomal multifunctional protein MFE-2. The final truncation step is carried out by DAF-22, a thiolase that shares strong homology to the mammalian peroxisomal 3-ketoacetyl-CoA thiolase SCPx.

Many of the head groups modifying the 4'-position of the ascarylose sugar groups including indole-3-carboxylic acid (icas), *p*-hydroxybenzoic acid (hbas) and (*E*)-2-methyl-2-butenic acid (mbas) are derived from amino acid metabolism (Figure 1.4). By studying metabolites produced by axenic *C. elegans* cultures supplemented with a specific amino acid, it has been demonstrated that the indole moiety of icas ascarosides is derived from tryptophan, whereas the head groups of hbas and mbas ascarosides could be synthesized from tyrosine and isoleucine, respectively.<sup>18</sup> Similarly, it is hypothesized that the *N*-succinylated

octopamine head group decorating osas ascarosides and the tyramine head group of tsas ascarosides may both be derived from tyrosine.<sup>20</sup> Ascaroside biosynthesis is therefore a complex system that incorporates building blocks derived from many parts of primary metabolism including carbohydrates, lipids, and amino acids.

The production of ascarosides is influenced by many factors including stage, environmental conditions, and sex. Whereas the total quantity of ascarosides produced increases as the worm progresses through larval stages, the production of individual ascarosides peak at different stages.<sup>21</sup> For example, ascr#3 production increases as the worm grows from the L1 to the L4 larval stages, but decreases as the worm reaches adulthood. Alternatively, the production of ascr#2 continues to increase as the worm ages and the modified ascarosides osas#9 and osas#10 are predominantly produced by L1 larva. Dauer larva, on the other hand, do not excrete ascarosides.<sup>21</sup>

Studies have shown that ascarosides are also produced in different quantities depending on the temperature at which worms are cultured. Jeong *et al* found that ascr#1 was produced highly in cultures at 20°C, whereas Butcher *et al* found ascr#3 levels to be dominant when worms were raised between 22.5 and 25°C.<sup>22-23</sup> This shift corresponds with worm behavior as dauer formation increases at higher temperatures and ascr#3 is a much more potent dauer pheromone compared to ascr#1.<sup>24-25</sup>

The availability of food also affects ascaroside production. For example, well-fed wildtype worms excrete larger amounts of ascr#3 than starved cultures, which secrete larger amounts of ascr#2.<sup>21</sup> Additionally, it was found that osas#9 is produced predominantly by starved L1 larva, whereas osas#10 is mainly produced by L1 larva when food is plentiful.<sup>20</sup>

The incorporation of various metabolically derived precursors and dependence upon stage and environmental conditions indicate that ascaroside biosynthesis is a complex and highly regulated process.

### 1.3 Ascarosides in Dauer Formation

Morphologically distinct from larva grown under favorable conditions, the dauer forms a more robust cuticle, forms a plug that blocks its oral orifice, does not pump, and has a higher fat content (Figure 1.5).<sup>26-27</sup> These physical attributes allow the dauer to survive for up to four months compared to the normal worm lifespan of 2-3 weeks.<sup>28</sup> If environmental conditions return to a favorable state, the worm will exit dauer diapause and resume development to reproductive maturity.

In *C. elegans*, ascarosides were first identified as molecules comprising the pheromone that regulates the formation of dauer larva.<sup>29-30</sup> Over 20 years later, using activity-guided fractionation, the structure of ascr#1, also known as daumone, was discovered and found to have a seven-carbon carboxylic acid side chain attached at the first position of the ascarylose sugar (Figure 1.6).<sup>22</sup> However, Gallo *et al* found that the levels of ascr#1 required to induce dauer formation were highly toxic to the worm and therefore indicated the involvement of additional molecules, then unknown.<sup>31</sup> Further studies utilizing activity-guided fractionation unveiled other related molecules involved in dauer formation bearing different fatty-acid like side chains, called ascr#2 and ascr#3.<sup>25</sup> A fourth ascaroside, called ascr#5, was found to act synergistically with ascr#2 and ascr#3.<sup>23</sup>

The synergistic activity of the ascarosides signifies that not all ascarosides may be detected when separated during activity-guided fractionation as certain ascarosides may only influence dauer formation in combination with other ascarosides. To expand the search for new dauer-inducing ascarosides, Pungaliya *et al* conducted NMR spectroscopy-based comparative metabolomic studies that revealed the additional dauer pheromone component called ascr#8, which contains a *p*-aminobenzoic acid group at the terminal end of the unsaturated fatty acid side chain.<sup>32</sup> Additionally, Butcher *et al* discovered an ascaroside containing an unusual indole-3-carbonyl group attached at the fourth position of the ascarylose core called icas#9.<sup>33</sup> Unlike other ascarosides that induce dauer formation in a manner positively correlated to pheromone concentration, icas#9 dauer formation activity decreases at higher concentrations. The synergistic abilities and different activity-concentration relationships between ascarosides may suggest that pheromone perception may involve multiple receptors.

#### **1.4 Ascarosides in Mate Attracting Behavior**

*C. elegans* nematodes are hermaphroditic, producing both oocytes and sperm, and can reproduce by self-fertilization (Figure 1.7). Male worms are naturally produced at low frequency and can fertilize hermaphrodites. Simon and Sternberg found that hermaphrodites emit a chemical cue that attracts males from a distance and it was found that on agar plates, male retention is increased in regions conditioned with hermaphrodite worms.<sup>34</sup>

Using activity-guided fractionation of hermaphrodite-conditioned media, Srinivasan *et al* identified ascr#2 and ascr#3 as major components of the male attracting pheromone.<sup>35</sup>

Although ascr#2 and ascr#3 are also known components of dauer pheromone, the concentrations required to attract males were in the picomolar to nanomolar ranges, and thus much lower than those required to elicit dauer formation. Furthermore, it was found that ascr#4 which is a glucosylated derivative of ascr#2, synergizes with ascr#2 and ascr#3 and enhances male attraction, but does not attract males alone (Figure 1.8). Additional NMR-based metabolomics studies revealed that ascr#8, another component of dauer pheromone, also synergizes with ascr#2 and ascr#3 to enhance male attracting activity. Ascarosides can therefore have distinct or redundant regulatory roles in *C. elegans* behavior.

Mate attracting cues are not exclusively generated by hermaphrodite worms. Analyses of sex-specific cultures demonstrated differences between male and hermaphrodite ascaroside profiles.<sup>36</sup> It was revealed that while hermaphrodite worms primarily produce ascr#3, male worms predominantly produce ascr#10, the  $\alpha,\beta$ -unsaturated version of ascr#3. While ascr#3 demonstrates strong male-attracting activity and repels hermaphrodite worms, ascr#10 is highly attractive to hermaphrodites.

## 1.5 Ascarosides in Social Behaviors

Foraging behavior naturally varies between different *C. elegans* strains. Although the laboratory strain N2 is considered solitary because it disperses around the bacterial lawn rather than aggregate, other wild type strains are considered social because they tend to gather in areas with a high abundance of food.<sup>37-38</sup> Ascarosides have been shown to influence these social behaviors (Figure 1.9).

Solitary N2 hermaphrodites are strongly repulsed by ascr#2, ascr#3, ascr#5, which were all shown to be attractive to male worms.<sup>39</sup> The studies conducted by Butcher *et al* that discovered the dauer-inducing ascaroside icas#9 also revealed the existence of an entire family of indolated ascaroside derivatives including icas#3 and icas#10.<sup>33</sup> At high concentrations, icas#3 and icas#9 attract both male and hermaphrodite worms, but only hermaphrodites, and not males remain attracted at low concentrations. At concentrations as low as 100 fM, both solitary and social hermaphrodites demonstrate significant levels of attraction, thus indicating icas#3 and icas#9 as effective aggregation pheromones.<sup>40</sup> The *p*-hydroxybenzoyl modified ascaroside hbas#3 was shown to attract hermaphrodites at concentrations as low as 10 fM and is therefore the most potent hermaphrodite aggregation signal reported.<sup>18</sup>

Although not involved in dauer formation, the *N*-succinylated octopamine modified ascaroside osas#9, primarily produced by starved L1 larva, has been identified as a strong deterrent to the worm in all stages of life.<sup>20</sup> It is hypothesized that when food is in limited supply, osas#9 may serve as a component of a dispersal signal.

## 1.6 Ascaroside Perception

The ascarosides are a complex family of more than 100 molecules with different structures producing many biological effects in *C. elegans*; however, the function of a single ascaroside may differ depending on conditions such as concentration. For example, at high concentrations, ascr#3 induces dauer formation, but at low concentrations, the same

ascaroside acts as a male attracting signal.<sup>25, 35</sup> This poses an interesting question of how worms sense ascarosides and respond accordingly.

Dauer formation signals are perceived and transduced through ciliated chemosensory neurons of the amphids, which are also known to play roles in recognizing soluble social cues and high osmolarity.<sup>41-42</sup> The chemosensory neurons shown to be involved in dauer formation include ADF, ASG, ASI, ASJ, and ASK.<sup>43</sup> Male mating behavior and hermaphrodite behaviors mediated by ascarosides, on the other hand, engage the ASK, ASI, and ADL neurons (Figure 1.10).<sup>35, 39-40, 44</sup>

Previous findings established that two GTP-binding protein (G protein) alpha subunits, GPA-2 and GPA-3, are expressed in chemosensory neurons and are involved in the dauer entry decision.<sup>45</sup> Constitutively active *gpa-2* and *gpa-3* mutants formed dauer larva even when grown under non-dauer-inducing conditions at rates of 99% and 95%, respectively. Conversely, worms containing null mutations in *gpa-2* and *gpa-3* displayed reduced responses to dauer pheromone. These results indicate that dauer formation is controlled, at least partially, by G proteins. It is also therefore suggested that the ciliated chemosensory neurons of the amphids express one or more G protein-coupled receptors (GPCRs) involved in mediating ascaroside perception.

Heterotrimeric G proteins, composed of  $\alpha$ ,  $\beta$ , and  $\gamma$  subunits, act as molecular switches that activate intracellular signaling pathways in response to the activation of a GPCR by an extracellular stimulus.<sup>46</sup> *C. elegans* encodes more than 1000 putative GPCRs with the majority being expressed in the chemosensory neurons, making them interesting candidates for ascaroside perception.<sup>43</sup>

Previous studies have identified two GPCRs, *srbc-64* and *srbc-66*, that mediate dauer formation in response to dauer pheromone and several of its individual components.<sup>47</sup> Loss-of-function mutations in *srbc-64* and *srbc-66* displayed dauer formation defects in response to several ascarosides. GFP-tagged SRBC-64 and SRBC-66 localized in the sensory cilia of the ASK chemosensory neurons. Furthermore, it was found that in the presence of *ascr#2*, *srbc-64; gpa-3* and *srbc-66; gpa-3* double loss-of-function mutant worms show similar defects in dauer formation when compared to their single mutation counterparts. Together, these results support the model that ascaroside signals promote dauer formation via SRBC-64 and SRBC-66 chemoreceptors and the GPA-3 G $\alpha$  protein in the ASK neuron. The precise mechanism by which GPA-2 influences dauer formation remains unknown.

McGrath *et al* determined that the genes *srg-36* and *srg-37* encode GPCRs required for the selective perception of *ascr#5*.<sup>48</sup> Furthermore, the two genes are partially redundant as rescue of either gene restores *ascr#5* sensitivity and both genes are expressed in the ASI neurons, which are shown to be involved in dauer formation. Mutants of two additional genes, *daf-37* and *daf-38* were shown to be defective in ascaroside perception.<sup>49</sup> While a *daf-38* mutant displayed a defective response to *ascr#2*, *ascr#3*, and *ascr#5*, the *daf-37* mutant was only defective in responding to *ascr#2*. It was later shown through a photo-affinity labeling experiment that *daf-37* directly binds to *ascr#2* and serves as the first example of direct binding of an ascaroside to a receptor. This combination of receptor specificity and redundancy indicates that ascaroside perception is a highly complex process.

## 1.7 Mass Spectrometry-Based Ascaroside Profiling

The *C. elegans* metabolome is complex and therefore, analysis by high performance liquid chromatography tandem mass spectrometry (HPLC-MS) produces crowded chromatograms which makes identifying individual ascarosides a difficult task. To surmount this issue, von Reuss *et al* examined MS/MS fragmentation patterns of various synthetic ascarosides and discovered that under negative-ion electrospray ionization (ESI), ascarosides typically fragment to produce a characteristic ion derived from the ascarylose sugar scaffold with a mass-to-charge ratio of 73.0 (Figure 1.11).<sup>18</sup>

By screening for this characteristic ion, HPLC-MS chromatogram peaks become well resolved. Furthermore, by examining fragmentation patterns of known synthetic ascarosides, unknown metabolites can be identified as derivatives or homologs. For example, two peaks in a HPLC-MS chromatogram of a wild type metabolome were found to contain a product ion at  $m/z$  301.1651, characteristic of ascr#3. Fractionation and subsequent 2D NMR spectroscopy later revealed these new ascarosides to be hbas#3 and mbas#3, 4'-modified derivatives of ascr#3. Using known retention times derived from synthetic ascarosides and characterized fragmentation patterns, many ascarosides can now be easily detected from the supernatant of *C. elegans* liquid cultures.

## 1.8 Thesis Summary

Ascarosides constitute a large family of signaling molecules that regulate crucial events in the life history of *C. elegans*. Although the molecular core remains consistent, small structural alterations to the attached moieties appear to be responsible for the vast differences

in biological effects amongst individual ascarosides. However, very little is known about the biological machinery and processes by which ascarosides are synthesized within the worm.

The primary focus of this thesis was to determine where and how ascarosides are produced. In Chapter 2, we found that by selectively driving the expression of DAF-22, an enzyme necessary for the production of biologically active ascarosides, within specific tissues, we were able to assess ascarosides produced within the intestine, hypodermis, and body wall muscles of the worm. Our results revealed that while the intestine is the major site of ascaroside biosynthesis, modest amounts of ascarosides are produced in the hypodermis and body wall muscle that are sufficient in quantity to rescue various ascaroside-regulated *C. elegans* behaviors.

In Chapter 3, we discuss studies on the enzyme ACS-7, which was found to be required for the attachment of head groups to the 4'-position of ascr#9. It was also discovered that although predicted to be peroxisomal, ACS-7 is expressed in lysosome-related organelles found in the intestine of *C. elegans*. These so-called gut granules are necessary for the production of 4'-modified ascarosides. The biosynthesis of ascarosides is a complex process that incorporates many aspects of primary metabolic pathways, and these studies serve to help elucidate how the worm's metabolic status is transduced into worm behavior via ascaroside signaling.

## 1.9 Figures

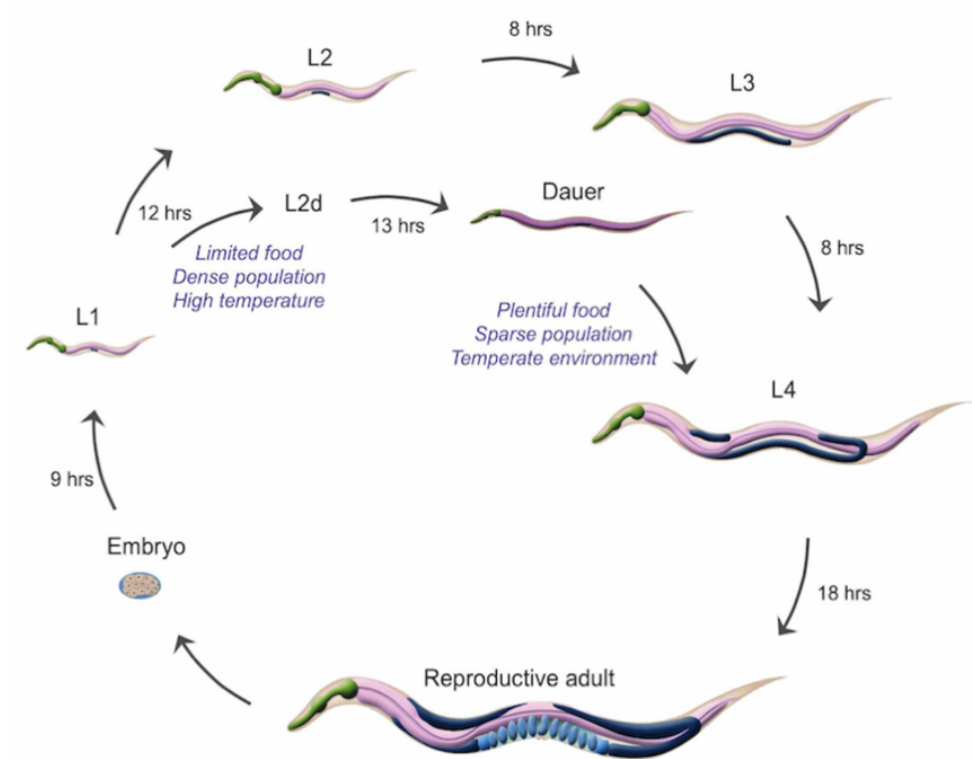


**Figure 1.1: The *C. elegans* Life Cycle.** Under favorable environmental conditions, *C. elegans* progresses through four larval stages, L1-L4, molting between each stage. In a stressful environment with a high population density, low food, and/or at a high temperature, L1 larva may develop into L2d larva and eventually develop into the alternative stress-resistant L3 larval stage, the dauer. When conditions turn favorable, the worm may exit dauer diapause and return to the normal life cycle as an L4 larva. (Unmodified figure from Wormatlas.<sup>50</sup>)

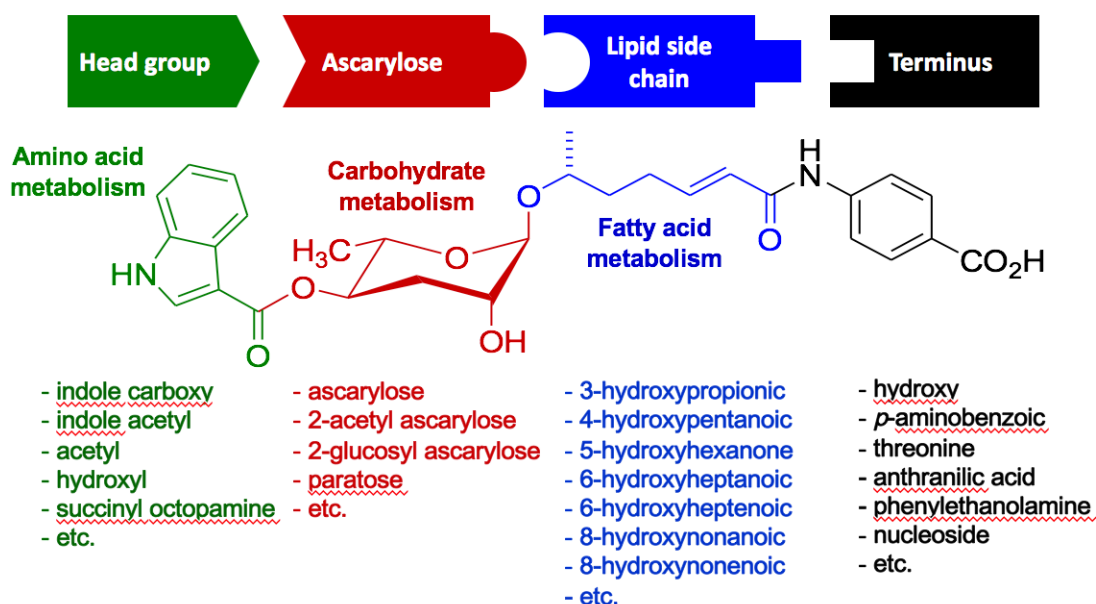


**Figure 1.2: Modular Ascaroside Structure.** Ascarosides are glycosides of the dideoxysugar ascarylose (red). Attached to the ascarylose core at the 1'-position is a fatty acid moiety that can differ in length, saturation, and oxidation (blue). Ascarosides are modular structures and can have additional groups attached to the 2'- or 4'-positions of the ascarylose sugar (green), or at the terminal end of the lipid side chain (black). (Modified figure from von Reuss *et al.*<sup>18</sup>)

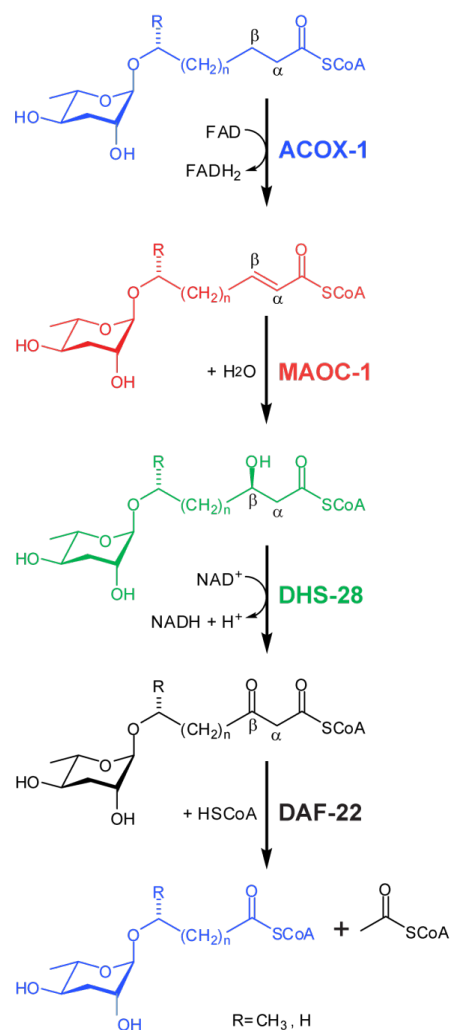


**Figure 1.3: Peroxisomal  $\beta$ -Oxidation of Ascaroside Lipid Side Chains.** Peroxisomal  $\beta$ -oxidation is a process that truncates a carbon chain by two carbons in a series of four steps. ACOX-1, an acyl-CoA oxidase, introduces a site of  $\alpha,\beta$ -unsaturation (blue). MAOC-1, a peroxisomal 2-enoyl-CoA hydratase, hydrates the double bond (red). DHS-28, a dehydrogenase, oxidizes the hydroxyl group to form a  $\beta$ -ketoacyl-CoA ester (green). DAF-22, a thiolase, truncates the lipid chain to release acetyl-CoA and a shortened ascaroside precursor (black). (Modified figure from von Reuss *et al.*<sup>18</sup>)

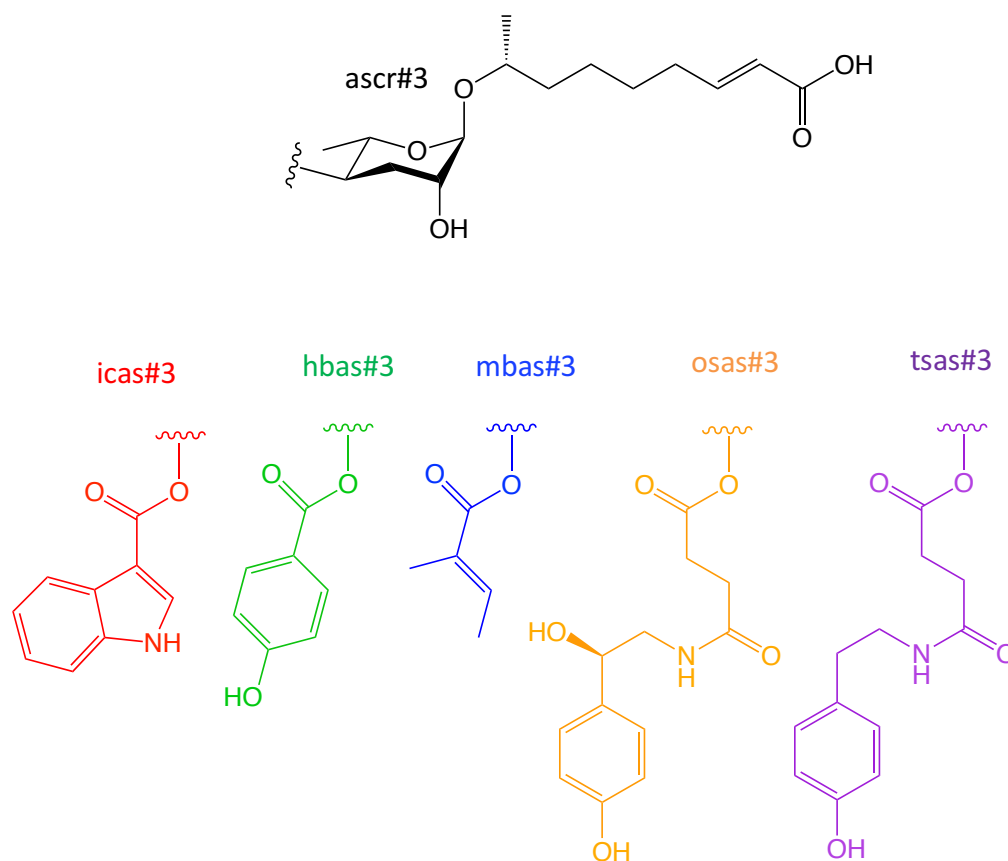


**Figure 1.4: 4'-Modification of Ascarosides.** Simple ascarosides such as ascr#3 (black) can be modified at the 4'-position with various head groups derived from primary metabolic pathways to form derivatives such as icas (red), hbas (green), mbas (blue), osas (orange), and tsas (purple) ascarosides. Note: tsas#3 is not known to exist, but the tsas head group does modify other simple ascarosides such as ascr#9.

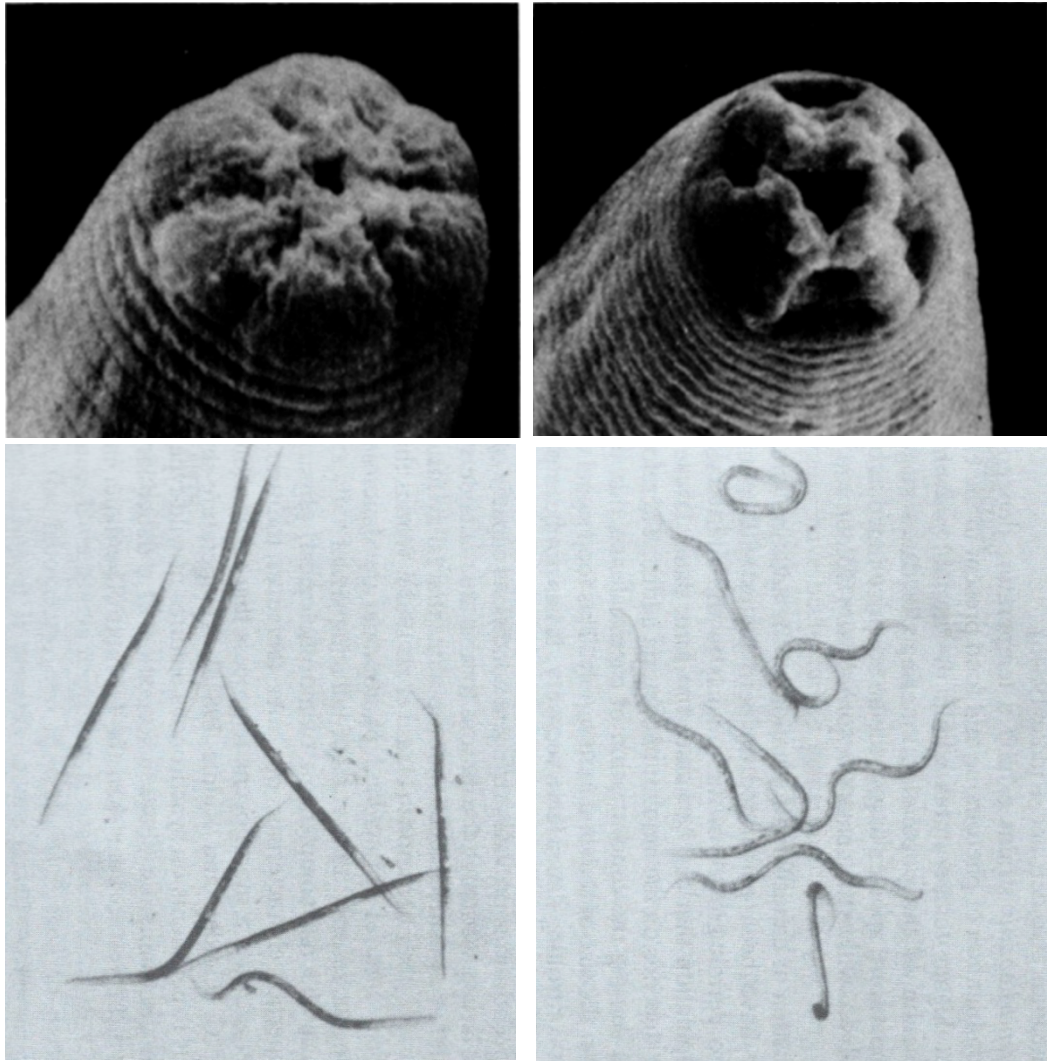


**Figure 1.5: The Dauer Larva.** The dauer is a stress-resistant alternative larval stage. Scanning electron microscopy reveals that the dauer forms a plug that blocks the mouth, preventing the ingestion of food and toxins from the environment (top panel, left), whereas the mouth of a well fed L2 larva remains open (top panel, right). Dauer larva (bottom panel, left) can be distinguished from L3 larva (bottom panel, right) by light microscopy. With a thicker cuticle, the dauer is rigid and motionless, and appears darker due to an increase in fat storage within the intestine. (Modified figure from Wood *et al.*<sup>13</sup>)

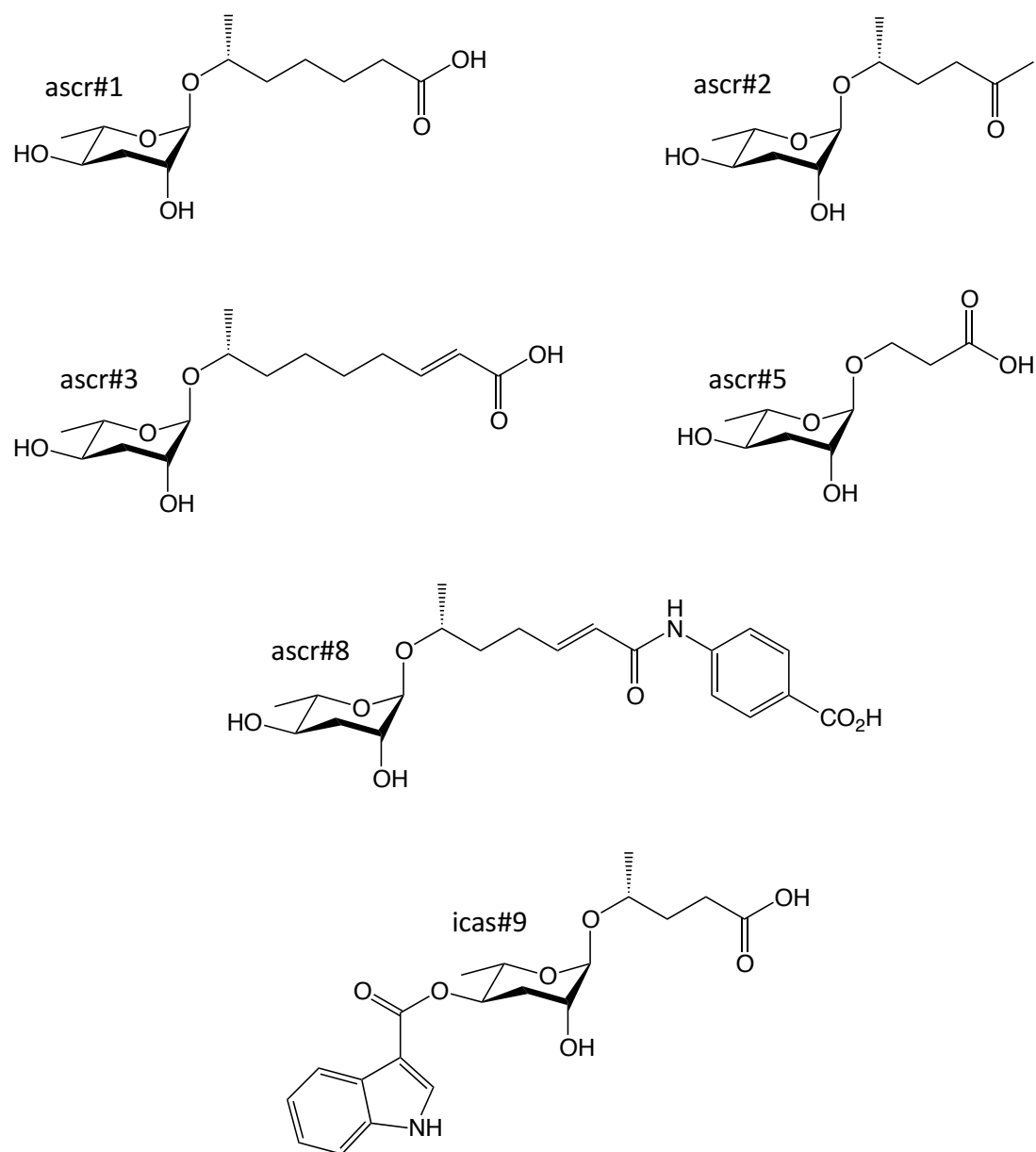


**Figure 1.6: Ascarosides Involved in Dauer Formation.**

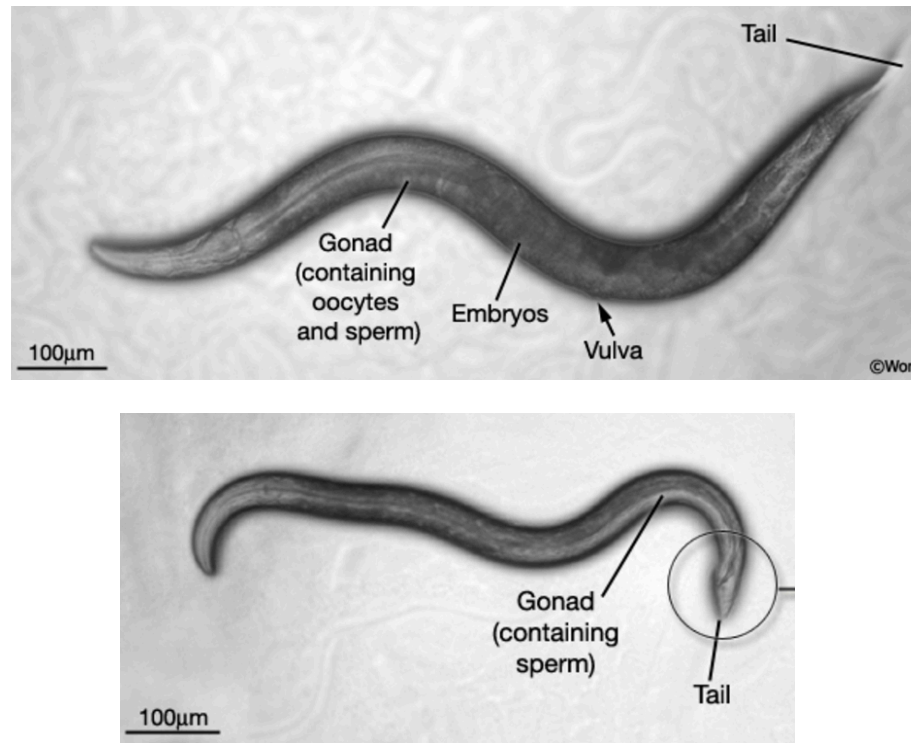


**Figure 1.7: Hermaphrodite vs. Male Worm Morphology.** *C. elegans* hermaphrodite worms produce both eggs and sperm and can therefore self-fertilize their own oocytes (top panel). Male *C. elegans* worms are smaller than hermaphrodites and have a hook-like copulatory tail that can be inserted into the vulva of a hermaphrodite worm to fertilize eggs (bottom panel). (Modified figure from Wormatlas.<sup>50</sup>)

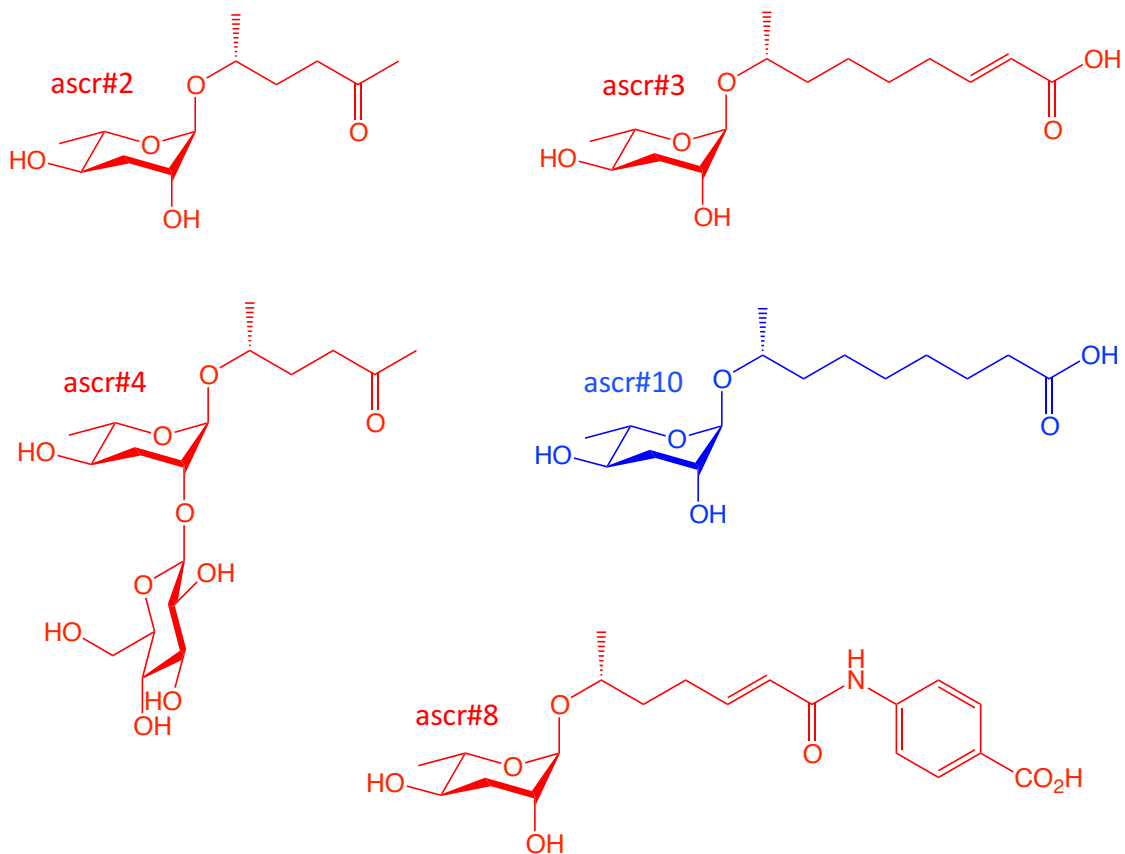


**Figure 1.8: Ascarosides Involved in Mate Attraction.** Several ascarosides are attractive to male *C. elegans* worms (red), whereas ascr#10, an ascaroside highly produced by male worms, is attractive to hermaphrodite worms (blue).

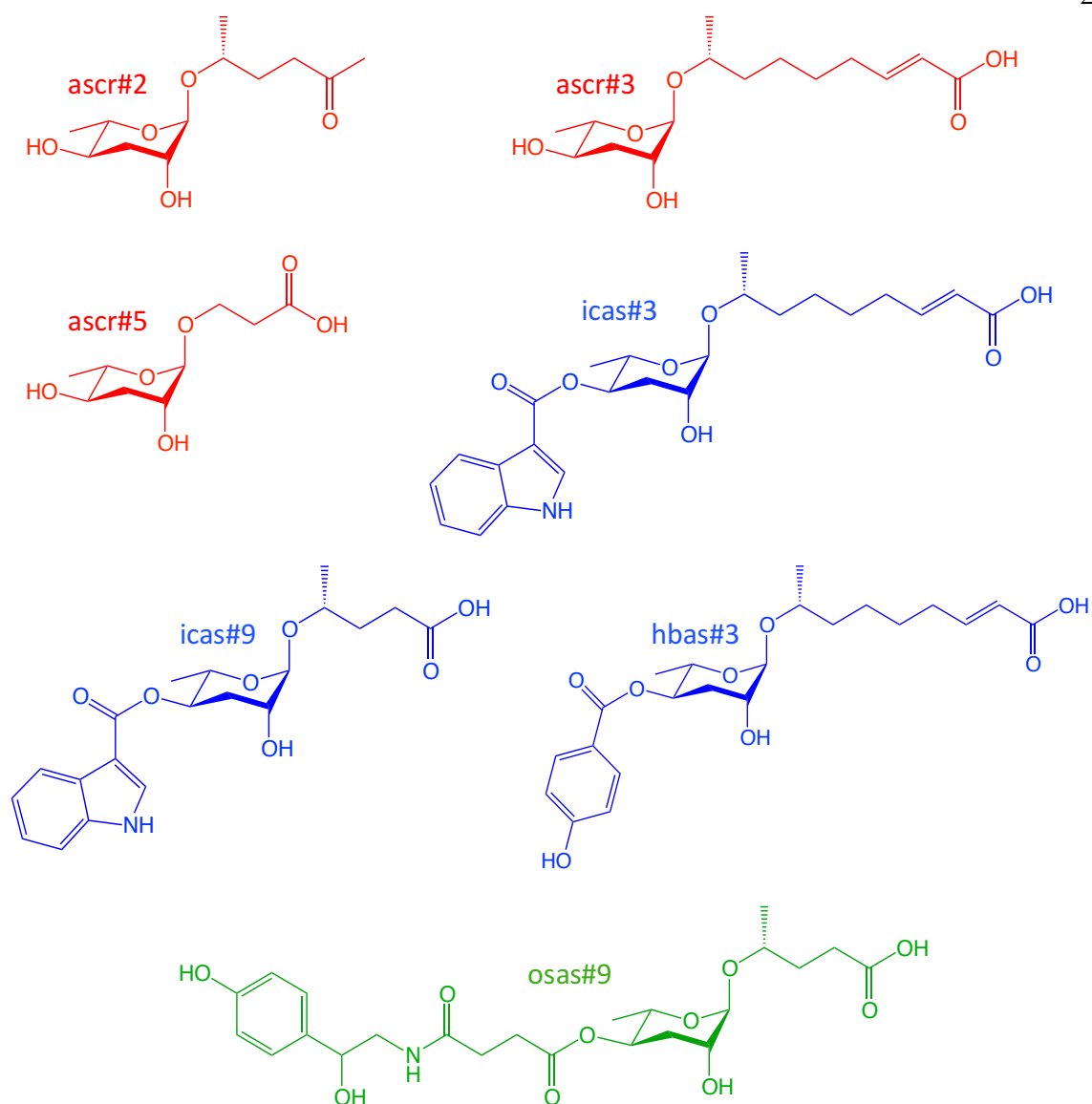


**Figure 1.9: Ascarosides Involved in Aggregation and Repulsion.** Ascarosides involved in other behaviors such as male attraction and dauer formation are repulsive to *C. elegans* hermaphrodite worms (red). Several 4'-modified ascarosides are hermaphrodite attractants (blue), but osas#9, produced mainly by starved L1 larva, act as deterrents to all larval stages (green).

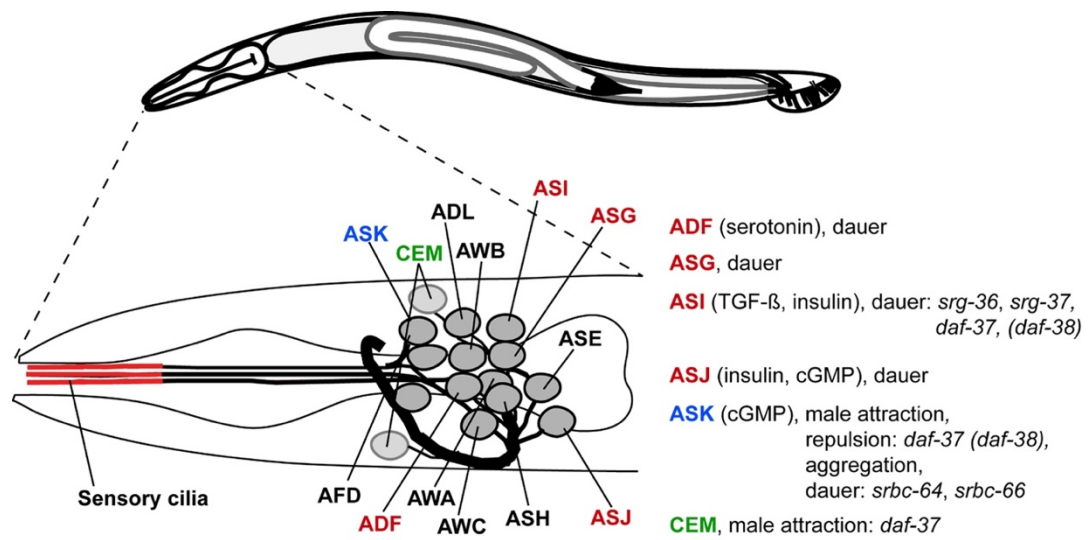


**Figure 1.10: Ciliated Sensory Neurons Involved in Ascaroside Perception.** *C. elegans* depends on chemosensation in order to locate food, avoid noxious chemicals, to mate, and in development. To do so, the worm relies on chemosensory neurons with cilia exposed to the environment. ADF, ASG, ASI, ASJ, ASK, and ADL neurons have been shown to play roles in perception of dauer pheromone as well as ascaroside-mediated social and mating behaviors. (Modified figure from Wormatlas.<sup>51</sup>)

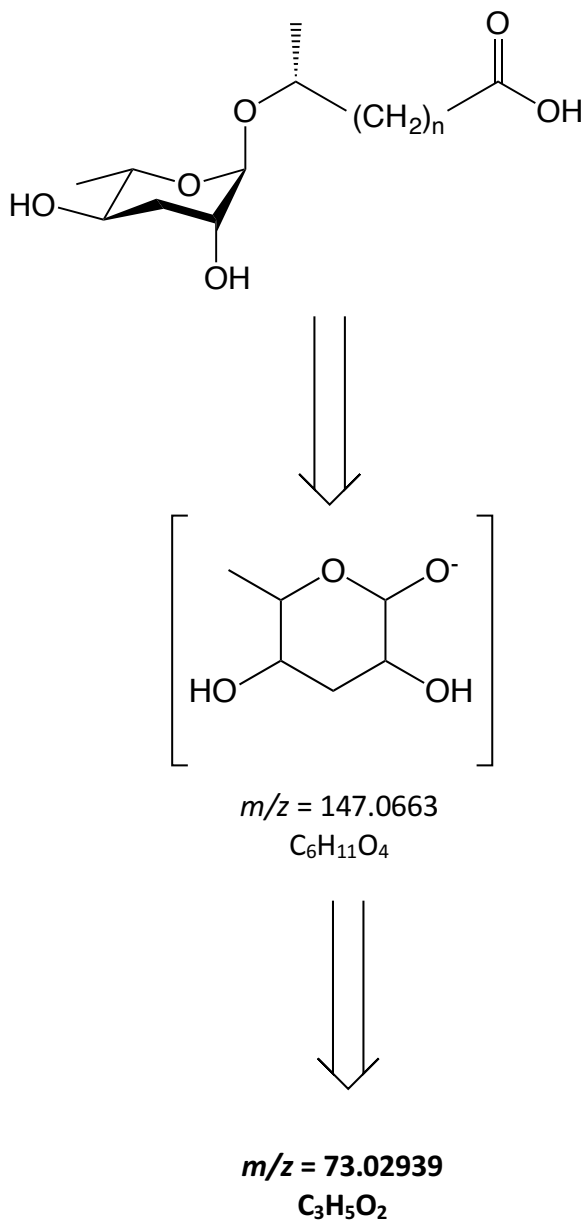


**Figure 1.11: MS/MS Fragmentation of Ascarosides.** Under ESI<sup>-</sup> conditions, most ascarosides produce an ion at  $m/z$  73.0 derived from the ascarylose sugar core. (Modified figure from von Reuss *et al.*<sup>18</sup>)

## 1.10 References

1. Riddle, D. L.; Blumenthal, T.; Meyer, B. J.; Priess, J. R., Introduction to *C. elegans*. In *C. elegans II*, 2nd ed.; Riddle, D. L.; Blumenthal, T.; Meyer, B. J.; Priess, J. R., Eds. Cold Spring Harbor (NY), 1997.
2. Wu, Y.; Luo, Y., Transgenic *C. elegans* as a model in Alzheimer's research. *Curr Alzheimer Res* **2005**, *2* (1), 37-45.
3. Kenyon, C. J., The genetics of ageing. *Nature* **2010**, *464* (7288), 504-12.
4. Morcos, M.; Hutter, H., The model *Caenorhabditis elegans* in diabetes mellitus and Alzheimer's disease. *J Alzheimers Dis* **2009**, *16* (4), 897-908.
5. Irazoqui, J. E.; Urbach, J. M.; Ausubel, F. M., Evolution of host innate defence: insights from *Caenorhabditis elegans* and primitive invertebrates. *Nat Rev Immunol* **2010**, *10* (1), 47-58.
6. Artal-Sanz, M.; Tavernarakis, N., Mechanisms of aging and energy metabolism in *Caenorhabditis elegans*. *IUBMB Life* **2008**, *60* (5), 315-22.
7. Felix, M. A.; Braendle, C., The natural history of *Caenorhabditis elegans*. *Curr Biol* **2010**, *20* (22), R965-9.
8. Steiernagle, T., *Maintenance of C. elegans*. Oxford University Press: 1999; p 51-67.
9. Sulston, J. E.; Horvitz, H. R., Post-embryonic cell lineages of the nematode, *Caenorhabditis elegans*. *Dev Biol* **1977**, *56* (1), 110-56.
10. Kamath, R. S.; Ahringer, J., Genome-wide RNAi screening in *Caenorhabditis elegans*. *Methods* **2003**, *30* (4), 313-21.

11. Meister, P.; Towbin, B. D.; Pike, B. L.; Ponti, A.; Gasser, S. M., The spatial dynamics of tissue-specific promoters during *C. elegans* development. *Genes Dev* **2010**, *24* (8), 766-82.
12. Dickinson, D. J.; Goldstein, B., CRISPR-Based Methods for *Caenorhabditis elegans* Genome Engineering. *Genetics* **2016**, *202* (3), 885-901.
13. Edgar, R. S.; Wood, W. B., The nematode *Caenorhabditis elegans*: a new organism for intensive biological study. *Science* **1977**, *198* (4323), 1285-6.
14. Hu, P. J., Dauer. *WormBook* **2007**, 1-19.
15. Flury, F., On the chemistry and toxicology of ascarides. *Arch. Exp. Path. Pharmacol.* **1912**, *67*, 275-392.
16. Fairbairn, D., The biochemistry of *Ascaris*. *Exp Parasitol* **1957**, *6* (5), 491-554.
17. Meier, J. L.; Burkart, M. D., The chemical biology of modular biosynthetic enzymes. *Chem Soc Rev* **2009**, *38* (7), 2012-45.
18. von Reuss, S. H.; Bose, N.; Srinivasan, J.; Yim, J. J.; Judkins, J. C.; Sternberg, P. W.; Schroeder, F. C., Comparative metabolomics reveals biogenesis of ascarosides, a modular library of small-molecule signals in *C. elegans*. *J Am Chem Soc* **2012**, *134* (3), 1817-24.
19. Joo, H. J.; Kim, K. Y.; Yim, Y. H.; Jin, Y. X.; Kim, H.; Kim, M. Y.; Paik, Y. K., Contribution of the peroxisomal *acox* gene to the dynamic balance of daumone production in *Caenorhabditis elegans*. *J Biol Chem* **2010**, *285* (38), 29319-25.
20. Artyukhin, A. B.; Yim, J. J.; Srinivasan, J.; Izrayelit, Y.; Bose, N.; von Reuss, S. H.; Jo, Y.; Jordan, J. M.; Baugh, L. R.; Cheong, M.; Sternberg, P. W.; Avery, L.; Schroeder, F. C., Succinylated octopamine ascarosides and a new pathway of

- biogenic amine metabolism in *Caenorhabditis elegans*. *J Biol Chem* **2013**, *288* (26), 18778-83.
21. Kaplan, F.; Srinivasan, J.; Mahanti, P.; Ajredini, R.; Durak, O.; Nimalendran, R.; Sternberg, P. W.; Teal, P. E.; Schroeder, F. C.; Edison, A. S.; Alborn, H. T., Ascaroside expression in *Caenorhabditis elegans* is strongly dependent on diet and developmental stage. *PLoS One* **2011**, *6* (3), e17804.
  22. Jeong, P. Y.; Jung, M.; Yim, Y. H.; Kim, H.; Park, M.; Hong, E.; Lee, W.; Kim, Y. H.; Kim, K.; Paik, Y. K., Chemical structure and biological activity of the *Caenorhabditis elegans* dauer-inducing pheromone. *Nature* **2005**, *433* (7025), 541-5.
  23. Butcher, R. A.; Ragains, J. R.; Kim, E.; Clardy, J., A potent dauer pheromone component in *Caenorhabditis elegans* that acts synergistically with other components. *Proc Natl Acad Sci U S A* **2008**, *105* (38), 14288-92.
  24. Golden, J. W.; Riddle, D. L., The *Caenorhabditis elegans* dauer larva: developmental effects of pheromone, food, and temperature. *Dev Biol* **1984**, *102* (2), 368-78.
  25. Butcher, R. A.; Fujita, M.; Schroeder, F. C.; Clardy, J., Small-molecule pheromones that control dauer development in *Caenorhabditis elegans*. *Nat Chem Biol* **2007**, *3* (7), 420-2.
  26. Cassada, R. C.; Russell, R. L., The dauerlarva, a post-embryonic developmental variant of the nematode *Caenorhabditis elegans*. *Dev Biol* **1975**, *46* (2), 326-42.
  27. Riddle, D. L.; Swanson, M. M.; Albert, P. S., Interacting genes in nematode dauer larva formation. *Nature* **1981**, *290* (5808), 668-71.

28. Wang, Y.; Ezemaduka, A. N.; Tang, Y.; Chang, Z., Understanding the mechanism of the dormant dauer formation of *C. elegans*: from genetics to biochemistry. *IUBMB Life* **2009**, *61* (6), 607-12.
29. Golden, J. W.; Riddle, D. L., A pheromone influences larval development in the nematode *Caenorhabditis elegans*. *Science* **1982**, *218* (4572), 578-80.
30. Golden, J. W.; Riddle, D. L., A gene affecting production of the *Caenorhabditis elegans* dauer-inducing pheromone. *Mol Gen Genet* **1985**, *198* (3), 534-6.
31. Gallo, M.; Riddle, D. L., Effects of a *Caenorhabditis elegans* dauer pheromone ascaroside on physiology and signal transduction pathways. *J Chem Ecol* **2009**, *35* (2), 272-9.
32. Pungaliya, C.; Srinivasan, J.; Fox, B. W.; Malik, R. U.; Ludewig, A. H.; Sternberg, P. W.; Schroeder, F. C., A shortcut to identifying small molecule signals that regulate behavior and development in *Caenorhabditis elegans*. *Proc Natl Acad Sci U S A* **2009**, *106* (19), 7708-13.
33. Butcher, R. A.; Ragains, J. R.; Clardy, J., An indole-containing dauer pheromone component with unusual dauer inhibitory activity at higher concentrations. *Org Lett* **2009**, *11* (14), 3100-3.
34. Simon, J. M.; Sternberg, P. W., Evidence of a mate-finding cue in the hermaphrodite nematode *Caenorhabditis elegans*. *Proc Natl Acad Sci U S A* **2002**, *99* (3), 1598-603.
35. Srinivasan, J.; Kaplan, F.; Ajredini, R.; Zachariah, C.; Alborn, H. T.; Teal, P. E.; Malik, R. U.; Edison, A. S.; Sternberg, P. W.; Schroeder, F. C., A blend of small

molecules regulates both mating and development in *Caenorhabditis elegans*.

*Nature* **2008**, *454* (7208), 1115-8.

36. Izrayelit, Y.; Srinivasan, J.; Campbell, S. L.; Jo, Y.; von Reuss, S. H.; Genoff, M. C.; Sternberg, P. W.; Schroeder, F. C., Targeted metabolomics reveals a male pheromone and sex-specific ascaroside biosynthesis in *Caenorhabditis elegans*. *ACS Chem Biol* **2012**, *7* (8), 1321-5.
37. Hodgkin, J.; Doniach, T., Natural variation and copulatory plug formation in *Caenorhabditis elegans*. *Genetics* **1997**, *146* (1), 149-64.
38. de Bono, M.; Bargmann, C. I., Natural variation in a neuropeptide Y receptor homolog modifies social behavior and food response in *C. elegans*. *Cell* **1998**, *94* (5), 679-89.
39. Macosko, E. Z.; Pokala, N.; Feinberg, E. H.; Chalasani, S. H.; Butcher, R. A.; Clardy, J.; Bargmann, C. I., A hub-and-spoke circuit drives pheromone attraction and social behaviour in *C. elegans*. *Nature* **2009**, *458* (7242), 1171-5.
40. Srinivasan, J.; von Reuss, S. H.; Bose, N.; Zaslaver, A.; Mahanti, P.; Ho, M. C.; O'Doherty, O. G.; Edison, A. S.; Sternberg, P. W.; Schroeder, F. C., A modular library of small molecule signals regulates social behaviors in *Caenorhabditis elegans*. *PLoS Biol* **2012**, *10* (1), e1001237.
41. Culotti, J. G.; Russell, R. L., Osmotic avoidance defective mutants of the nematode *Caenorhabditis elegans*. *Genetics* **1978**, *90* (2), 243-56.
42. Ward, S.; Thomson, N.; White, J. G.; Brenner, S., Electron microscopical reconstruction of the anterior sensory anatomy of the nematode *Caenorhabditis elegans*. *J Comp Neurol* **1975**, *160* (3), 313-37.

43. Bargmann, C. I., Chemosensation in *C. elegans*. *WormBook* **2006**, 1-29.
44. White, J. Q.; Nicholas, T. J.; Gritton, J.; Truong, L.; Davidson, E. R.; Jorgensen, E. M., The sensory circuitry for sexual attraction in *C. elegans* males. *Curr Biol* **2007**, *17* (21), 1847-57.
45. Zwaal, R. M., J.; Sternberg, P.; Plasterk, R., Two Neuronal G Proteins are Involved in Chemosensation of the *Caenorhabditis elegans* Dauer-Inducing Pheromone. *Genetics* **1996**, *145*, 715-727.
46. Oldham, W. M.; Hamm, H. E., Heterotrimeric G protein activation by G-protein-coupled receptors. *Nat Rev Mol Cell Biol* **2008**, *9* (1), 60-71.
47. Kim, K.; Sato, K.; Shibuya, M.; Zeiger, D. M.; Butcher, R. A.; Ragains, J. R.; Clardy, J.; Touhara, K.; Sengupta, P., Two chemoreceptors mediate developmental effects of dauer pheromone in *C. elegans*. *Science* **2009**, *326* (5955), 994-8.
48. McGrath, P. T.; Xu, Y.; Ailion, M.; Garrison, J. L.; Butcher, R. A.; Bargmann, C. I., Parallel evolution of domesticated *Caenorhabditis* species targets pheromone receptor genes. *Nature* **2011**, *477* (7364), 321-5.
49. Park, D.; O'Doherty, I.; Somvanshi, R. K.; Bethke, A.; Schroeder, F. C.; Kumar, U.; Riddle, D. L., Interaction of structure-specific and promiscuous G-protein-coupled receptors mediates small-molecule signaling in *Caenorhabditis elegans*. *Proc Natl Acad Sci U S A* **2012**, *109* (25), 9917-22.
50. Hall, D. H. A., Z.F., *C. elegans atlas*. Cold Spring Harbor Laboratory Press: 2008.
51. Altun, Z. H., L.; Wolkow, C.; Crocker, C.; Lints, R.; Hall, D. WormAtlas. <http://www.wormatlas.org/>.

## A LOCALIZATION STUDY OF ASCAROSIDE PRODUCTION

### **2.1 Abstract**

According to earlier studies, loss-of-function *daf-22* mutants are unable to produce the short-chain ascarosides necessary for entry into dauer diapause or for behaviors such as male attraction. DAF-22, a thiolase responsible for the truncation step of peroxisomal  $\beta$ -oxidation of the ascaroside fatty-acid side chain and therefore necessary for the production of biologically active ascarosides, has been reported to be expressed in the intestine, hypodermis, and body wall muscle of the worm. In order to examine potential tissue-specific aspects of ascaroside production, we have selectively driven the expression of DAF-22 under tissue-specific promoters, conducted mass spectrometry-based analyses of the excretomes of each strain, and assessed several ascaroside-regulated worm behaviors. HPLC-MS analysis reveals that the intestine is the major site of ascaroside biosynthesis. However, several ascarosides are produced when a GFP::DAF-22 fusion is expressed in the body wall muscle and hypodermis of the worm. Furthermore, intestinal GFP::DAF-22 expression restored a large amount of dauer formation activity, while GFP::DAF-22 expression in all three individual tissues restored male attraction behavior to wild type-like levels.

### **2.2 Introduction**

Despite its small size, *C. elegans* is comprised of multiple, well-defined tissues and organs that serve vital functions in the life of the worm. For example, the intestine is a large

organ that comprises approximately one third of the worm's entire body. Its main functions include the digestion of food following the grinding of bacteria in the pharynx, as well as the absorption and storage of nutrients.<sup>1</sup> The hypodermis forms the base of the nematode's body, stores nutrients, and secretes the worm's protective cuticle.<sup>2-3</sup> The body wall muscle, on the other hand, is responsible for the worm's sinusoidal movement. There are therefore many potential sites of ascaroside biosynthesis within the worm.

Although much of the biosynthetic pathway of ascarosides has yet to be elucidated, previous studies have shown that DAF-22, a thiolase responsible for the last step of peroxisomal  $\beta$ -oxidation of the lipid moiety attached to the 1'-position of the ascarylose sugar core, is necessary for the production of biologically active short-chain ascarosides (Figure 2.1).<sup>4-5</sup> Transgenic expression of an N-terminally tagged GFP DAF-22 fusion protein (GFP::DAF-22) under the control of the native *daf-22* gene promoter revealed that the protein is expressed in the intestine, the hypodermis, and the body wall muscle of the worm.<sup>4</sup> Furthermore, when exclusively expressed in the intestine under the control of the *vha-6* promoter, GFP::DAF-22 rescue was able to restore some dauer inducing activity. It was therefore hypothesized that the intestine is the major site of ascaroside biosynthesis; however, the possible roles of DAF-22 expressed in the hypodermis and body wall muscle in the biosynthesis of ascarosides remained unexamined.<sup>4</sup> An additional hypothesis could be made that ascaroside production may occur at different locations within the worm and that the ascarosides produced may vary from tissue to tissue.

To investigate this issue, we created three strains of worms that drive the expression of GFP::DAF-22 specifically within the intestine, the hypodermis, or the body wall muscle

using tissue-specific gene promoters within a *daf-22(ok693)* mutant background. The ascaroside profile in each strain was examined by HPLC-MS analysis. Pheromone cues collected in each strain were then tested for activity in dauer formation, male attraction, and hermaphrodite repulsion.

## 2.3 Results and Discussion

### 2.3.1 Driving GFP::DAF-22 Expression within Individual Tissues

To selectively rescue DAF-22 function within a specific tissue, we integrated transgenes into the worm's genome that contained the sequence of a GFP::DAF-22 fusion protein under the direction of one of three different gene promoter sequences. For intestinal expression, we selected the promoter for the gene *vha-6*, which encodes an ortholog of subunit A of the membrane-bound domain of a vacuolar proton-translocating ATPase. This promoter was the same promoter sequence used previously by Butcher *et al*, and the *Pvha-6::gfp::daf-22* transgene in this study produced a similar expression pattern (Figure 2.2).<sup>4</sup>

To drive expression in the hypodermis, we used the short promoter sequence for the *dpy-7* gene, which encodes a collagen that is necessary for normal development and structure of the cuticle.<sup>7</sup> The *Pdpy-7::gfp::daf-22* transgene used in this study was expressed in a punctate manner within the hypodermis. This punctate pattern, which can also be seen in the expression pattern of the intestinal *Pvha-6::gfp::daf-22* transgene, may be due to the three amino acid serine-lysine-isoleucine peroxisomal tag at the C-terminus of the DAF-22 protein.

Expression was driven in the body wall muscle using the promoter sequence of *myo-3*, a gene which encodes the minor isoform of the myosin heavy chain. Expression of the *Pmyo-3::gfp::daf-22* transgene can be seen in the muscle running along the dorsal and ventral axes of the worm.

### 2.3.2 Ascarosides are Primarily Produced in the Intestine

In order to assess the ascaroside profile of each tissue-specific GFP::DAF-22 expressing strain, synchronized liquid cultures were grown from egg to young adult. Ascarosides excreted by the worms were extracted with ethanol from the lyophilized remnants of the culture supernatant, and identified from HPLC-MS chromatograms based on known fragmentation patterns, as previously described (Figure 2.3).<sup>6, 8-9</sup> As expected, the supernatant from *daf-22(ok693)* mutant cultures did not contain any short-chain ascarosides, as DAF-22 is required for the truncation of the lipid side chain. Worms expressing the GFP::DAF-22 fusion within the body wall muscle produced minimal amounts of *ascr#3*, typically one of the most abundantly produced ascarosides, as well as *ascr#10*, and *ascr#18*.

As hypothesized, the intestine does appear to be the major source of ascaroside biosynthesis, with *Pvha-6::gfp::daf-22* transgenic worms producing 50-100% of each ascaroside compared to levels generated by wild type N2 worms, including both simple ascarosides and ascarosides modified at the 4'-position of the ascarylose sugar. As digestion and absorption of nutrients occurs in the intestine, as well as nutrient storage, it makes sense that ascaroside production occurs where the building blocks are most likely to be found.

Worms expressing the GFP::DAF-22 fusion protein within the hypodermis also produce a significant amount of ascarosides, albeit generally less than the quantities

displayed by intestinal expression of GFP::DAF-22. Hypodermal GFP::DAF-22 expression resulted in *ascr#3* levels similar to intestinal rescue, but significantly less quantities of *ascr#5*, and 2'-glucosylated *ascr#4*. Although previous studies did not predict the hypodermis as potential location for ascaroside biosynthesis, the tissue is known to play a role in nutrient storage, and therefore could harbor the building blocks necessary for ascaroside production. Interestingly, hypodermal GFP::DAF-22 rescue demonstrated wild type levels of *ascr#10* and its 4'-modified derivatives, *icas#10* and *osas#10*. Research has shown that lysosome-like organelles within the intestine, called the gut granules, are required for the 4'-modification of ascarosides. Therefore, the question arises as to whether the hypodermis contains the machinery necessary to modify 4'-modified ascarosides, whether simple ascarosides are synthesized in the hypodermis and then transported to the intestine for 4'-modification, or whether there is leaky expression of the *Pdpy-7::gfp::daf-22* transgene within the intestine.

### 2.3.3 Intestinal Rescue of GFP::DAF-22 Restores Dauer Formation

Originally, ascarosides were identified as the major components of dauer pheromone, a chemical signal that directs entry into and exit out of dauer diapause.<sup>10</sup> Previous research demonstrated that a *daf-22* loss-of-function mutant is unable to produce the pheromone necessary to induce entry into dauer diapause; however, partial dauer formation activity can be restored through transgenic expression of GFP::DAF-22 within the intestine.<sup>4, 11</sup>

In order to probe whether driving DAF-22 expression in the body wall muscle and hypodermis, the two other tissues in which DAF-22 is naturally expressed within the worm,

can restore dauer formation activity, integrated strains containing either a *Pmyo-3::gfp::daf-22* or *Pdpy-7::gfp::daf-22* transgene were grown in liquid culture. Dauer pheromone was then collected via ethanol extraction of the boiled supernatant. Exogenous pheromone was then added to plate agar on which eggs were allowed to hatch and develop, and dauer formation activity was assessed (Figure 2.4).

As expected, exogenous pheromone collected from *daf-22(ok693)* loss-of-function mutant worms induced no dauer formation in N2 worms, whereas wild type dauer pheromone elicited dauer formation in  $70 \pm 5\%$  ( $\pm$  SD) of larva. Pheromone generated by intestinal expression of GFP::DAF-22 restored approximately half of the dauer formation activity compared to the N2 control ( $35 \pm 4\%$ ). GFP::DAF-22 rescue within the body wall muscle and hypodermis produced dauer pheromone that induced much lower levels of dauer formation at  $6 \pm 2\%$  and  $4 \pm 2\%$ , respectively. This is consistent with the initial hypothesis that ascaroside biosynthesis primarily occurs within the intestine. However, although very modest, GFP::DAF-22 expression in both the body wall muscle and hypodermis does restore dauer formation compared to the *daf-22(ok693)* mutant. This correlates with the HPLC-MS analysis that reveals ascaroside biosynthesis occurs within the hypodermis, and to a lesser extent, within the body wall muscle.

The main components of dauer pheromone are *ascr#1*, *ascr#2*, *ascr#3*, *ascr#5*, *ascr#8*, and *icas#9*. Although the low resolution HPLC-MS data could not resolve *ascr#1* from other metabolites, it was revealed that *ascr#3* is produced in all three rescue strains, though minimally in the body wall muscle. Furthermore, *ascr#5* was found in the supernatant of intestinal and hypodermal GFP::DAF-22 rescue cultures, as well as *icas#9*. The intestine

produces greater quantities of all the aforementioned dauer-inducing ascarosides compared to the hypodermis, which may explain why dauer pheromone derived from *Pvha-6::gfp::daf-22* worms rescues higher levels of dauer formation than pheromone derived from worms expressing the *Pdpy-7::gfp::daf-22* transgene. It is important to note that the conditions in which cultures were grown for HPLC-MS analysis and dauer pheromone collection were vastly different. As ascaroside production is regulated by the nutritional status of the worm, this may explain why dauer-inducing pheromones ascr#2 and ascr#8 were not detected in the well-fed cultures from the HPLC-MS analysis.<sup>12</sup>

#### 2.3.4 GFP::DAF-22 Rescue Restores Male Attraction Behavior

Hermaphrodite worms are known to produce a chemical cue that attracts males.<sup>13-</sup>  
<sup>14</sup> Guided fractionation studies revealed ascr#2 and ascr#3 as the major components of the male attracting signal. Although incapable of attracting *C. elegans* males alone, ascr#4 was shown to synergize with ascr#2 and ascr#3 to enhance male attraction.<sup>5</sup> We therefore sought to examine whether or not tissue-specific GFP::DAF-22 expression could rescue male-attracting activity in pheromone-deficient worms.

Pheromone cues were collected from *Pvha-6::gfp::daf-22*, *Pmyo-3::gfp::daf-22*, and *Pdpy-7::gfp::daf-22* expressing worms by soaking thoroughly washed synchronized adult hermaphrodites in buffer. The biological activity of each cue was tested by measuring the number of male worms in regions containing cue compared to a control buffer region and calculating a chemotaxis index (Figure 2.5). Media conditioned with *C. elegans* hermaphrodites from each tissue-specific GFP::DAF-22 strain demonstrated the ability to attract male worms to a similar degree as media conditioned with wild type N2 worms

(Figure 2.6). The male attraction chemotaxis indexes of cues collected from *Pvha-6::gfp::daf-22*, *Pmyo-3::gfp::daf-22*, and *Pdpy-7::gfp::daf-22* expressing hermaphrodite worms were  $0.72 \pm 0.16$ ,  $0.71 \pm 0.14$ , and  $0.71 \pm 0.06$ , respectively. In comparison, pheromone collected from wild type N2 worms produced a male attraction chemotaxis index of  $0.82 \pm 0.10$ . As expected, all cues were significantly more attractive than the buffer control (chemotaxis index of  $0.03 \pm 0.28$ ) and pheromone collected from the *daf-22* loss-of-function mutant (chemotaxis index of  $0.28 \pm 0.31$ ).

Although *ascr#2* was not detected in any culture including N2, *ascr#3* was detected in cultures of all three tissue-specific rescue strains. Furthermore, *ascr#4* was produced in worms expressing the *Pvha-6::gfp::daf-22* transgene at levels similar to wild type, and to a lesser extent in *Pdpy-7::gfp::daf-22* expressing worms. Although *ascr#3* levels produced by rescue of GFP::DAF-22 in the body wall muscle were very low compared to wild type and the other rescue strains, the concentrations of *ascr#3* required to induce male attraction lies within the pico- to nanomolar range. Therefore, only very small quantities of *ascr#3*, such as those displayed by the HPLC-MS data for GFP::DAF-22 rescue in the body wall muscle, are required to attract male *C. elegans* worms, which could explain the near wild type levels of male attraction achieved by pheromone cues collected from *Pmyo-3::gfp::daf-22* rescue worms.

### 2.3.5 Hermaphrodite Conditioned Media Does Not Induce Repulsive Behavior Amongst Hermaphrodites

Ascarosides have also been shown to regulate social behaviors such as aggregation and repulsion. Dauer pheromone components *ascr#2*, *ascr#3*, and *ascr#5* were all shown to be repulsive to *C. elegans* hermaphrodite worms.<sup>15</sup> On the other hand, *icas#3* and *icas#9* were shown to be effective hermaphrodite aggregation signals.<sup>16</sup>

In order to test whether tissue-specific rescue of GFP::*DAF-22* causes differences in social behavior, we collected pheromone cues from each transgenic strain by soaking synchronized hermaphrodite worms in buffer for either 6 or 24 hours, and compared how hermaphrodite worms react to each cue compared to a buffer control in a four-quadrant assay (Figure 2.7). A chemotaxis index of 1 indicates a high level of attraction, whereas a chemotaxis index of -1 indicates a high level of repulsion.

Calculated chemotaxis indexes from the repulsion assay were all close to a value of zero, and therefore revealed worms were neither repelled nor attracted to the 6 and 24 hour cues (Figure 2.8). In fact, cues derived from all three tissue-specific GFP::*DAF-22* rescue strains, wild type N2 worms, and *daf-22(ok693)* loss-of-function mutant worms produced chemotaxis indexes similar to the buffer control. While the *daf-22(ok693)* cue may not have attracted or repelled hermaphrodite worms due to a complete lack of ascarosides, it may be possible that the cues generated by wild type worms and each tissue-specific strain contained conflicting signals. While all three tissue-specific GFP::*DAF-22* rescue strains produce *ascr#3*, a repulsive ascaroside, all three tissues also produce *icas#3*, an aggregation pheromone. It is therefore possible that the two signals cancel each other out.

## 2.4 Conclusions

In summary, we have found that driving the expression of GFP::DAF-22 within the intestine, hypodermis, or body wall muscle within a *daf-22* loss-of-function background is able to rescue varying levels of ascaroside biosynthesis. HPLC-MS analysis of liquid culture supernatants reveals that the intestine is the main site of ascaroside biosynthesis with hypodermal GFP::DAF-22 rescue also producing significant levels of biologically active ascarosides.

The expression of the *Pdpy-7::gfp::daf-22* transgene did not diffuse through the entire hypodermis, but rather appeared in a punctate pattern. While this may be due to the three amino acid serine-lysine-isoleucine peroxisomal tag, whether GFP::DAF-22 expression is localized to the peroxisomes should be confirmed. This may be accomplished by constructing and injecting a *Pdpy-7::mcherrySKL* peroxisomal marker into the gonads of *Pdpy-7::gfp::daf-22* worms. Fluorescence microscopy may then be used to assess potential colocalization of the mCherry marker and GFP::DAF-22 within the peroxisomes.

Our results also indicated that hypodermal rescue of GFP::DAF-22 results in the production of 4'-modified derivatives of asc#10. Previous research has indicated that 4'-modification of ascarosides requires the gut granules, lysosome-like organelles within the intestine. To assess possible leaky expression of GFP:DAF-22 within the gut of the hypodermal rescue worms, one could cross the *Pdpy-7::gfp::daf-22* expressing worms with *glo-1(zu39)* or *pgp-2(kx48)* strains, which contain mutations that cause a complete lack or have a reduced number of gut granules, respectively. The presence of 4'-modified

ascarosides in the excretome of such an animal would indicate that the hypodermis does contain the biological machinery required for 4'-modification.

Furthermore, the quantities of ascr#10 derivatives produced by hypodermal rescue of GFP::DAF-22 surpass the levels displayed by intestinal rescue. While higher resolution HPLC-MS studies would be needed to confirm this result, it may indicate that the 4'-modified ascarosides observed may not be due to leaky expression of the transgene. Other genes necessary for the formation of gut granules such as *pgp-2*, a member of the ABC transporter family, and *apb-3*, an adaptin, are also expressed in the hypodermis. Therefore, combined with the punctate expression pattern of *Pdpy-7::gfp::daf-22*, these results could suggest the presence of gut granule-like structures in the hypodermis. To probe this issue, worms expressing the *Pdpy-7::gfp::daf-22* transgene could be stained with LysoTracker Red, a dye that labels lysosome-related gut granules. Fluorescence microscopy could then be used to test for colocalization of GFP::DAF-22 with possible gut granule-like structures within the hypodermis.

Although dauer formation activity restored by GFP::DAF-22 rescue in each tissue roughly correlates with the quantities of dauer-inducing ascarosides observed in the HPLC-MS analysis, it is likely that the ascaroside profile of the dauer pheromone used in the dauer formation assays differs from that observed in the cultures used in our HPLC-MS studies. Ascaroside production varies upon multiple environmental factors, including nutritional state. Therefore, in future, it may be necessary to run an additional HPLC-MS analysis on the dauer pheromone, which was collected from starved worm cultures, in order to get a more complete ascaroside profile of actual dauer pheromone produced by each tissue-specific GFP::DAF-22 rescue strain.

Overall, this study demonstrates that ascaroside biosynthesis is a complex process that involves multiple tissues and organelles. Furthermore, ascarosides can have both distinct and redundant functions in regulating worm behavior, and thus further studies in ascaroside perception are also important.

## 2.5 Figures

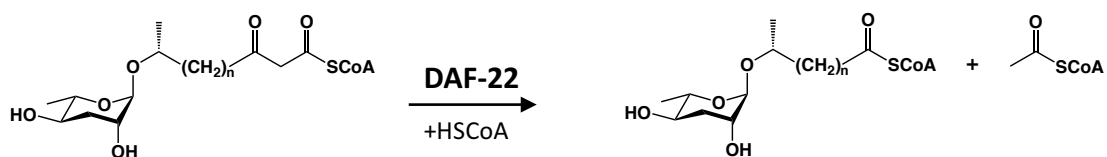


**Figure 2.1: The Role of DAF-22 in Short-Chain Ascaroside Biosynthesis.** DAF-22 comprises the fourth and last step of peroxisomal  $\beta$ -oxidation of the ascaroside lipid side chain in which the carbon chain is truncated by two carbons, which are released in the form of acetyl-CoA.

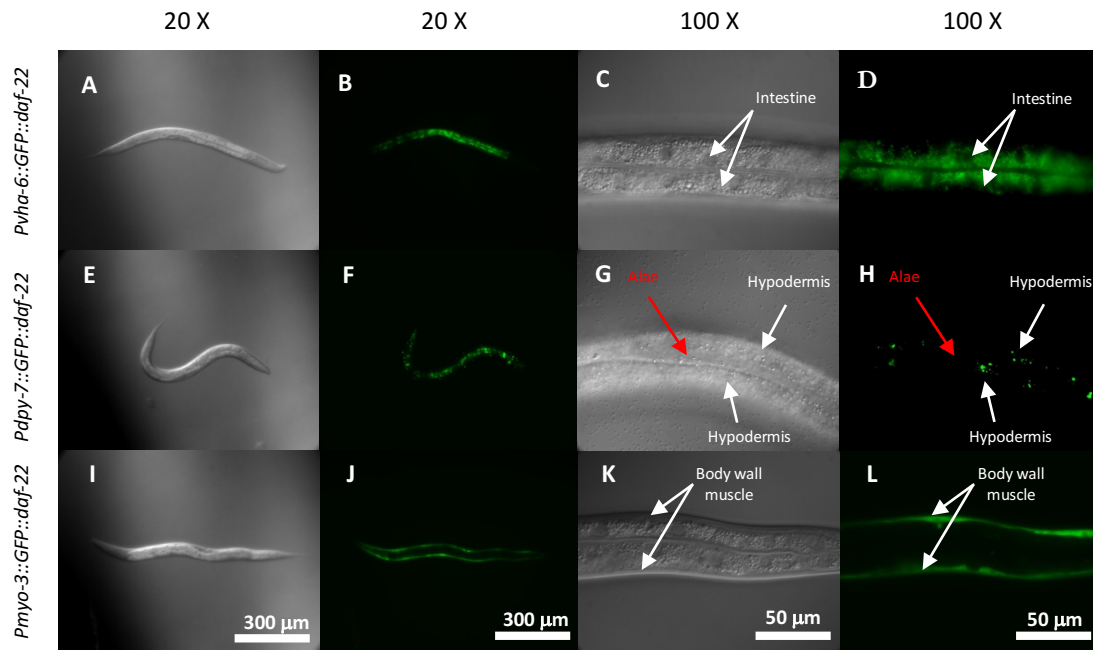


**Figure 2.2: Tissue-Specific GFP::DAF-22 Expression.** DIC and GFP fluorescence microscopy images of L4 larva expressing a GFP::DAF-22 transgene at 20X and 100X magnification. (A-D) *Pvha-6::gfp::daf-22* expresses in the intestine (white arrows). (E-H) *Pdpi-7::gfp::daf-22* expresses in a punctate manner within the hypodermis (white arrows). The top focal plane is in focus, displaying the alae (red arrow). (I-L) *Pmyo-3::gfp::daf-22* expresses within the body wall muscle (white arrows).

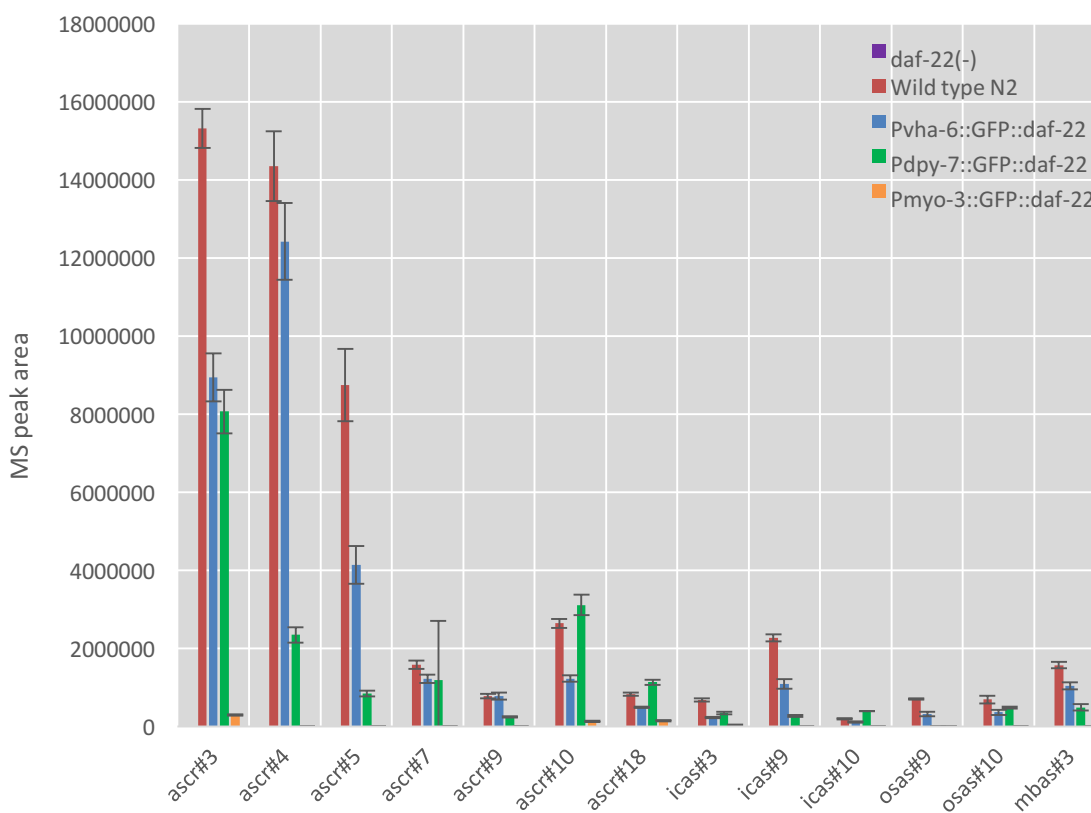


**Figure 2.3: Tissue-Specific Ascaroside Profiles.** HPLC-MS analysis of liquid culture supernatant reveals ascaroside profiles of worms expressing GFP::DAF-22 in the intestine (*Pvha-6::gfp::daf-22*), the hypodermis (*Pdpy-7::gfp::daf-22*), and the body wall muscle (*Pmyo-3::gfp::daf-22*). Averages and standard error of the mean were calculated from three biological replicates. Daumone, or ascr#1, could not be resolved from other metabolites and therefore could not be assessed.

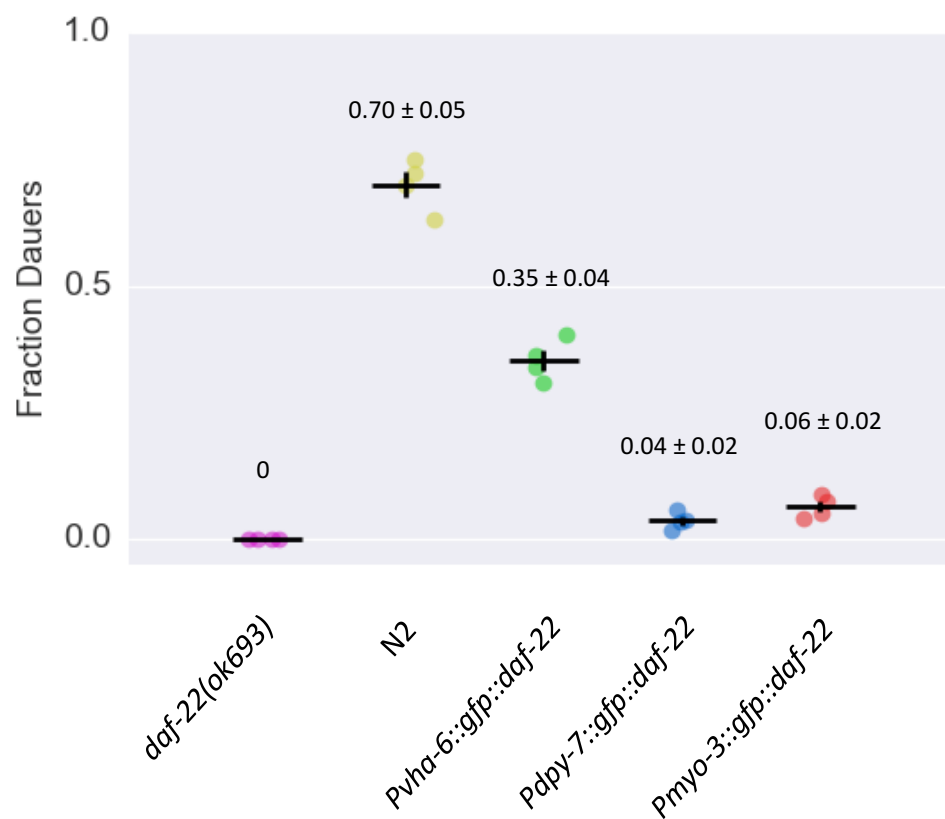


**Figure 2.4: Dauer Formation Activity is Restored by GFP::DAF-22 Rescue.** Dauer formation activity, based on worm morphology, was measured in N2 worms exposed to exogenous dauer pheromone collected from *daf-22(ok693)* loss-of-function worms, wild type N2 worms, and worms expressing GFP::DAF-22 in the intestine (*Pvha-6::gfp::daf-22*), hypodermis (*Pdpi-7::gfp::daf-22*), or body wall muscle (*Pmyo-3::gfp::daf-22*). Dauer pheromone collected from all three tissue-specific transgenic GFP::DAF-22 strains demonstrated partially restored dauer formation ability compared to pheromone derived from loss-of-function *daf-22(ok693)* worms. However, intestinal GFP::DAF-22 expression restored the most activity. Averages and standard error of the mean were calculated from a minimum of four trials.

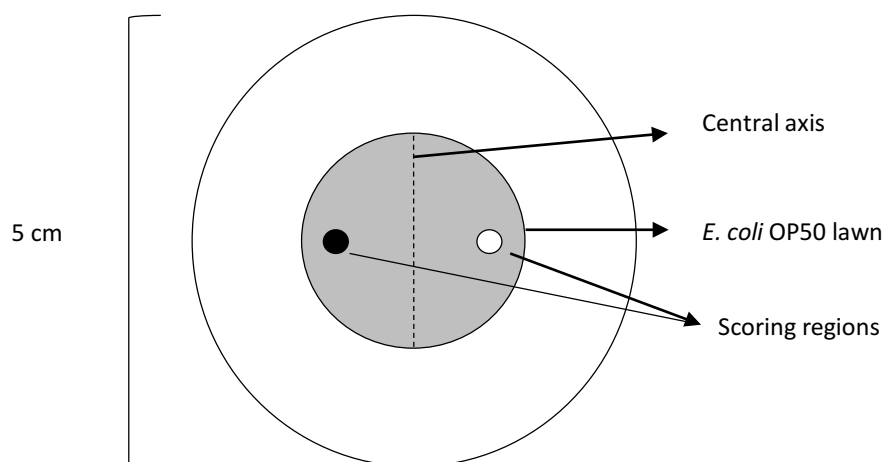


**Figure 2.5: Male Retention Bioassay.** A representation of the bioassay used to measure male retention by a hermaphrodite generated cue. Media conditioned with adult hermaphrodites was spotted on one side of the plate with wash buffer placed on the other side as a control. Male worms were placed along the central axis and behavior was recorded for 20 minutes, from which a chemotaxis index was computed.

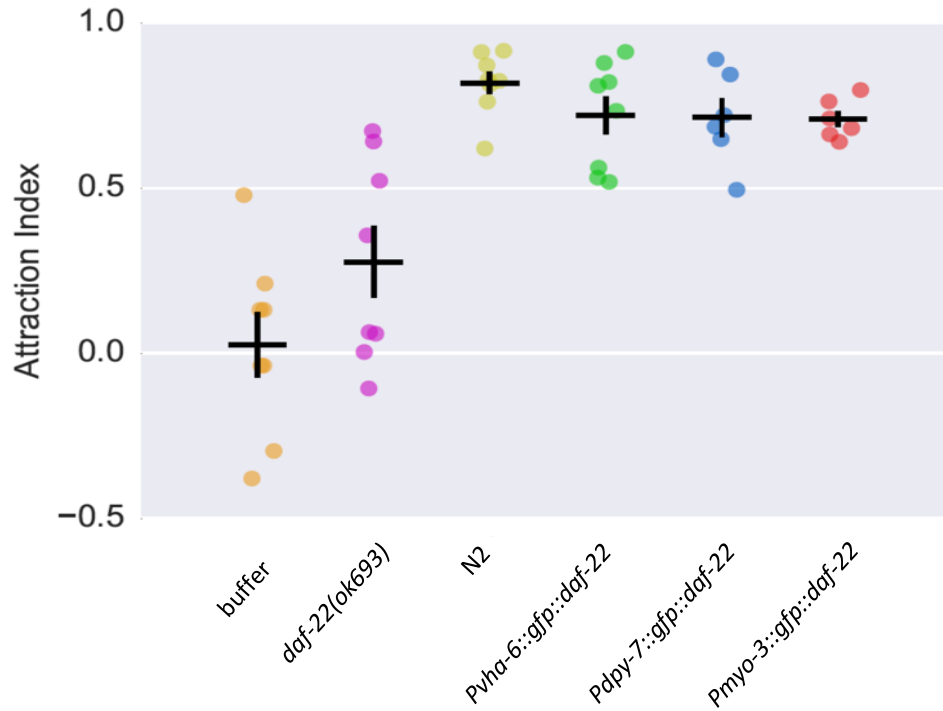


**Figure 2.6: Male Attraction is Restored by GFP::DAF-22 Rescue.** Male worm response (attraction index) to cues generated by hermaphrodites expressing GFP::DAF-22 in the intestine (*Pvha-6::gfp::daf-22*), hypodermis (*Pdpi-7::gfp::daf-22*), and body wall muscle (*Pmyo-3::gfp::daf-22*) are compared to cues generated by wild type N2 or *daf-22(ok693)* worms and a buffer control. Pheromone cues collected over a period of four hours from each tissue-specific GFP::DAF-22 transgenic strain were sufficient to restore male attractive behavior similar to wild type levels. Averages were calculated from a minimum of 6 trials. Error bars represent the standard error of the mean between trials.

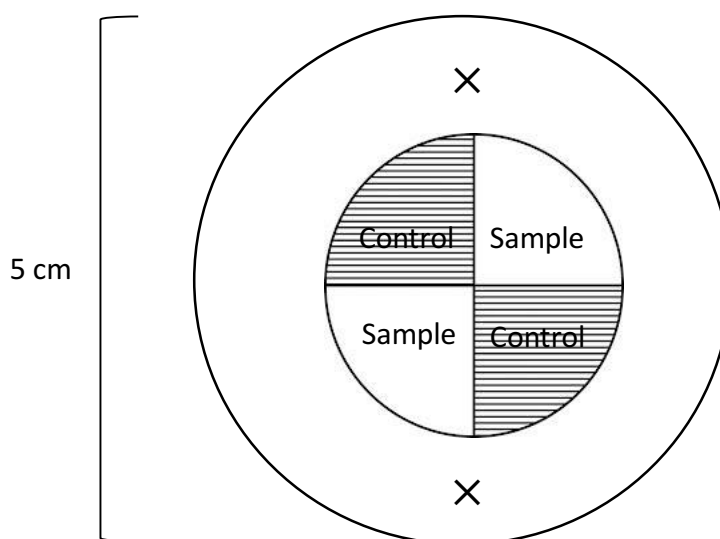


**Figure 2.7: Hermaphrodite Repulsion Assay.** A representation of the bioassay used to measure repulsion behavior. Buffer control was applied to the shaded quadrants and pheromone cue collected from hermaphrodite worms was applied to the white quadrants. The two X's denote where washed hermaphrodite worms were placed on the plate. Behavior was recorded for 10 minutes, from which a chemotaxis index was calculated.

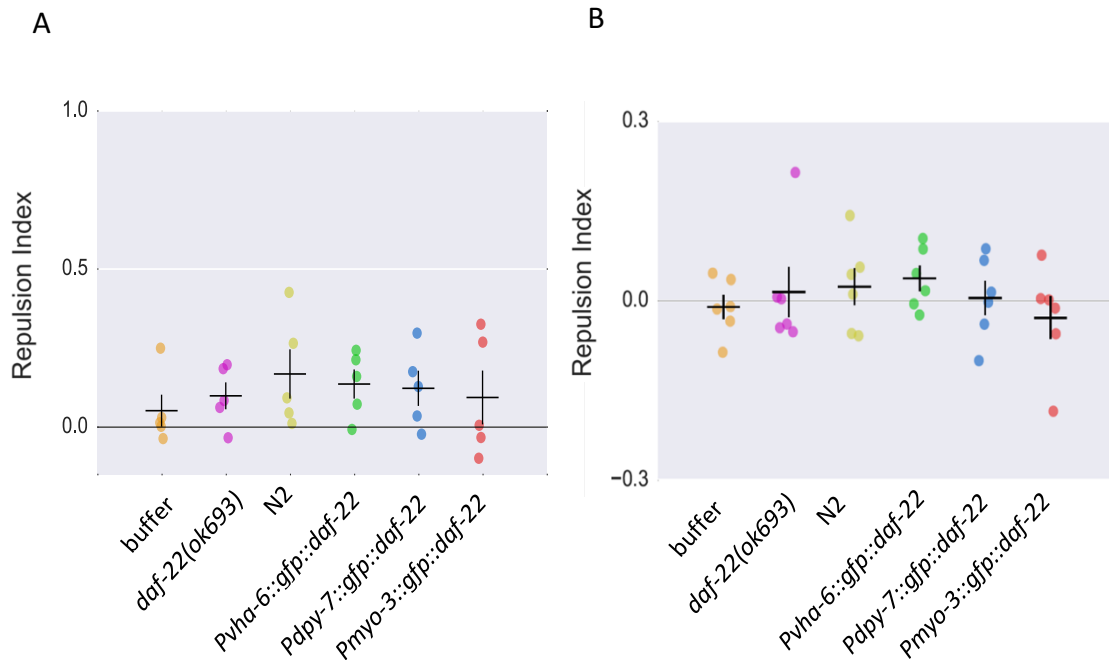


**Figure 2.8: Hermaphrodites Neither Attract nor Repel Each Other.** Adult hermaphrodite worm response (repulsion index) to cues generated by hermaphrodites expressing GFP::DAF-22 in the intestine (*Pvha-6::gfp::daf-22*), hypodermis (*Pdpv-7::gfp::daf-22*), and body wall muscle (*Pmyo-3::gfp::daf-22*) compared to cues generated by wild type N2 or *daf-22(ok693)* worms and a buffer control. Cues were collected either over (A) 6 hours, or (B) 24 hours. Averages were calculated from a minimum of 5 trials. Error bars represent the standard error of the mean between trials.

## 2.6 Materials and Methods

### 2.6.1 *C. elegans* Strains and General Culture Methods

All strains were maintained at room temperature on standard Nematode Growth Medium (NGM) agar plates, which were made with Bacto agar (BD Biosciences) and seeded with *Escherichia coli* OP50 bacteria grown overnight as food.<sup>17</sup> Wild type reference Bristol strain N2, CB1490 *him-5(e1490)*, and RB859 *daf-22(ok693)* mutant strains were obtained from the Caenorhabditis Genetics Center (Minneapolis, MN).

### 2.6.2 Construction and Expression of GFP::*DAF-22*

To construct plasmid pAEA1 (*Pvha-6::gfp::daf-22*), the *gfp::daf-22* cDNA fragment and *vha-6* promoter sequence were amplified by PCR from plasmid HYM433, generously provided by H.Y. Mak using primers oAA017, oAA018, oAA019, and oAA020.<sup>4</sup> The 3'UTR region of the *unc-54* gene was PCR amplified from plasmid pPH93, a gift from the Bargmann Lab, using primers oAA015 and oAA016. These three segments were inserted into backbone vector pBluescript SK(+) between KpnI and ClaI restriction sites using the Gibson assembly system (New England BioLabs, USA).<sup>18</sup>

To construct plasmids pAEA3 (*Pdpy-7::gfp::daf-22*) and pAEA4 (*Pmyo-3::gfp::daf-22*) and, the *dpy-7* promoter was amplified by PCR from genomic DNA using 5' primer oAA013 and 3' primer oAA014 and the *myo-3* promoter sequence was PCR amplified from plasmid jc10ssfo es1 using 5' primer oAA011 and 3' primer oAA012. Each promoter was subsequently inserted between KpnI and AscI restriction sites of a pAEA1 vector backbone. Transgenic lines were generated by microinjecting a mixture containing

either pAEA1, pAEA3, or pAEA4 (10 ng/ $\mu$ L), a *Pmyo-2::dsRed* co-injection marker (5 ng/ $\mu$ L), and 1 kb DNA ladder (New England BioLabs, Massachusetts, 85 ng/ $\mu$ L) into the germ line of adult hermaphrodite *daf-22(ok693)* worms using standard techniques.<sup>19</sup> Extrachromosomal arrays were integrated into the background genome via X-ray irradiation. All integrated strains were outcrossed ten times with *daf-22(ok693)*, which had previously been outcrossed ten times with wild type N2 worms.

### 2.6.3 Preparation of Nematode Culture and Metabolite Extracts

Gravid hermaphrodite worms were collected and treated with a 2:1:7 mixture of 5% NaClO, 5M NaOH, and double distilled water for 2 minutes. Eggs were washed three times with M9 buffer and resuspended at a concentration of 2 eggs/ $\mu$ L in 100 mL of S-complete medium supplemented with *E. coli* HB101. Cultures were grown at 22°C on a rotary shaker until worms reached the young adult stage. Metabolite extractions were performed as previously reported.<sup>9</sup> Liquid cultures were centrifuged, and the supernatant and worm pellets were frozen separately. After lyophilization, the dried supernatant was extracted with 35 mL of 95% ethanol at room temperature for 12 hours. Extracts were then dried *in vacuo*, resuspended in methanol and analyzed by LC-MS. All cultures were grown in three biological replicates.

### 2.6.4 HPLC-MS Analysis

As performed previously, low resolution HPLC-MS was performed using the Agilent 1100 Series HPLC system equipped with an Agilent Eclipse XDB-C18 column (250 mm x

9.4 mm, particle size 5  $\mu\text{m}$ ), connected to a Quattro II or Quattro Ultima mass spectrometer.<sup>6,9</sup> A 0.1% acetic acid-acetonitrile solvent gradient was used starting with an acetonitrile content of 5% for 5 minutes after injection which was then increased to 100% over a period of 40 minutes. Metabolic extracts were analyzed by HPLC-ESI-MS in the negative ionization mode using a capillary voltage of 3.5 kV and a cone voltage of -40 V. Ascarosides were detected as  $[\text{M-H}]^-$  ions and confirmed through comparisons with the retention times of synthetic standards.

#### *2.6.5 Dauer Formation Assay*

The preparation of crude dauer pheromone and dauer formation assay were performed as previously described with modification.<sup>20</sup> Crude pheromone was extracted with 95% ethanol from exhausted liquid culture medium and resuspended with double distilled water. Assay plates were prepared the day before each experiment by adding crude pheromone to NGM agar containing no peptone and dried overnight at room temperature. Heat-killed *E. coli* OP50 was used as a limited food source and was prepared by resuspending overnight OP50 cultures in S-basal at a concentration of 8 g/mL and heating at 100°C for 5 minutes. On the day of the experiment, 2  $\mu\text{L}$  of heat-killed *E. coli* OP50 was spotted onto each pheromone plate. Ten young adult worms were picked onto each plate and allowed to lay 50-60 eggs before being removed. Another 18  $\mu\text{L}$  of heat-killed OP50 was added to the plates as a food source for the unhatched larvae. Plates were incubated for 48 hours at 25°C, after which dauers and non-dauer worms were counted based on morphology.

### 2.6.6 Male Retention Assay

To collect pheromone cues, worms were selected as L4 larva and allowed to grow overnight into adult worms. Synchronized adults were washed four times in M9 buffer, then allowed to soak in M9 buffer in the cap of an inverted 1.5 mL Eppendorf tube at a concentration of 1 worm/ $\mu$ L. After 4 hours, and centrifugation, the supernatant was collected and stored at  $-20^{\circ}\text{C}$ . As described by Choe *et al.*, a 16 mm lawn of *E. coli* OP50 was grown overnight on 5 cm NGM agar plates at  $20^{\circ}\text{C}$  the day prior to the experiment.<sup>21</sup> Two 0.6  $\mu$ L spots, one a control consisting of the last M9 wash cycle and the other the pheromone cue, were placed on opposite sides of the bacterial lawn using a transparent template. The liquid was allowed to settle into the agar. 10 male worms, isolated as L4 larva the night before the experiment, were placed along the central axis of the bacterial lawn and video recording began immediately upon worm placement. Trials were recorded for 20 minutes at a frame rate of 1 frame per second using the behavior chamber and camera set up described by Chai *et al.*<sup>22</sup> The results were averaged from at least six different trials. To compare worm occupancy in each scoring region, automated software was used to calculate the Chemotaxis Index, as outlined by Bargmann *et al.*<sup>23</sup>

### 2.6.7 Hermaphrodite Repulsion Assay

Pheromone cues were generated similarly to those used for the male retention assay, but were collected over a period of 6 or 24 hours. Repulsion behavior was assessed using the protocol outlined previously.<sup>22</sup> On day 1, 10 well-fed gravid hermaphrodite worms were picked onto NGM agar plates seeded with *E. coli* OP50 the night before, and allowed to lay

eggs for six hours. The worms were then removed from the plates and progeny were allowed to grow at 20°C for three days into adults. On day 3, 35 mm chemotaxis agar plates were prepared and allowed to dry overnight at room temperature. On day 4, synchronized adult worms from two NGM plates were washed three times in chemotaxis buffer. During the second wash, 1  $\mu$ L of M9 buffer (quadrants 1 and 4) or cue (quadrants 2 and 3) were added to the 35 mm assay plate using a transparent template. After complete washing, worms were transferred to the assay plate above and below the circular treated region and a folded tissue was used to absorb excess wash buffer. Using video capture software, behavior was recorded for 10 minutes at a frame rate of 1 frame per second. The experiment was repeated at least 5 times for each pheromone cue.

## 2.7 References

1. McGhee, J. D., The *C. elegans* intestine. *WormBook* **2007**, 1-36.
2. Kramer, J. M., Extracellular Matrix. In *C. elegans II*, 2nd ed.; Riddle, D. L.; Blumenthal, T.; Meyer, B. J.; Priess, J. R., Eds. Cold Spring Harbor (NY), 1997.
3. Wood, W. B., *The Nematode Caenorhabditis elegans*. Cold Spring Harbor Laboratory: Cold Spring Harbor, N.Y., 1988; p xiii, 667 p.
4. Butcher, R. A.; Ragains, J. R.; Li, W.; Ruvkun, G.; Clardy, J.; Mak, H. Y., Biosynthesis of the *Caenorhabditis elegans* dauer pheromone. *Proc Natl Acad Sci USA* **2009**, *106* (6), 1875-9.
5. Srinivasan, J.; Kaplan, F.; Ajredini, R.; Zachariah, C.; Alborn, H. T.; Teal, P. E.; Malik, R. U.; Edison, A. S.; Sternberg, P. W.; Schroeder, F. C., A blend of small molecules regulates both mating and development in *Caenorhabditis elegans*. *Nature* **2008**, *454* (7208), 1115-8.
6. von Reuss, S. H.; Bose, N.; Srinivasan, J.; Yim, J. J.; Judkins, J. C.; Sternberg, P. W.; Schroeder, F. C., Comparative metabolomics reveals biogenesis of ascarosides, a modular library of small-molecule signals in *C. elegans*. *J Am Chem Soc* **2012**, *134* (3), 1817-24.
7. McMahon, L.; Muriel, J. M.; Roberts, B.; Quinn, M.; Johnstone, I. L., Two sets of interacting collagens form functionally distinct substructures within a *Caenorhabditis elegans* extracellular matrix. *Mol Biol Cell* **2003**, *14* (4), 1366-78.
8. Artyukhin, A. B.; Yim, J. J.; Srinivasan, J.; Izrayelit, Y.; Bose, N.; von Reuss, S. H.; Jo, Y.; Jordan, J. M.; Baugh, L. R.; Cheong, M.; Sternberg, P. W.; Avery, L.;

- Schroeder, F. C., Succinylated octopamine ascarosides and a new pathway of biogenic amine metabolism in *Caenorhabditis elegans*. *J Biol Chem* **2013**, *288* (26), 18778-83.
9. Panda, O.; Akagi, A. E.; Artyukhin, A. B.; Judkins, J. C.; Le, H. H.; Mahanti, P.; Cohen, S. M.; Sternberg, P. W.; Schroeder, F. C., Biosynthesis of Modular Ascarosides in *C. elegans*. *Angew Chem Int Ed Engl* **2017**, *56* (17), 4729-4733.
  10. Golden, J. W.; Riddle, D. L., A pheromone influences larval development in the nematode *Caenorhabditis elegans*. *Science* **1982**, *218* (4572), 578-80.
  11. Golden, J. W.; Riddle, D. L., A gene affecting production of the *Caenorhabditis elegans* dauer-inducing pheromone. *Mol Gen Genet* **1985**, *198* (3), 534-6.
  12. Kaplan, F.; Srinivasan, J.; Mahanti, P.; Ajredini, R.; Durak, O.; Nimalendran, R.; Sternberg, P. W.; Teal, P. E.; Schroeder, F. C.; Edison, A. S.; Alborn, H. T., Ascaroside expression in *Caenorhabditis elegans* is strongly dependent on diet and developmental stage. *PLoS One* **2011**, *6* (3), e17804.
  13. Simon, J. M.; Sternberg, P. W., Evidence of a mate-finding cue in the hermaphrodite nematode *Caenorhabditis elegans*. *Proc Natl Acad Sci U S A* **2002**, *99* (3), 1598-603.
  14. White, J. Q.; Nicholas, T. J.; Gritton, J.; Truong, L.; Davidson, E. R.; Jorgensen, E. M., The sensory circuitry for sexual attraction in *C. elegans* males. *Curr Biol* **2007**, *17* (21), 1847-57.
  15. Macosko, E. Z.; Pokala, N.; Feinberg, E. H.; Chalasani, S. H.; Butcher, R. A.; Clardy, J.; Bargmann, C. I., A hub-and-spoke circuit drives pheromone attraction and social behaviour in *C. elegans*. *Nature* **2009**, *458* (7242), 1171-5.

16. Srinivasan, J.; von Reuss, S. H.; Bose, N.; Zaslaver, A.; Mahanti, P.; Ho, M. C.; O'Doherty, O. G.; Edison, A. S.; Sternberg, P. W.; Schroeder, F. C., A modular library of small molecule signals regulates social behaviors in *Caenorhabditis elegans*. *PLoS Biol* **2012**, *10* (1), e1001237.
17. Brenner, S., The genetics of *Caenorhabditis elegans*. *Genetics* **1974**, *77* (1), 71-94.
18. Gibson, D. G.; Young, L.; Chuang, R. Y.; Venter, J. C.; Hutchison, C. A., 3rd; Smith, H. O., Enzymatic assembly of DNA molecules up to several hundred kilobases. *Nat Methods* **2009**, *6* (5), 343-5.
19. Mello, C. C.; Kramer, J. M.; Stinchcomb, D.; Ambros, V., Efficient gene transfer in *C.elegans*: extrachromosomal maintenance and integration of transforming sequences. *EMBO J* **1991**, *10* (12), 3959-70.
20. Golden, J. W.; Riddle, D. L., The *Caenorhabditis elegans* dauer larva: developmental effects of pheromone, food, and temperature. *Dev Biol* **1984**, *102* (2), 368-78.
21. Choe, A.; von Reuss, S. H.; Kogan, D.; Gasser, R. B.; Platzer, E. G.; Schroeder, F. C.; Sternberg, P. W., Ascaroside signaling is widely conserved among nematodes. *Curr Biol* **2012**, *22* (9), 772-80.
22. Chai, C. M., Automated analysis of a nematode population-based chemosensory preference assay. *JoVE* **2017**, *In press*.
23. Bargmann, C. I.; Hartweg, E.; Horvitz, H. R., Odorant-selective genes and neurons mediate olfaction in *C. elegans*. *Cell* **1993**, *74* (3), 515-27.

*Chapter 3*IDENTIFYING GENES INVOLVED IN THE BIOSYNTHESIS OF  
MODULAR ASCAROSIDES IN *CAENORHABDITIS ELEGANS*

Panda, O.; Akagi, A.E.; Artyukhin, A.B.; Judkins, J.C.; Le, H.H.; Mahanti, P.; Cohen, S. M.; Sternberg, P.W.; Schroeder, F.C. (2017). "Biosynthesis of modular ascarosides in *C. elegans*." In: *Angewandte Chemie International Edition English* 56.17, pp. 4729-4733. doi: 10.1002/anie.201700103.

**3.1 Abstract**

*C. elegans* and other related nematodes produce a large family of small molecule signals, collectively called ascarosides, by linking together multiple building blocks derived from primary metabolic pathways. In each ascaroside, the dideoxysugar ascarylose acts as a scaffold to which different modalities are attached in a modular fashion. Although these structural differences have been shown to be responsible for the variation in behaviors regulated by individual ascarosides, the mechanisms by which specific components are linked together are unknown. We demonstrate that ACS-7, a predicted acyl-CoA synthetase that localizes in lysosome-related organelles within the intestine, is necessary for the attachment of different metabolically derived moieties to the 4'-position of the ascarylose sugar in *ascr#9*. Additional examination revealed that ACS-10, another putative acyl-CoA synthetase, does not appear to play a significant role in ascaroside biosynthesis.

## 3.2 Introduction

*C. elegans* and other related nematodes produce a large family of small signaling molecules known as ascarosides that control many aspects in the life of the nematode, often through conserved signaling pathways.<sup>1-7</sup> All ascarosides are glycosides of the dideoxysugar ascarylose with a fatty acid-like moiety attached at the 1'-position of the sugar core (Figure 3.1). The fatty acid can vary in length, level of saturation, and level of oxidation to produce different simple ascarosides (ascr). However, some ascaroside variants contain an additional head group derived from primary metabolic pathways at the 4'-position of ascarylose (Figure 3.2). For example, the indole-3-carbonyl group characteristic of icas ascarosides has previously been shown to be derived from tryptophan,<sup>8</sup> and the *N*-succinylated octopamine building block found attached in osas ascarosides is a product derived from tyrosine.<sup>9</sup> Although microorganisms are known to contain the necessary biological machinery for the synthesis of large libraries of structures, it was presumed that animals do not, and therefore the ascarosides serve as an unexpected example of structural diversity.<sup>10-11</sup>

Studies have shown that the small structural alterations between ascarosides are associated with substantial differences in biological function (Figure 3.3). For instance, ascr#3, the most abundantly produced ascaroside by wild type *C. elegans* hermaphrodites, is a potent male attractant and acts as a dauer formation signal. On the other hand, ascr#10 which contains a lipid side chain of equal length to that of ascr#3, but lacks a site of  $\alpha,\beta$ -unsaturation, attracts hermaphrodites and not males.<sup>5, 12</sup> Another example, icas#3, which consists of an indole-3 carbonyl attached to an ascr#3 core, acts as a hermaphrodite attractant.<sup>8</sup> Although the structural elements of ascarosides have known significant impacts

on worm biology, the biological machinery involved in piecing together the building blocks of ascarosides is largely unknown.

Additionally, the modular assembly of ascarosides appears to be a highly selective process. In *ascr#8*, the *p*-aminobenzoic terminal group attaches to the terminus of the unsaturated 7-carbon side chain of an *ascr#7* core despite the fact that *ascr#1* and *ascr#3*, which contain saturated 7-carbon and unsaturated 9-carbon side chains respectively, are more abundantly produced (Figure 3.4). This high level of specificity suggests that there may be well-regulated pathways dedicated to the biosynthesis of ascarosides. Elucidating these pathways will therefore demonstrate how the metabolic status drives the production of pheromones that regulate the behavior and development of the worm.

Using HPLC-MS analyses of the worm excretome, we found that ACS-7, a putative acyl-CoA synthetase, plays a role in the attachment of different head groups to the 4'-position of the ascarylose sugar scaffold of the simple ascaroside *ascr#9*. Staining and GFP-tagging studies indicate that ACS-7 localizes to the gut granules, lysosome-like organelles that are significant sites of ascaroside biosynthesis. On the other hand, ACS-10, another putative acyl-CoA synthetase, does not appear to play a role in ascaroside production.

### **3.3 Results and Discussion**

#### *3.3.1 Screening for Candidate Genes*

Up to this point, the only enzymes known to play a role in the production of ascarosides are those involved in the peroxisomal  $\beta$ -oxidation of the fatty acid side chain.<sup>13-</sup>

<sup>17</sup> In order to identify additional genes involved in the biosynthesis of ascarosides, our collaborator, Oishika Panda in the Schroeder Lab at Cornell University, screened the

supernatant of different loss-of-function mutant worm cultures for ascaroside biosynthetic defects using HPLC-MS in comparison to a wild type control. Mutant strains were selected for testing from a collection of already available strains based on either their predicted function for creating ester bonds (Table 3.1), or their subcellular location in the peroxisomes.

Previous studies have found that samples of synthetic *ascr#1* and *ascr#3* fed to worms in liquid culture can be converted into their indolated derivatives *icas#1* and *icas#3*, respectively.<sup>13</sup> This suggests that ascaroside modification at the 4'-position occurs after the attachment and peroxisomal  $\beta$ -oxidation of the fatty acid side chain. The headgroups attached to the 4'-position of ascarylose are connected by ester bonds, making genes encoding *O*-acyltransferases prime candidates as potential players in the ascaroside biosynthetic pathway.

In *C. elegans*, 61 genes are annotated as putative *O*-acyltransferases based on homology, and out-crossed knockout mutants were available readily for only three genes: *oac-39(gk149)*, *nrf-6(sa525)*, and *ndg-4(sa529)*. To expand our examination of the *oac* family, we also studied strains obtained from the Million Mutant Project (MMP). These strains are derived from the mutagenesis of wild type animals with ethylmethanesulfonate, *N*-ethyl-*N*-nitrosourea, or a mixture of both. As such, these strains contain a large number of mutations, but we specifically selected strains containing amber, ochre, or opal stop codons within the *oac* gene sequences, which are likely to disrupt proper translation and therefore have a higher probability of disrupting enzyme function.<sup>18</sup> As truncation of the fatty acid side chain occurs in the peroxisomes, we also selected genes containing peroxisome targeting sequences including three putative acyl-CoA synthetase genes from the *acs* gene family.<sup>19</sup>

From the initial LC-MS screen, four of the 19 MMP strains examined demonstrated reduced levels of *mbas#3* compared to a wild type control. These strains contained mutations in *oac-14(gk519224)*, *oac-38(gk648702)*, *oac-29(gk646323)*, and *oac-50(gk402144)*. The potent aggregation pheromone *mbas#3* is a derivative of *ascr#3* and contains a tiglic acid moiety on the 4'-position of the ascarylose sugar.

Although all four *oac* mutant strains produced decreased levels of *mbas#3*, levels of the precursor ascaroside *ascr#3* were similar to wild type. To rule out the possibility that the lower *mbas#3* levels observed were not due a decrease in tiglic acid, cultures of *oac-38(gk648702)* and *oac-50(gk402144)* mutant worms, which produced the lowest *mbas#3* levels of the four strains, were supplemented with tiglic acid or an ethanol control (Figure 3.5). The results demonstrate that *mbas#3* production was rescued in *oac-38(gk648702)* with the addition of tiglic acid, but not in *oac-50(gk402144)*. This suggests that *oac-50* may play a role in the biosynthesis of *mbas#3*, but that the change in *mbas#3* production observed in the *oac-38(gk648702)* is most likely due to a change in tiglyl-CoA metabolism.

Initial HPLC-MS screening of putative peroxisomal genes revealed that the *acs-7(tm6781)* mutant is unable to produce the modular ascarosides *icas#9* and *osas#9*, although the levels of other modular ascarosides such as *icas#3*, *icas#10*, and *osas#10* were similar to wild type (Figure 3.6). This result suggests that *acs-7* may be important in the modification of the simple ascaroside *ascr#9* at the 4'-position.

### 3.3.2 Examining the Role of *oac-50* in Ascaroside Biosynthesis

The MMP strain containing the *oac-50(gk402144)* mutation contains 218 additional mutations (Figure 3.7). To ensure the observed defects in *mbas#3* production were

specifically due to a loss of function in *oac-50* and not another gene, the MMP strain was outcrossed three times with wild type N2 worms to eliminate background mutations. The outcrossed *oac-50(gk402144)* worms were then fed either tiglic acid or ethanol as a control to confirm that any observed reduction in *mbas#3* production is due to an ascaroside biosynthetic defect caused by the *oac-50* mutation and not due to a background mutation.

Results from the feeding assay revealed that the outcrossed *oac-50* mutant strain produces *mbas#3* levels similar to wild type when fed either tiglic acid or ethanol (Figure 3.8). This rescue of *mbas#3* production indicates that *oac-50* does not play a role in ascaroside production. It is possible that the reduced *mbas#3* phenotype previously observed is due to one of the background mutations eliminated through the outcrossing process, however which specific mutation is responsible is not immediately apparent based on the predicted functions of each gene based on homology.

### 3.3.3 Transgenic Rescue of ACS-7 Restores the Production of *ascr#9* Derivatives

The gene *acs-7* is an ortholog of human acyl-CoA synthetase bubblegum family member 1 and is therefore predicted to be an acyl-CoA synthetase; however, the specific function of the gene within *C. elegans* has not previously been identified. In order to confirm the role of ACS-7 in the biosynthesis of the modular ascarosides *icas#9* and *osas#9* as indicated by our initial screen, we drove the expression of a C-terminal green fluorescent protein (GFP)-tagged ACS-7 fusion protein (ACS-7::GFP) under the native *acs-7* promoter (*Pacs-7:acs-7::gfp*) within an *acs-7(tm6781)* loss-of-function mutant background.

HPLC-MS analysis of the supernatant obtained from *Pacs-7::acs-7::gfp* liquid cultures demonstrated rescue of the production of *icas#9* and *osas#9* (Figure 3.9). Other

ascaroside levels remained similar to wild type. Furthermore, although *ascr#9* levels remained consistent amongst wild type N2, the *acs-7(tm6781)* loss-of-function mutant, and the *Pacs-7::acs-7::gfp* rescue strain, restoration of *osas#9*, *icas#9*, and *tsas#9* indicate that ACS-7 is specifically involved in the biosynthesis of *ascr#9* derivatives (Figure 3.10). Our collaborators went on to demonstrate through *in vitro* assays using recombinant ACS-7 protein that ACS-7 activates head groups prior to attachment to the ascarylose core by adenylating the precursors.<sup>20</sup> ACS-7 does not carry out the esterification, or *O*-acyltransferase, step.

#### 3.3.4 The Role of LROs in Modular Ascaroside Biosynthesis

Although the *acs-7* gene contains a peroxisomal targeting sequence (PTS) and was therefore predicted to encode a peroxisomal protein, the localization of ACS-7 had not previously been examined. Fluorescence microscopy of worms co-expressing an ACS-7::GFP fusion protein along with an mCherry fluorescent protein containing an SKL peroxisomal tag and driven under the intestine-specific promoter for the *vha-6* gene (*Pvha-6::mCherrySKL*) revealed that the ACS-7::GFP protein does not colocalize with the peroxisomal marker (Figure 3.11). Therefore, although the *acs-7* gene contains a PTS tag, the protein is not peroxisomal.

*C. elegans* is known to contain punctate, birefringent organelles in the intestine called the gut granules.<sup>21-22</sup> Although there are several types of gut granules, acidic lysosome-related organelles (LROs) are known to play significant roles in breaking down digestive waste, regenerating biomolecular building blocks, and are hypothesized to be involved in the biosynthesis of various metabolites.<sup>23-24</sup> Through staining studies using LysoTracker red, a

dye that selectively stains LROs, it was revealed that ACS-7::GFP colocalizes with the dye, indicating that ACS-7::GFP localizes in the LROs within the intestine of *C. elegans* (Figure 3.12). Our collaborators in the Schroeder Lab found that strains with mutations in genes required to produce gut granules such as *glo-1*, a member of the Rab family of small GTPases, and *pgp-2*, a member of the ABC transporter family, are unable to produce or product reduced quantities of ascarosides modified at the 4'-position, suggesting that these more complex ascarosides are synthesized specifically in the LROs (Figure 3.13).<sup>20</sup> Our localization data and rescue experiments for the *acs-7* gene further support this hypothesis.

### 3.3.5 Knockout of *acs-10* Does Not Impact Ascaroside Biosynthesis

As *acs-7* was shown to be involved in the biosynthesis of modified derivatives of ascr#9, we hypothesized that other members in the *acs* gene family may be involved in the production of 4'-modified versions of other simple ascarosides. There are 22 members in the *acs* gene family, all predicted to be fatty acid-CoA synthetases based on homology and orthology data; however, there are only mutant strains available from the Caenorhabditis Genetics Center for seven of the genes. We therefore utilized the CRISPR/Cas9 gene editing system to create an additional loss-of-function mutant strain for the gene *acs-10*.

The *acs-10* gene shares 30% homology to *acs-7*. We generated a mutant that contains a 1182 base pair deletion that covers the most of last two exons and a significant portion of the 3'UTR region (Figure 3.14). We predict that this is a loss-of-function deletion as it includes 16 of the 19 residues in the predicted active site and 15 of 16 residues in the predicted AMP binding site. However, HPLC-MS analysis of mutant *acs-10* liquid cultures revealed that all known ascarosides were produced at similar levels to a wild type control

(Figure 3.14). Therefore, we conclude that unlike *acs-7*, *acs-10* plays no significant role in the biosynthesis of ascarosides modified at the 4'-position.

### 3.4 Conclusions

In summary, by driving the expression of a GFP-tagged *acs-7* transgene within a mutant *acs-7* loss-of-function mutant background, we found that ACS-7 rescues the production of *icas#9*, *osas#9*, and *tsas#9*, and thus plays a role in the creation of *ascr#9* derivatives. This also suggests that other enzymes are required to play similar roles in the biosynthesis of modular ascarosides containing different fatty acid side chains. Although loss of function in the gene *acs-10* did not demonstrate any ascaroside biosynthetic defects, we suggest conducting further screens on other mutants from the *acs* gene family.

Through colocalization and staining studies, we discovered that ACS-7 is expressed in acidic LROs. Furthermore, abolishment or reduction of gut granules resulted in a loss or reduction in the production of ascarosides modified at the 4'-position, but not the corresponding precursor simple ascarosides. These results demonstrate that *C. elegans* homologs of genes from canonical metazoan metabolic pathways act in specific organelles to create complex metabolites. In future, it may be useful to perform organelle-specific proteomics studies to identify other proteins that may be involved in the attachment of head groups to other simple ascarosides such as *ascr#3* and *ascr#10*.

Although our initial study of an *oac-50* loss-of-function mutant failed to display any defects in ascaroside biosynthesis, the *oac* family of genes is still a prime target for screening. Our initial screen may have failed due to MMP strains containing too many mutations. Ascaroside biosynthesis is a highly regulated process that is influenced by many

environmental factors including temperature, nutrient density and population. Therefore, an additional mutation may alter ascaroside biosynthesis indirectly by influencing the worm's metabolism. We therefore suggest the creation of mutant strains containing loss-of-function mutations in single *oac* genes using the CRISPR-Cas9 genome editing system.

### 3.5 Figures

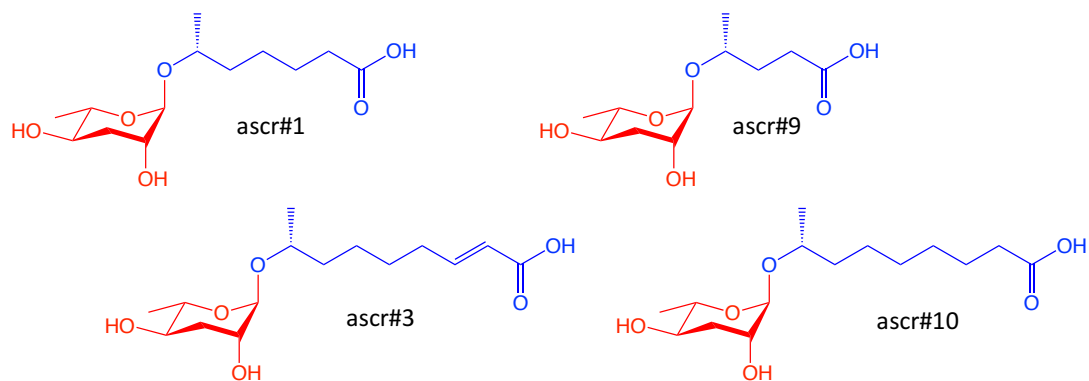


**Figure 3.1: Simple Ascaroside Structures.** The simple ascarosides ascr#1, ascr#3, ascr#9 and ascr#10 all consist of an ascrylose sugar core (red) with different fatty acid-like moieties at the 1'-position (blue).

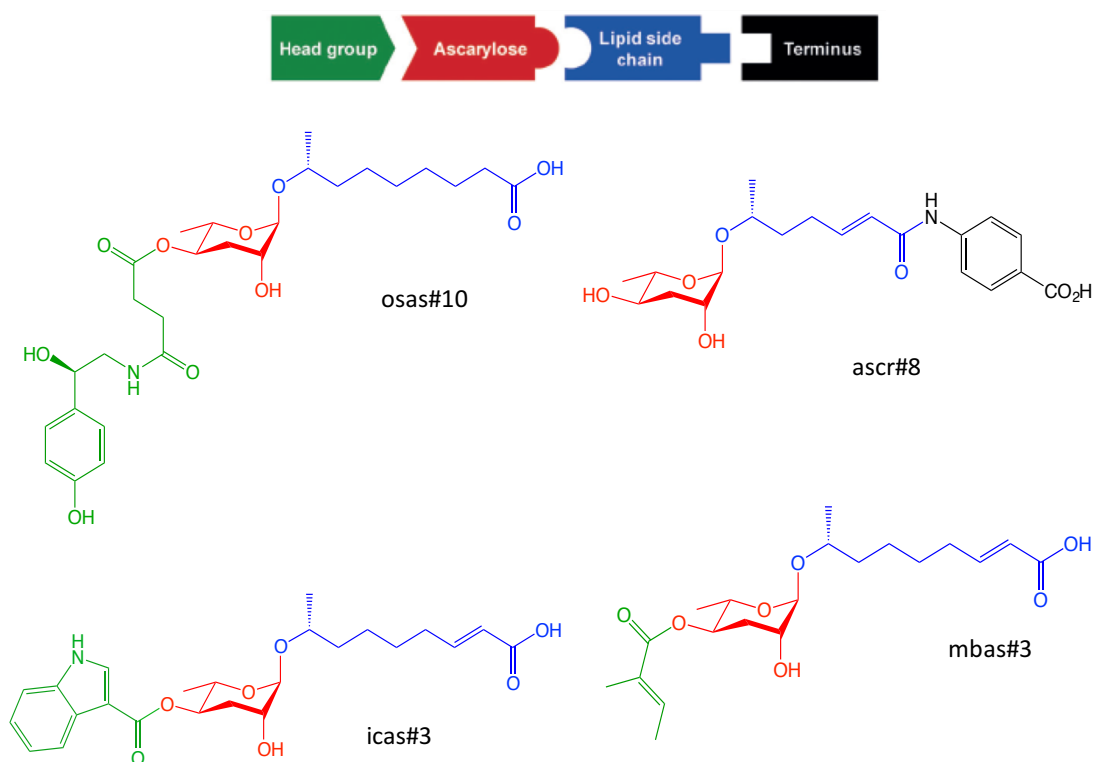


**Figure 3.2: Modular Ascarioside Structures.** Modular ascariosides consisting of a simple ascarioside core (red) with a head (green) or terminal (black) group derived from neurotransmitter (osas#10), amino acid (icas#3), fatty-acid (mbas#3), or folate (ascr#8) metabolic pathways.

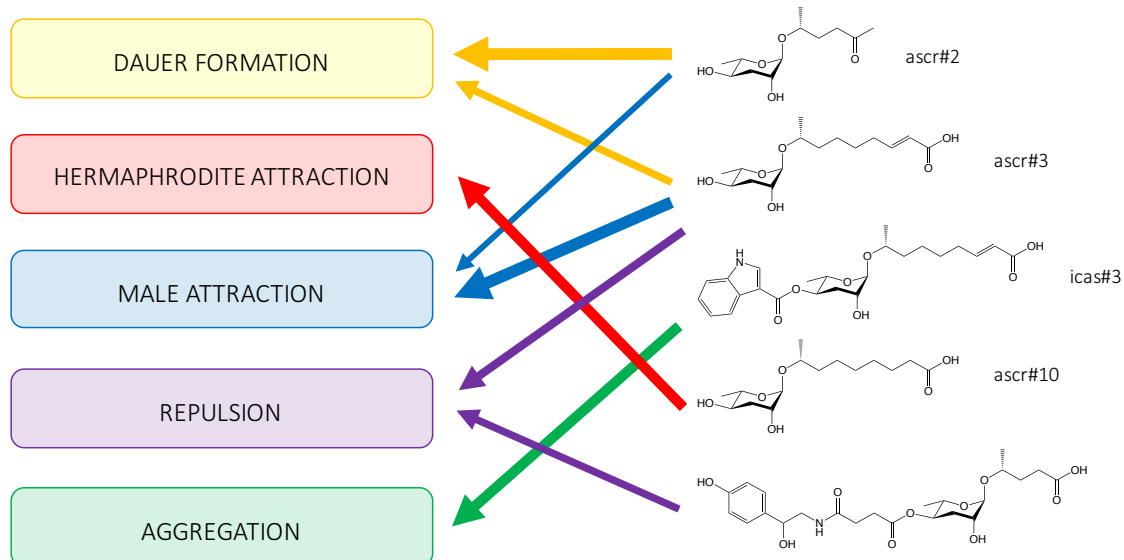


**Figure 3.3: Ascaroside Structure Determines Biological Function.** Although ascr#3 is a major component of dauer pheromone and known to attract male *C. elegans* worms, ascr#10, which has a carbon chain of similar length, but lacks a site of unsaturation, is a hermaphrodite attractant. Furthermore, when ascr#3 is modified with an indole-3-carbonyl at the 4'-position, icas#3, an aggregation pheromone, is formed. Small structural differences amongst ascarosides thus result in large differences between behaviors demonstrated by the worm. Width of arrows represent the relative potency of the ascaroside in each specific behavior.

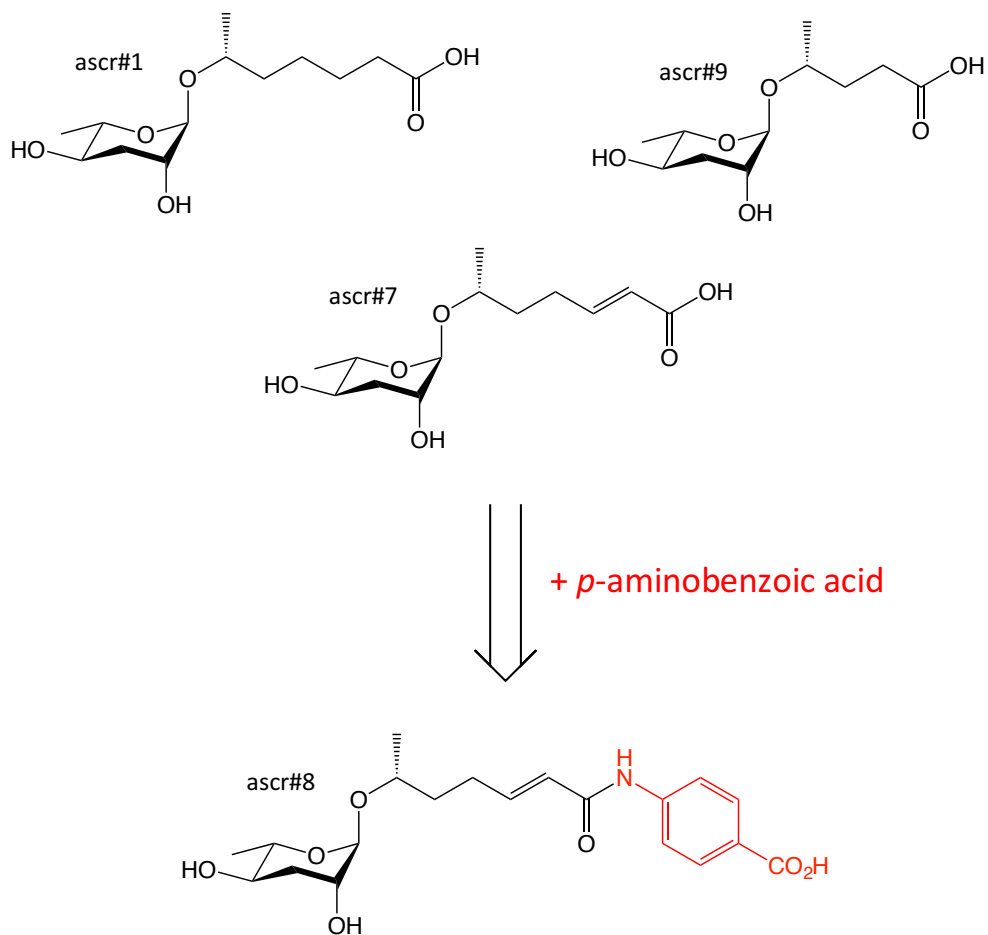


**Figure 3.4: Specificity in Ascaroside Modification.** A *p*-aminobenzoic acid group preferentially attaches to the terminal end of the lipid side chain of ascr#7 to form its derivative ascr#8, despite the fact that ascr#1 and ascr#9, which contain lipid side chains of similar length and level of saturation, respectively, are more abundantly produced.

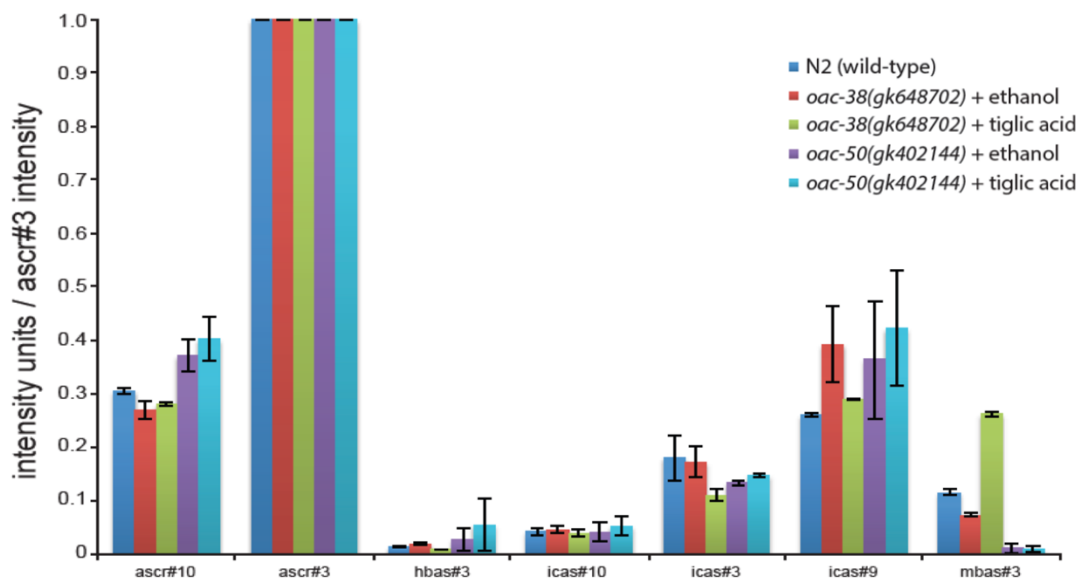


**Figure 3.5: Tiglic Acid Feeding Assay with *oac* Mutants.** Upon the addition of tiglic acid to worm cultures, *mbas#3* production was rescued in the *oac-38(gk648702)* mutant, but not the *oac-50(gk402144)* mutant. Averages and standard deviations were calculated from at least two biological replicates.

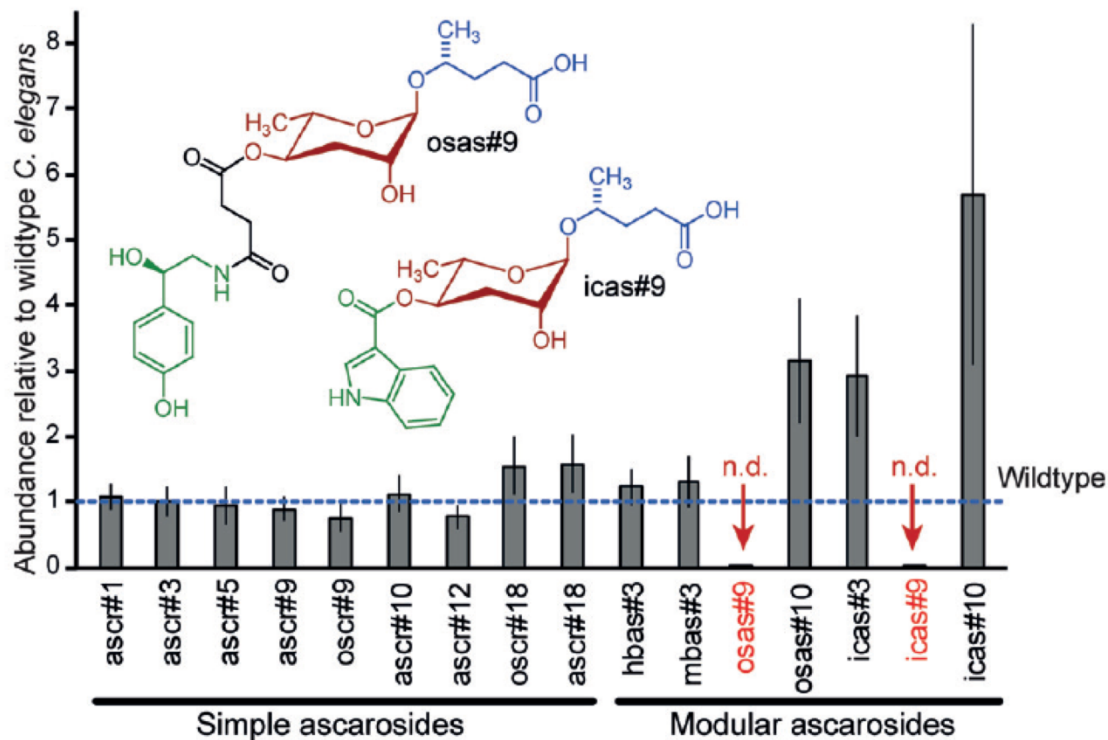


**Figure 3.6: The Mutant *acs-7(tm6781)* Lacks *ascr#9* Derivatives.** A comparison of ascaroside abundance in *acs-7(tm6781)* mutants normalized to ascaroside levels produced by wild type *C. elegans* as determined by HPLC-MS analysis. The presence of *icas#9* and *osas#9* were not detected (n.d.). (Figure from Panda *et al.*<sup>20</sup>)

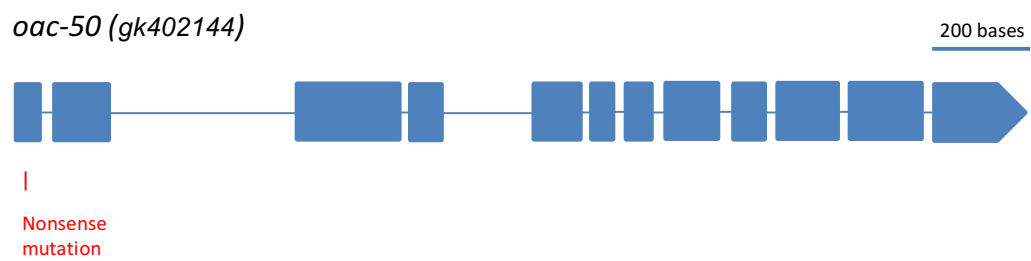


**Figure 3.7: The *oac-50(gk402144)* Mutant.** The Million Mutation strain VC20784 contained 219 mutations including the *oac-50(gk402144)* allele which contained a nonsense mutation in the first exon of the gene.

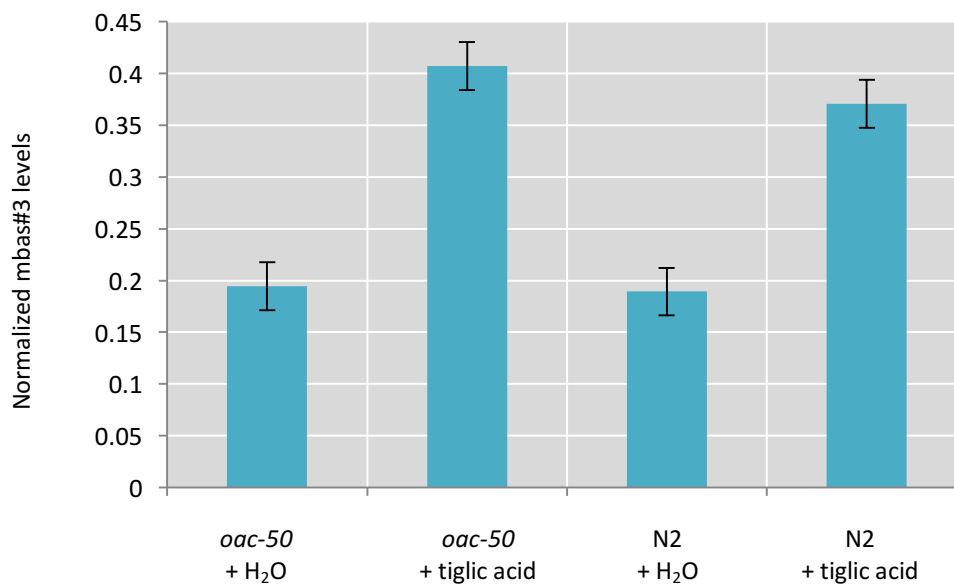


**Figure 3.8: Feeding Tiglic Acid to an Outcrossed *oac-50(-)* Mutant.** When fed tiglic acid or ethanol, the outcrossed *oac-50* mutant produced mbas#3 levels similar to N2. The levels of mbas#3 are normalized to ascr#3 levels. Error bars represent the standard deviation between three biological replicates.

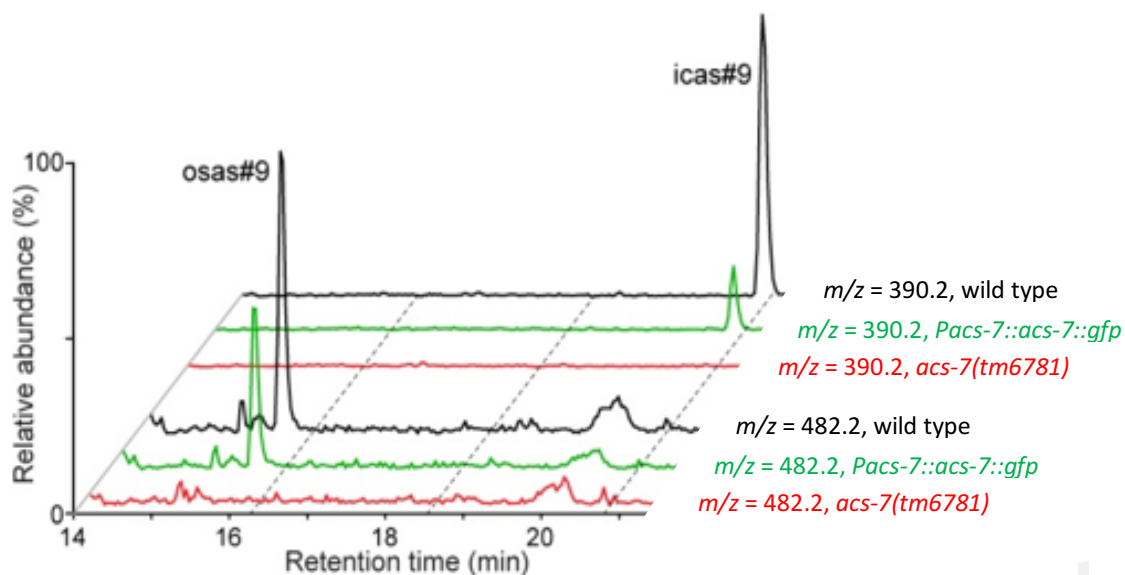


**Figure 3.9: ACS-7::GFP Rescue Restores *ascr#9* Derivatives.** HPLC-MS (ESI-) ion chromatograms for *icas#9* and *osas#9* demonstrate rescue of *icas#9* and *osas#9* production in *Pacs-7::acs-7::gfp* transgenic worms (green) compared to the *acs-7(tm6781)* loss-of-function mutant (red). Wild type N2 worms (black) produce both *ascr#9* derivatives. (Modified figure from Panda *et al.*<sup>20</sup>)

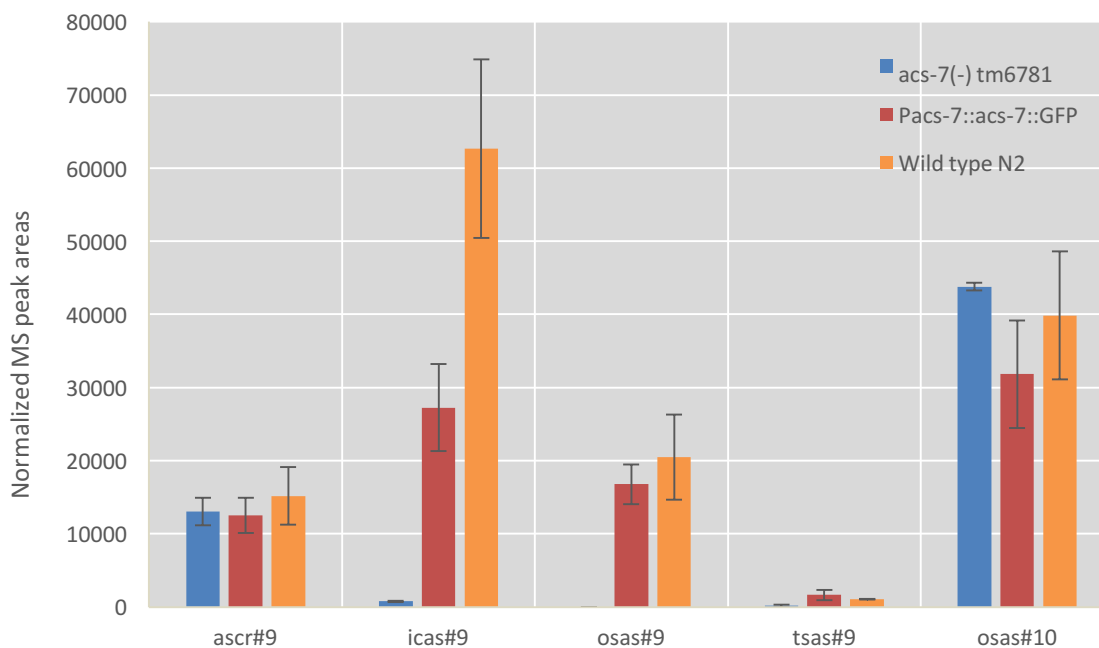


**Figure 3.10: Rescuing Production of *ascr#9* Derivatives.** As determined by HPLC-MS analysis of liquid worm culture supernatant, the production of *icas#9*, *tsas#9*, and *osas#9* is restored in worms expressing an ACS-7::GFP fusion protein. The levels of *ascr#9* remain consistent in all three worm strains. MS peaks are normalized to worm pellet mass. Error bars represent the standard deviation between two biological replicates.

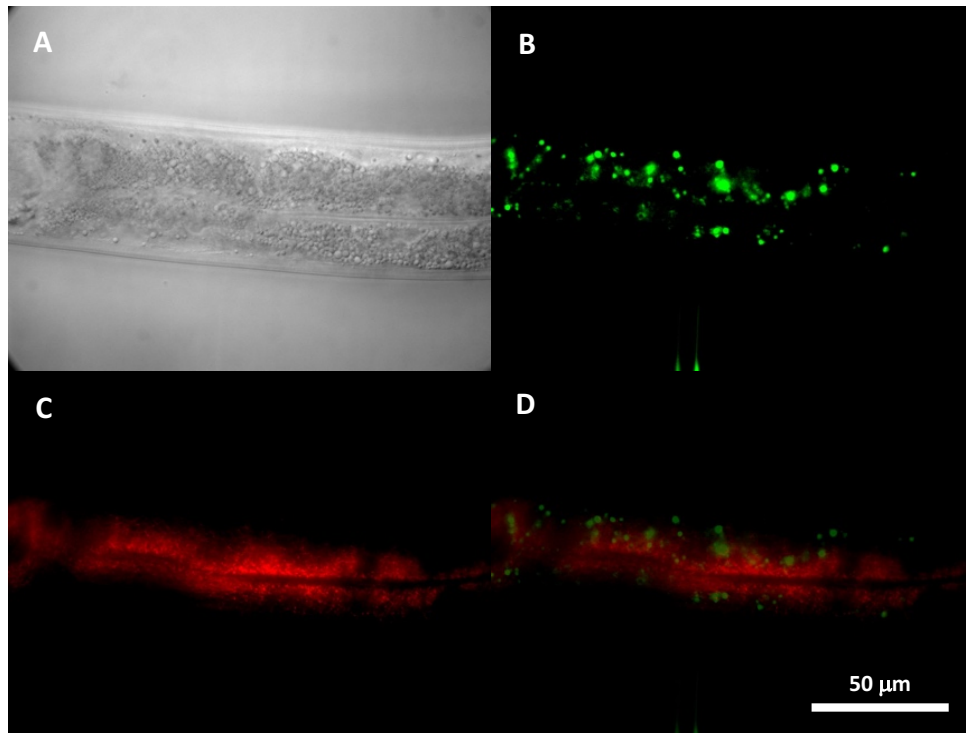


**Figure 3.11: ACS-7::GFP Does Not Localize to the Peroxisomes.** A) A DIC image of the midsection of a young adult worm expressing an ACS-7::GFP fusion protein under the *acs-7* promoter, an mCherry peroxisomal marker, and an *unc-119(+)* rescue construct within an *unc-119(-)* mutant background. B) ACS-7::GFP expression is localized to punctate organelles within the intestine. C) mCherry fluorescent protein with a peroxisomal tag is expressed under the *vha-6* intestinal promoter. D) Overlay of (B) and (C) reveal that ACS-7::GFP does not colocalize with the peroxisomal mCherry marker.

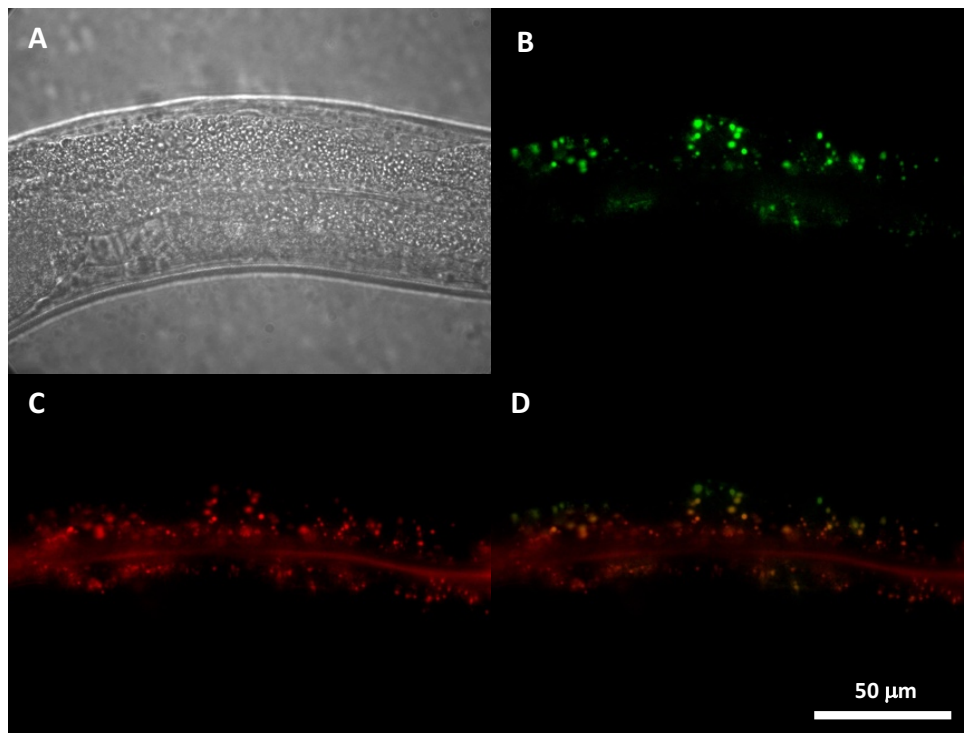


**Figure 3.12: ACS-7::GFP Localizes to the LROs.** A) A DIC image of the midsection of a young adult worm expressing ACS-7::GFP under the native *acs-7* promoter. B) ACS-7::GFP localizes to punctate organelles within the intestine. C) Staining of LROs with LysoTracker Red. D) Overlay of (B) and (C) reveal that ACS-7::GFP localizes to the LROs.

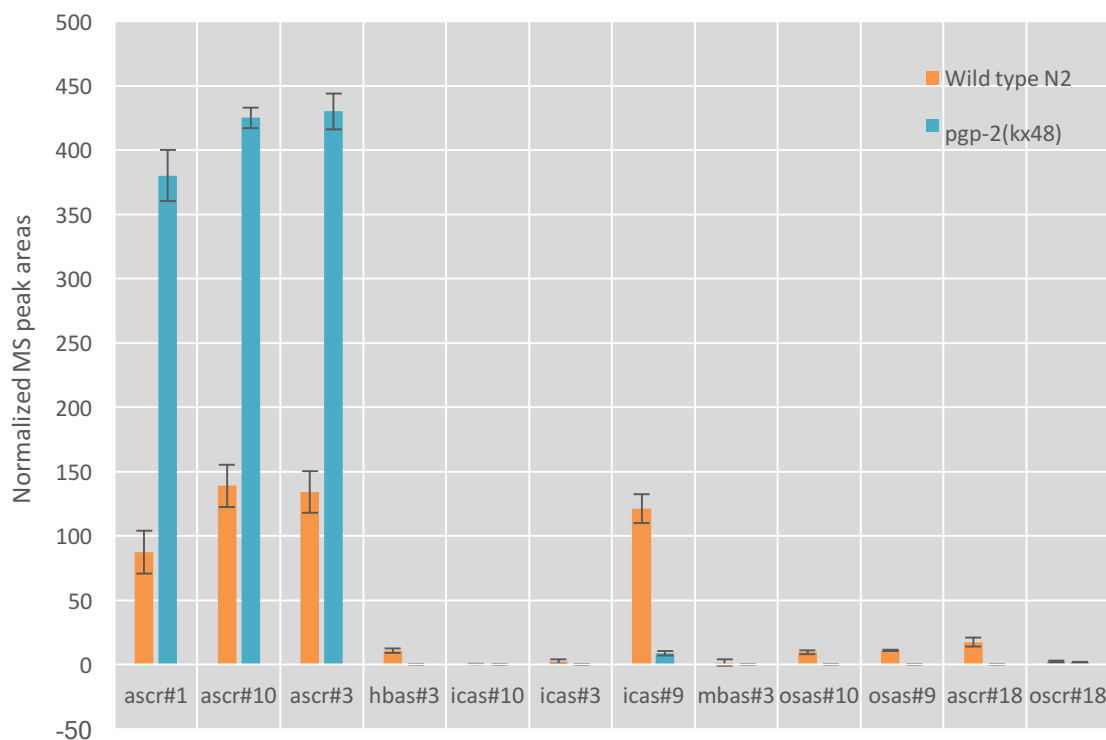


**Figure 3.13: LRO Mutants Do Not Produce 4'-Modified Ascarosides.** The gene *pgp-2* is a member of the ABC transporter family. Mutants with a loss-of-function in *pgp-2* are unable to form gut granules in the intestine. HPLC-MS analyses reveal that *pgp-2(kx48)* mutant worms do not make appreciable quantities of ascarosides modified at the 4'-position. Error bars represent the standard deviation between biological replicates.

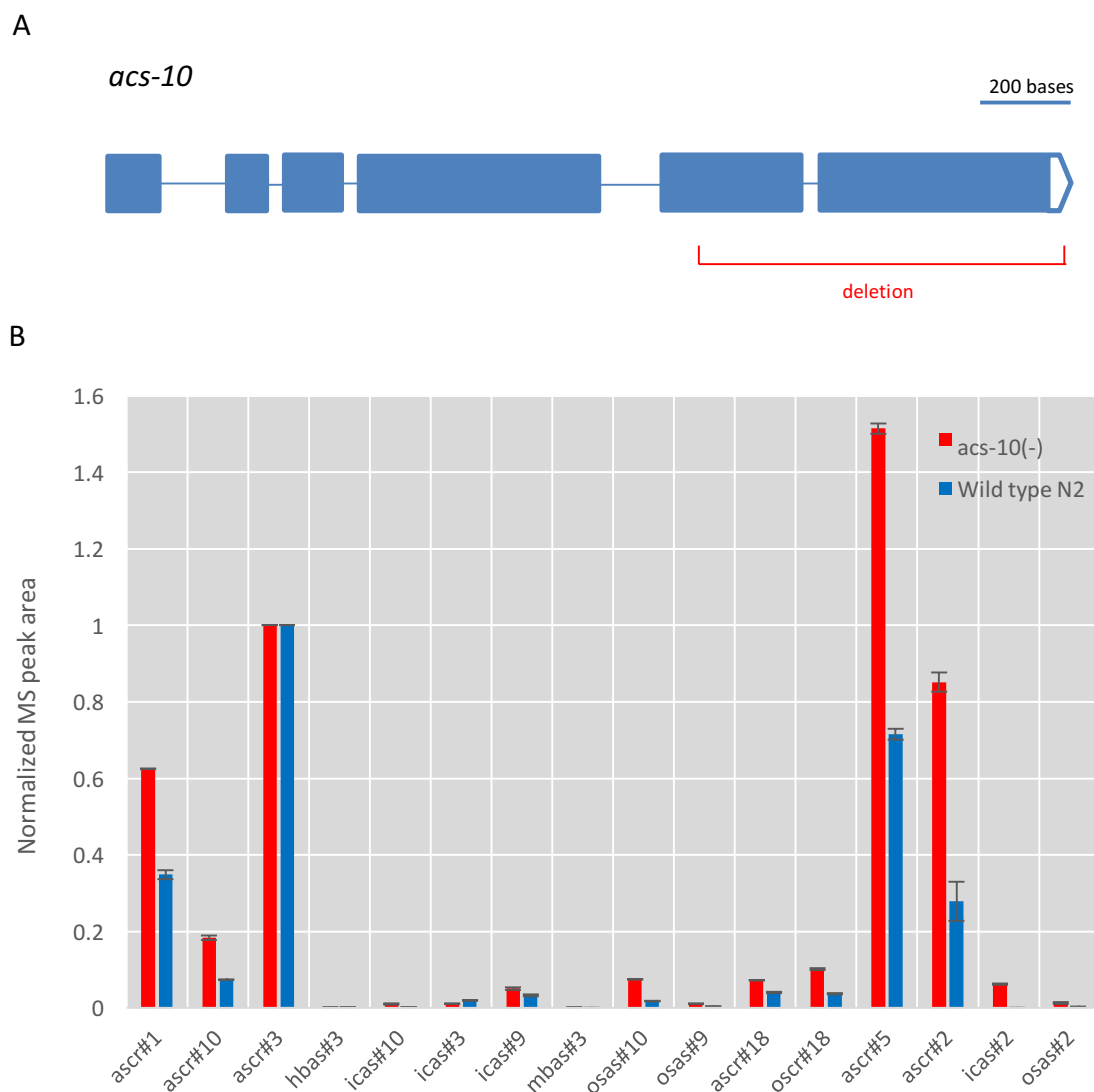


**Figure 3.14: The *acs-10* Gene Does Not Play a Role in 4'-Modification.** A) Schematic of the 1182 base pair deletion spanning the last two exons and part of the 3'UTR region of the *acs-10* gene. B) HPLC-MS analysis of an *acs-10* mutant metabolome reveals no significant difference in ascaroside production compared to a wild type control. Peak areas from HPLC-MS chromatogram are normalized to ascr#3 levels. Data represents two biological replicates for each strain. Error bars represent the standard deviation between replicates.

### 3.6 Tables

**Table 3.1** *O*-acyltransferase mutant strains screened by HPLC-MS for ascaroside biosynthetic defects.

Gene	Strain	Source	Initial Screen Result
<i>ndg-4(sa529)</i>	JT529	Deletion mutant from CGC	Wild type
<i>nrf-6(sa525)</i>	JT525	Deletion mutant from CGC	Wild type
<i>oac-11(gk531381)</i>	VC40243	Million Mutation Project	Wild type
<i>oac-14(gk519224)</i>	VC40217	Million Mutation Project	Wild type
<i>oac-14(gk786954)</i>	VC40738	Million Mutation Project	Reduced mbas#3
<i>oac-16(gk914989)</i>	VC40988	Million Mutation Project	Wild type
<i>oac-20(gk256989)</i>	VC10128	Million Mutation Project	Wild type
<i>oac-23(gk445127)</i>	VC30240	Million Mutation Project	Wild type
<i>oac-27(gk694121)</i>	VC40561	Million Mutation Project	Wild type
<i>oac-29(gk646323)</i>	VC40455	Million Mutation Project	Reduced mbas#3
<i>oac-3(gk252641)</i>	VC20209	Million Mutation Project	Wild type
<i>oac-34(gk652397)</i>	VC40469	Million Mutation Project	Wild type
<i>oac-35(gk883174)</i>	VC40922	Million Mutation Project	Wild type
<i>oac-36(gk124636)</i>	VC20551	Million Mutation Project	Wild type
<i>oac-38(gk648702)</i>	VC40461	Million Mutation Project	Reduced mbas#3
<i>oac-39(gk145)</i>	VC247	Deletion mutant from CGC	Wild type
<i>oac-4(gk363869)</i>	VC20633	Million Mutation Project	Wild type
<i>oac-40(gk242459)</i>	VC20235	Million Mutation Project	Wild type
<i>oac-41(gk242464)</i>	VC20211	Million Mutation Project	Wild type
<i>oac-41(gk766757)</i>	VC40696	Million Mutation Project	Wild type
<i>oac-42(WBVar00026105)</i>	CB4856	Wild isolate	Wild type
<i>oac-43(gk737013)</i>	VC40638	Million Mutation Project	Wild type
<i>oac-49(gk264009)</i>	VC20294	Million Mutation Project	Wild type
<i>oac-5(gk398429)</i>	VC30020	Million Mutation Project	Wild type
<i>oac-50(gk402144)</i>	VC20784	Million Mutation Project	Reduced mbas#3
<i>oac-51(gk533438)</i>	VC40246	Million Mutation Project	Wild type
<i>oac-54(gk684785)</i>	VC40540	Million Mutation Project	Wild type
<i>oac-6(gk735518)</i>	VC40635	Million Mutation Project	Wild type
<i>oac-7(gk586689)</i>	VC40345	Million Mutation Project	Wild type
<i>oac-8(gk211086)</i>	VC20046	Million Mutation Project	Wild type
<i>oac-9(gk662463)</i>	VC40490	Million Mutation Project	Wild type

## 3.7 Materials and Methods

### 3.7.1 Maintenance of *C. elegans* Strains

Wild type (N2, Bristol), GH10 *glo-1(zu437)*, RB811 *glo-4(ok623)*, RB662 *apb-3(ok429)*, FX06781 *acs-7(tm6781)*, GH378 *pgp-2(kx48)*, and PS7396 *acs-7(tm6781);syIs459[Pacs-7::ACS-7::GFP::unc-54 3'UTR, 10 ng/μL; Pmyo-2::dsRed, 5 ng/μL]* strains were maintained on NGM plates with *Escherichia coli* OP50 as the food source at room temperature as originally described, unless otherwise stated.<sup>25</sup> Some strains were obtained from the Caenorhabditis Genetics Center (CGC, USA) and the National BioResource Project (NBRP, Japan). GH10 was provided by D. Gems and *daf-22(ok693)* was a gift from H.Y. Mak. A list of *O*-acyltransferase mutants can be seen in Table 3.1. FCS10 *acs-7(tm6781)* was obtained by outcrossing FX06781 10x against GE1710 *rol-6(e187);unc-4(e120)*. FCS10 was used for all experiments reported for *acs-7(tm6781)*.

### 3.7.2 Molecular Biology

Plasmids were constructed using standard molecular cloning techniques and Gibson Assembly (New England BioLabs, USA). To construct the *Pacs-7::ACS-7::gfp* rescue construct, pAEA10, the native *acs-7* promoter was PCR amplified from genomic DNA using 5' primer oAA065 and 3' primer oAA066 (see Appendix C) and inserted between FseI and AscI sites of pPH92, a gift from the Bargmann Lab. The cDNA sequence of the *acs-7* gene was amplified from plasmid pU57 provided by H. H. Le using 5' primer oAA067 and 3' primer oAA068 and inserted between AgeI and NheI sites upstream of the GFP coding region.

To assemble the *Pvha-6::mCherrySKL* peroxisomal marker construct, pAEA15, the mCherry coding sequence was PCR amplified from pPH93, a gift from the Bargmann Lab, using the 5' primer oAA093 and the 3' primer oAA094 which contains a nine nucleotide sequence encoding the SKL peroxisomal tag.<sup>26</sup> The fragment was then inserted between XmaI and KpnI sites of plasmid HYM433, kindly donated by H.Y. Mak.<sup>15</sup> The mCherrySKL sequence was placed downstream of the *vha-6* promoter and upstream of the 3'UTR region of the *unc-54* gene.

### 3.7.3 Transformation

For *acs-7* rescue experiments, a DNA mixture of 10 ng/μL of pAEA10, 5 ng/μL of a *Pmyo-2::dsRed* co-injection marker, and 85 ng/μL of 1 kb ladder (New England BioLabs, USA) were injected into adult gonads of *acs-7(tm6781)* hermaphrodites using standard microinjection techniques.<sup>27</sup> Extrachromosomal arrays were then integrated into the genome via X-ray irradiation and integrants were outcrossed ten times with wild type strain N2 to create strain PS7396. For *acs-7* localization experiments, a DNA mixture of 30 ng/μL pAEA10 rescue construct, 30 ng/μL pAEA15, and 30 ng/μL *unc-119(+)* rescue construct were injected into adult gonads of PS6018 *unc-119(ed4)* hermaphrodites.<sup>28</sup>

### 3.7.4 CRISPR Knockout of *acs-10*

An *acs-10* knockout mutant was created using the CRISPR/Cas9 genome editing system as previously described by Arribere *et al.*<sup>29</sup> Guide RNA (gRNA) templates were generated for four different binding sites within the *acs-10* gene by ligating corresponding

5' and 3' primers at the BsaI restriction site within the pRB1017 gRNA expression cassette vector provided by the Fire Lab (Stanford). For binding site 1, pAEA5 was generated using 5' primer oAA001 and 3' primer oAA002. For binding site 2, pAEA6 was generated using 5' primer oAA003 and 3' primer oAA004. For binding site 3, pAEA7 was generated using 5' primer oAA005 and 3' primer oAA006. For binding site 4, pAEA8 was created using 5' primer oAA007 and 3' primer oAA008.

A mixture of gRNA templates pAEA5, pAEA6, pAEA7, and pAEA8 (25 ng/ $\mu$ L each), plasmid pJA58 containing a gRNA directed at the gene *dpy-10* (25 ng/ $\mu$ L), a plasmid encoding *Peft-3::cas9* (Addgene #46168, 50 ng/ $\mu$ L), and the roller *dpy-10* repair oligo oHW36f (500 nM/ $\mu$ L) was injected into the adult gonad of wild type N2 hermaphrodite worms. Isolated injected animals were grown at room temperature and F1 progeny of the roller phenotype were selected and individually plated. After three days, plates were screened for F2 progeny displaying a roller phenotype, signaling likely co-conversion CRISPR positive plates.

Worms from each potentially CRISPR positive plate were lysed in 2.5  $\mu$ L of worm lysis buffer supplemented with 0.5 mg/mL Proteinase K and genotyped by PCR using primer oAA009 and primer oAA010. PCR products were analyzed by gel electrophoresis and bands of shorter length than the predicted product were excised and sent for DNA sequencing to confirm a deletion. F2 progeny from those plates were individually plated to isolate a homozygote of the deletion mutant.

### 3.7.5 *Nematode Culture and Extraction*

Worms of mixed stages were washed from a 10 cm NGM agar plate seeded with *E. coli* OP50 into 25 mL of S-complete medium. Cultures were grown for 7 days at 22°C while shaking at 220 rpm for 7 days. Cultures were fed *E. coli* OP50 on days 1, 3, and 5. On day 7, cultures were centrifuged and worm pellets and supernatant were frozen separately, lyophilized, and extracted with 35 mL of 95% ethanol at room temperature for 12 hours. The extracts were dried *in vacuo*, resuspended in 200 µL of methanol and analyzed by HPLC-MS. All cultures were grown in at least two biological replicates.

### 3.7.6 *Mass Spectrometric Analysis*

High resolution HPLC-MS analysis was performed on a Dionex 3000 UPLC coupled with a Thermo Q Exactive high-resolution mass spectrometer as described previously.<sup>30</sup> Metabolites were separated using a water-acetonitrile gradient on an Agilent Zorbax Eclipse XDB-C18 column (150 mm x 2.1 mm, particle size 1.8 µm) maintained at 40°C. Solvent A: 0.1% formic acid in water; Solvent B: 0.1% formic acid in acetonitrile. A/B gradient started at 5% B for 5 minutes after injection and increased linearly to 100% B at 12.5 minutes. Most ascarosides were detected as [M-H]<sup>-</sup> ions or [M-Cl]<sup>-</sup> adducts in the negative ionization mode (spray voltage 3 kV) and confirmed based on their high-resolution masses (<1 ppm), fragmentation spectra, and comparison of retention times with those of synthetic standards.

Low resolution HPLC-MS was performed using the Agilent 1100 Series HPLC system equipped with an Agilent Eclipse XDB-C18 column (250 mm x 9.4 mm, particle size 5 µm), connected to a Quattro II or Quattro Ultima mass spectrometer.<sup>13</sup> Solvent A: 0.1%

acetic acid in water; Solvent B: 0.1% acetic acid in acetonitrile. A/B gradient started at 5% B for 5 minutes after injection and increased linearly to 100% B over a period of 40 minutes. Ascarosides were detected as  $[M-H]^-$  ions in the negative ionization mode (spray voltage 3.5 kV, cone voltage -40 V) and confirmed based on comparison of retention times with those of synthetic standards.

### 3.7.7 Microscopy

LysoTracker staining was performed as previously reported by Hermann *et al.*<sup>23</sup> A 1 mM stock solution of LysoTracker Red (Thermo Fisher, USA) was diluted to 2  $\mu$ M in M9 buffer, of which 0.5 mL was added to an NGM plate seeded with *E. coli* OP50 and incubated overnight at 20°C. Worms were added to the plate and grown overnight in the dark.

For imaging, worms were removed from the plate and transferred onto a glass slide with a thin 2% agarose pad containing 5 mM levamisole. Microscopic analysis was performed with a wide-field epifluorescence Zeiss Axioskop microscope equipped with a 100x oil objective. Images were taken with a Hamamatsu ORCA-ER digital camera using Openlab imaging software.

### 3.8 References

1. Jeong, P. Y.; Jung, M.; Yim, Y. H.; Kim, H.; Park, M.; Hong, E.; Lee, W.; Kim, Y. H.; Kim, K.; Paik, Y. K., Chemical structure and biological activity of the *Caenorhabditis elegans* dauer-inducing pheromone. *Nature* **2005**, *433* (7025), 541-5.
2. Butcher, R. A.; Fujita, M.; Schroeder, F. C.; Clardy, J., Small-molecule pheromones that control dauer development in *Caenorhabditis elegans*. *Nat Chem Biol* **2007**, *3* (7), 420-2.
3. Butcher, R. A.; Ragains, J. R.; Kim, E.; Clardy, J., A potent dauer pheromone component in *Caenorhabditis elegans* that acts synergistically with other components. *Proc Natl Acad Sci U S A* **2008**, *105* (38), 14288-92.
4. Srinivasan, J.; Kaplan, F.; Ajredini, R.; Zachariah, C.; Alborn, H. T.; Teal, P. E.; Malik, R. U.; Edison, A. S.; Sternberg, P. W.; Schroeder, F. C., A blend of small molecules regulates both mating and development in *Caenorhabditis elegans*. *Nature* **2008**, *454* (7208), 1115-8.
5. Pungaliya, C.; Srinivasan, J.; Fox, B. W.; Malik, R. U.; Ludewig, A. H.; Sternberg, P. W.; Schroeder, F. C., A shortcut to identifying small molecule signals that regulate behavior and development in *Caenorhabditis elegans*. *Proc Natl Acad Sci U S A* **2009**, *106* (19), 7708-13.
6. Ren, P.; Lim, C. S.; Johnsen, R.; Albert, P. S.; Pilgrim, D.; Riddle, D. L., Control of *C. elegans* larval development by neuronal expression of a TGF-beta homolog. *Science* **1996**, *274* (5291), 1389-91.

7. Kimura, K. D.; Tissenbaum, H. A.; Liu, Y.; Ruvkun, G., *daf-2*, an insulin receptor-like gene that regulates longevity and diapause in *Caenorhabditis elegans*. *Science* **1997**, *277* (5328), 942-6.
8. Srinivasan, J.; von Reuss, S. H.; Bose, N.; Zaslaver, A.; Mahanti, P.; Ho, M. C.; O'Doherty, O. G.; Edison, A. S.; Sternberg, P. W.; Schroeder, F. C., A modular library of small molecule signals regulates social behaviors in *Caenorhabditis elegans*. *PLoS Biol* **2012**, *10* (1), e1001237.
9. Artyukhin, A. B.; Yim, J. J.; Srinivasan, J.; Izrayelit, Y.; Bose, N.; von Reuss, S. H.; Jo, Y.; Jordan, J. M.; Baugh, L. R.; Cheong, M.; Sternberg, P. W.; Avery, L.; Schroeder, F. C., Succinylated octopamine ascarosides and a new pathway of biogenic amine metabolism in *Caenorhabditis elegans*. *J Biol Chem* **2013**, *288* (26), 18778-83.
10. Walsh, C. T., The chemical versatility of natural-product assembly lines. *Acc Chem Res* **2008**, *41* (1), 4-10.
11. Meier, J. L.; Burkart, M. D., The chemical biology of modular biosynthetic enzymes. *Chem Soc Rev* **2009**, *38* (7), 2012-45.
12. Edison, A. S., *Caenorhabditis elegans* pheromones regulate multiple complex behaviors. *Curr Opin Neurobiol* **2009**, *19* (4), 378-88.
13. von Reuss, S. H.; Bose, N.; Srinivasan, J.; Yim, J. J.; Judkins, J. C.; Sternberg, P. W.; Schroeder, F. C., Comparative metabolomics reveals biogenesis of ascarosides, a modular library of small-molecule signals in *C. elegans*. *J Am Chem Soc* **2012**, *134* (3), 1817-24.

14. Izrayelit, Y.; Srinivasan, J.; Campbell, S. L.; Jo, Y.; von Reuss, S. H.; Genoff, M. C.; Sternberg, P. W.; Schroeder, F. C., Targeted metabolomics reveals a male pheromone and sex-specific ascaroside biosynthesis in *Caenorhabditis elegans*. *ACS Chem Biol* **2012**, *7* (8), 1321-5.
15. Butcher, R. A.; Ragains, J. R.; Li, W.; Ruvkun, G.; Clardy, J.; Mak, H. Y., Biosynthesis of the *Caenorhabditis elegans* dauer pheromone. *Proc Natl Acad Sci U S A* **2009**, *106* (6), 1875-9.
16. Izrayelit, Y.; Robinette, S. L.; Bose, N.; von Reuss, S. H.; Schroeder, F. C., 2D NMR-based metabolomics uncovers interactions between conserved biochemical pathways in the model organism *Caenorhabditis elegans*. *ACS Chem Biol* **2013**, *8* (2), 314-9.
17. Zhang, X.; Feng, L.; Chinta, S.; Singh, P.; Wang, Y.; Nunnery, J. K.; Butcher, R. A., Acyl-CoA oxidase complexes control the chemical message produced by *Caenorhabditis elegans*. *Proc Natl Acad Sci U S A* **2015**, *112* (13), 3955-60.
18. Moerman, D. G., Strasbourger, P., Thompson, O., Adair, R., Au, V., Chaudhry, I., Edgley, M., Ewing, B., Fernando, L., Flibotte, S., High, A., Hillier, L., Hutter, H., Lau, J., Lee, N., Miller, A., Raymant, G., Shendure, J., Taylor, J., Turner, E.H., Waterston, R. , The million mutation project a genetic resource for *C. elegans*. *Worm Breeder's Gazette* **2012**, *19.2* (3).
19. Gould, S. J.; Keller, G. A.; Hosken, N.; Wilkinson, J.; Subramani, S., A conserved tripeptide sorts proteins to peroxisomes. *J Cell Biol* **1989**, *108* (5), 1657-64.

20. Panda, O.; Akagi, A. E.; Artyukhin, A. B.; Judkins, J. C.; Le, H. H.; Mahanti, P.; Cohen, S. M.; Sternberg, P. W.; Schroeder, F. C., Biosynthesis of Modular Ascarosides in *C. elegans*. *Angew Chem Int Ed Engl* **2017**, *56* (17), 4729-4733.
21. Chitwood, B. G.; Chitwood, M. B. H., *Introduction to nematology*. Consolidated ed.; University Park Press: Baltimore,, 1974; p 334 p.
22. Laufer, J. S.; Bazzicalupo, P.; Wood, W. B., Segregation of developmental potential in early embryos of *Caenorhabditis elegans*. *Cell* **1980**, *19* (3), 569-77.
23. Hermann, G. J.; Schroeder, L. K.; Hieb, C. A.; Kershner, A. M.; Rabbitts, B. M.; Fonarev, P.; Grant, B. D.; Priess, J. R., Genetic analysis of lysosomal trafficking in *Caenorhabditis elegans*. *Mol Biol Cell* **2005**, *16* (7), 3273-88.
24. Mony, V. K.; Benjamin, S.; O'Rourke, E. J., A lysosome-centered view of nutrient homeostasis. *Autophagy* **2016**, *12* (4), 619-31.
25. Brenner, S., The genetics of *Caenorhabditis elegans*. *Genetics* **1974**, *77* (1), 71-94.
26. Thieringer, H.; Moellers, B.; Dodt, G.; Kunau, W. H.; Driscoll, M., Modeling human peroxisome biogenesis disorders in the nematode *Caenorhabditis elegans*. *J Cell Sci* **2003**, *116* (Pt 9), 1797-804.
27. Mello, C. C.; Kramer, J. M.; Stinchcomb, D.; Ambros, V., Efficient gene transfer in *C.elegans*: extrachromosomal maintenance and integration of transforming sequences. *EMBO J* **1991**, *10* (12), 3959-70.
28. Maduro, M.; Pilgrim, D., Identification and cloning of *unc-119*, a gene expressed in the *Caenorhabditis elegans* nervous system. *Genetics* **1995**, *141* (3), 977-88.

29. Arribere, J. A.; Bell, R. T.; Fu, B. X.; Artiles, K. L.; Hartman, P. S.; Fire, A. Z., Efficient marker-free recovery of custom genetic modifications with CRISPR/Cas9 in *Caenorhabditis elegans*. *Genetics* **2014**, *198* (3), 837-46.
30. Markov, G. V.; Meyer, J. M.; Panda, O.; Artyukhin, A. B.; Claassen, M.; Witte, H.; Schroeder, F. C.; Sommer, R. J., Functional Conservation and Divergence of daf-22 Paralogs in *Pristionchus pacificus* Dauer Development. *Mol Biol Evol* **2016**, *33* (10), 2506-14.

## MITOCHONDRIAL $\beta$ -OXIDATION OF THE ASCAROSIDE SIDE CHAIN

### **A.1 Introduction**

Whereas the sequence and significance of peroxisomal  $\beta$ -oxidation is well characterized and understood, the bulk of ascaroside biosynthesis including precursor origins and participating enzymes is largely unknown.<sup>1</sup> Due to the fact that metabolites derived from tryptophan metabolism are incorporated into the biogenesis of indolated ascarosides, and other ascaroside structures suggest the possible incorporation of head groups derived from isoleucine and tyrosine degradation, we hypothesized that ascaroside biosynthesis may occur in the mitochondria, where amino acid catabolism occurs.<sup>2-3</sup>

Furthermore, although the digestion and truncation of long-chained lipids is a peroxisomal process, medium- and short-chained lipids are degraded in the mitochondria.<sup>4</sup> As it was previously observed by von Reuss *et al* that long-chained ascarosides undergo  $\beta$ -oxidation in the peroxisomes, we questioned whether ascarosides bearing shorter lipid side chains may be digested in the mitochondria in a similar fashion. In order to do so, we examined the ascaroside profiles produced by strains containing mutations in genes homologous to those involved in mammalian mitochondrial  $\beta$ -oxidation pathways. In this screen, we examined strains with loss-of-function mutations in *acdH-1* and *acdH-13*, two mitochondrial acyl-CoA dehydrogenases paralogous to the peroxisomal gene *acox-1*, and the enoyl-CoA-hydratase *ech-2*, a paralog of the peroxisomal gene *maoc-1*.

## A.2 Results and Discussion

Compared to wild type N2, the ascaroside profile of the *ech-2* mutant was largely similar, demonstrating no major changes in ascaroside biosynthesis (Figure A.1). Levels of indolated ascarosides were affected to a larger degree in the *acdH* loss-of-function mutants. For example, the ascaroside profile of *acdH-13(ok3004)* demonstrated elevated levels of hbas and icas ascarosides (Figure A.2). Although HPLC-MS analysis of the mutant excretomes revealed the *acdH-1(ok1514)* mutant ascaroside profile to be largely wild type, a second mutant allele for the same gene *acdH-1(ok1489)* demonstrated greater penetrance and produced elevated levels of hbas and icas ascarosides, to an even larger degree than *acdH-13(ok3004)*. The *acdH-1(ok1514)* allele remains uncurated, but the lower penetrance observed may be the result of a deletion mutation that leaves the active site intact. Levels of hbas#3 produced by *acdH-1(ok1498)* were 12 times larger than wild type and each indolated ascaroside, including icas#3, icas#9, and icas#10, were increased by a factor of 3 to 5.

These results suggest that the *acdH-1* and *acdH-13* genes may be involved in the regulation of icas and hbas ascaroside production despite the precise mechanism remaining unknown. Previous research has shown that ACDH-1 expression depends upon nutritional state with expression upregulated in animals that are well-fed and downregulated in starved animals.<sup>5-7</sup> As such, ACDH-1 has been used as a *C. elegans* dietary sensor.<sup>7</sup> In summary, ACDH-1 may serve as a link between ascaroside production and the nutritional state of the worm. This also indicates that the mitochondria may be involved in regulating ascaroside production as the energetic needs of the worm changes due to food availability.

### A.3 Figures

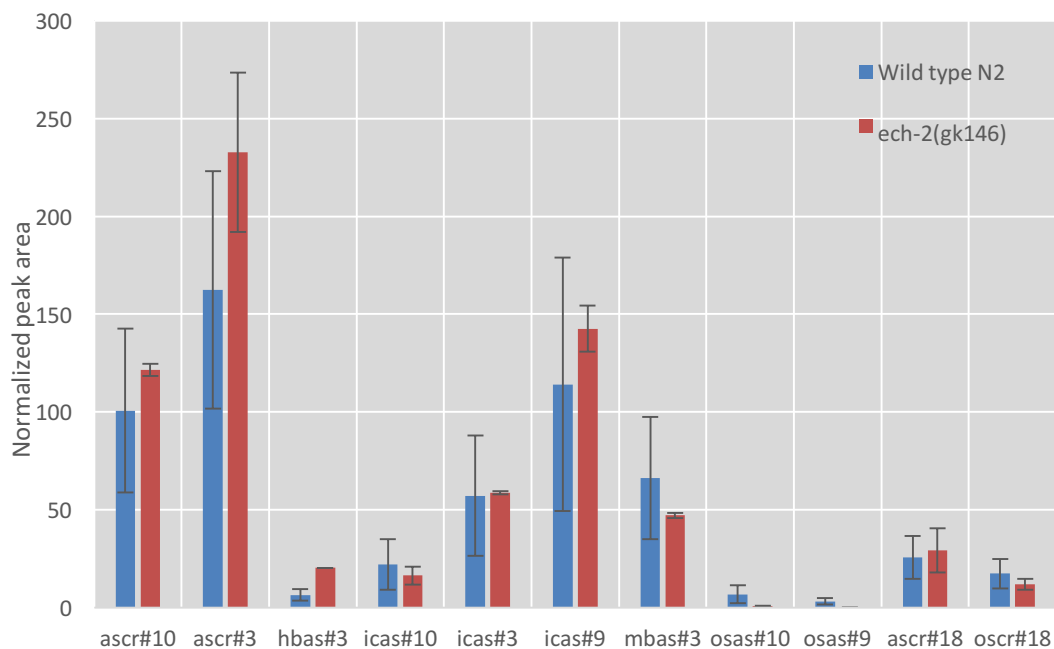


**Figure A.1: Examining the Role of *ech-2*.** The *ech-2* gene encodes a putative mitochondrial enoyl-CoA hydratase that is a paralog of *maoc-1*, the gene that encodes the protein responsible for hydrating the site of  $\alpha,\beta$ -unsaturation during peroxisomal  $\beta$ -oxidation of the ascaroside lipid side chain. Loss of *ech-2* function produces a mostly wild type ascaroside profile. Excretomes were derived from mixed stage cultures. MS peaks are normalized to worm pellet mass. Averages are of two biological replicates.

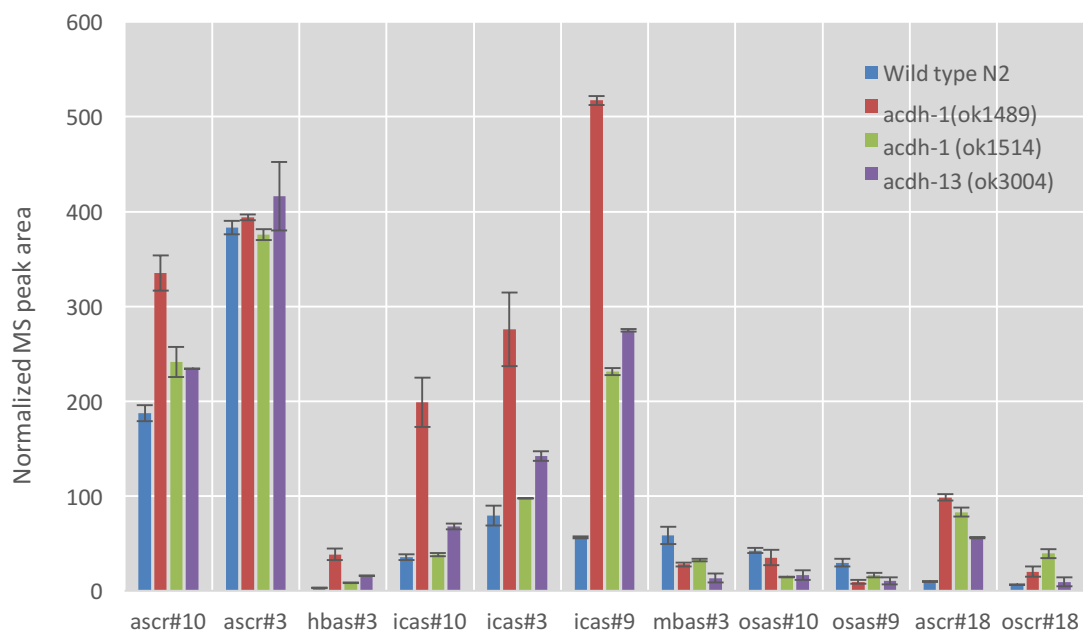


**Figure A.2: Examining the Role of Acyl-CoA Dehydrogenases.** The *acdh* genes are mitochondrial paralogs of *acox-1*, the gene that encodes the protein responsible for the first site of peroxisomal  $\beta$ -oxidation by introducing a site of  $\alpha,\beta$ -unsaturation. Loss of function in *acdh-1* and *acdh-13* genes result in higher levels of hbas and icas ascarosides, with the *acdh-1(ok1489)* allele being more penetrant than the *acdh-1(ok1514)* allele. Excretomes were derived from mixed stage cultures. MS peaks are normalized to worm pellet mass. Averages are of two biological replicates.

## A.4 References

1. von Reuss, S. H.; Bose, N.; Srinivasan, J.; Yim, J. J.; Judkins, J. C.; Sternberg, P. W.; Schroeder, F. C., Comparative metabolomics reveals biogenesis of ascarosides, a modular library of small-molecule signals in *C. elegans*. *J Am Chem Soc* **2012**, *134* (3), 1817-24.
2. Guda, P.; Guda, C.; Subramaniam, S., Reconstruction of pathways associated with amino acid metabolism in human mitochondria. *Genomics Proteomics Bioinformatics* **2007**, *5* (3-4), 166-76.
3. Harper, A. E.; Miller, R. H.; Block, K. P., Branched-chain amino acid metabolism. *Annu Rev Nutr* **1984**, *4*, 409-54.
4. Reddy, J. K.; Hashimoto, T., Peroxisomal beta-oxidation and peroxisome proliferator-activated receptor alpha: an adaptive metabolic system. *Annu Rev Nutr* **2001**, *21*, 193-230.
5. Taubert, S.; Van Gilst, M. R.; Hansen, M.; Yamamoto, K. R., A Mediator subunit, MDT-15, integrates regulation of fatty acid metabolism by NHR-49-dependent and -independent pathways in *C. elegans*. *Genes Dev* **2006**, *20* (9), 1137-49.
6. Van Gilst, M. R.; Hadjivassiliou, H.; Yamamoto, K. R., A *Caenorhabditis elegans* nutrient response system partially dependent on nuclear receptor NHR-49. *Proc Natl Acad Sci U S A* **2005**, *102* (38), 13496-501.
7. MacNeil, L. T.; Watson, E.; Arda, H. E.; Zhu, L. J.; Walhout, A. J., Diet-induced developmental acceleration independent of TOR and insulin in *C. elegans*. *Cell* **2013**, *153* (1), 240-52.

*Appendix B*

## ADDITIONAL MUTANTS SCREENED FOR BIOSYNTHETIC DEFECTS

**B.1 Introduction**

Foundational ascaroside studies have demonstrated or indicated that ascarosides are constructed from metabolites from various primary metabolic pathways. For example, the ascarylose scaffold is a carbohydrate, the lipid side chains are modified by peroxisomal  $\beta$ -oxidation enzymes, and head groups attached to the 4'-position are derived from amino acid catabolism.<sup>1-4</sup> In our initial screens, we prioritized mutants involved in primary metabolic pathways and those homologous to genes involved in the biosynthesis of ascaroside components in other organisms.

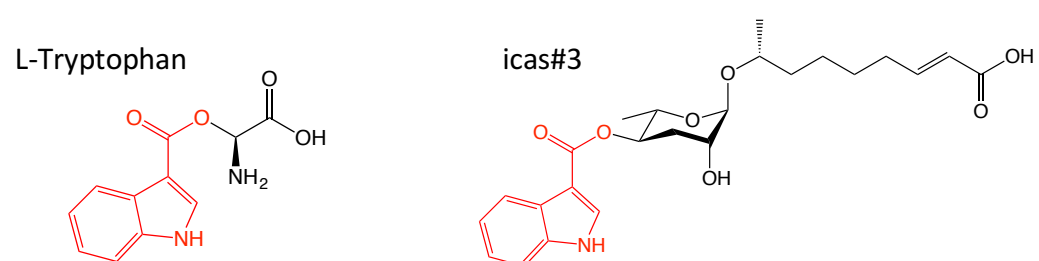
**B.2 Results and Discussion**

The indole-3-carbonyl group attached to the 4'-position of ascarylose in the icas ascarosides is known to be derived from tryptophan based on feeding assays (Figure B.1).<sup>5</sup> Indole-3-carboxylic acid is also a well-known auxin, a plant hormone that directs cell growth. In *Arabidopsis thaliana*, it was found that tryptophan is converted first into indole-3-pyruvate by a tryptophan aminotransferase and subsequently, a YUCCA monooxygenase converts the indole-3-pyruvate into indole-3-carboxylic acid (Figure B.2).<sup>6-7</sup> Although the indole-3-carboxylic acid auxin contains an extra carbon compared to the indole-3-carbonyl moiety on icas ascarosides, paralogous *C. elegans* genes may serve similar roles in the biosynthesis of

the icas head group. Cytochrome p450s are a family of enzymes that carry out monooxygenase functions, therefore we screened knockout mutants of five *cyp* genes: *cyp-13A7(gk31)*, *cyp-13B2(gk726)*, *cyp-14A2(gk289)*, *cyp-31A1(gk154)*, and *cyp-35A3(ok2709)*. HPLC-MS analysis of the mutant excretomes revealed no decrease in icas ascaroside biosynthesis (Figure B.3). In future, it might prove useful to examine the *fmo* gene family, which encodes flavin-containing monooxygenases with higher homology to the *A. thaliana* gene YUCCA1. Mutants are available from the CGC for *fmo-4(ok294)*, *fmo-3(ok354)*, and *fmo-2(ok2147)*.

The bacterium *Chromobacterium violaceum* and plants from the genus *Orobanche* are known to be able to synthesize indole-3-carboxylic acid, a process which involves the conversion of tryptophan into tryptamine, mediated by a decarboxylase enzyme.<sup>8</sup> We therefore screened three mutants that encode putative histidine decarboxylase enzymes based on homology: *hdl-1(ok956)*, *hdl-2(ok440)*, and *basl-1(ok703)*. HPLC-MS analysis of the liquid culture supernatant revealed that none of the three mutants screened resulted in a substantial reduction in icas production, suggesting that none of the enzymes tested are involved in the biosynthesis of the indole-3-carboxylic acid precursor (Figure B.4).

Another subset of genes screened came from the *elo* gene family. The *elo* genes encode elongase proteins that catalyzes the lengthening of a fatty acid carbon chain. We screened three *elo* mutants: *elo-1(gk48)*, *elo-5(gk182)*, and *elo-6(gk233)*. We found that *elo-1(gk48)* and *elo-5(gk183)* mutants produced higher amounts of the longer chain ascaroside ascr#18 and oscr#18, but did not significantly diminish the production of any particular ascaroside (Figure B.5).

**B.3 Figures**

**Figure B.1: The icas Ascarosides.** The indole-3-carbonyl group attached to icas ascarosides is derived from tryptophan.

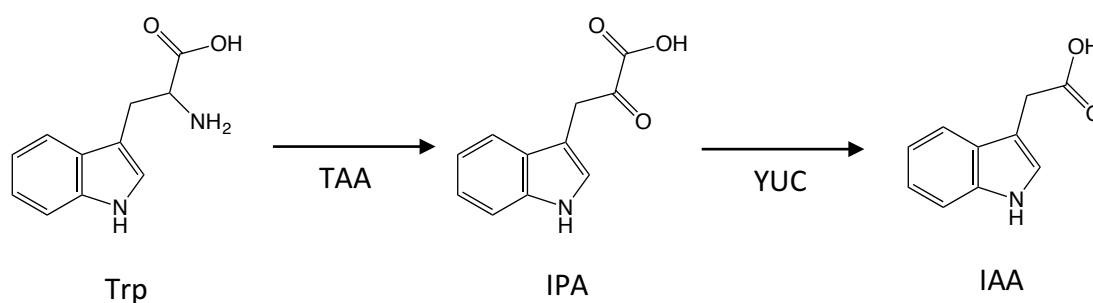


**Figure B.2: Indole-3-carboxylic Acid Biosynthesis in *A. thaliana*.** Tryptophan aminotransferase (TAA) converts tryptophan (Trp) into indole-3-pyruvate (IPA), which is then converted into indole-3-carboxylic (IAA) acid by YUCCA (YUC). (Modified figure from Won *et al.*<sup>6</sup>)

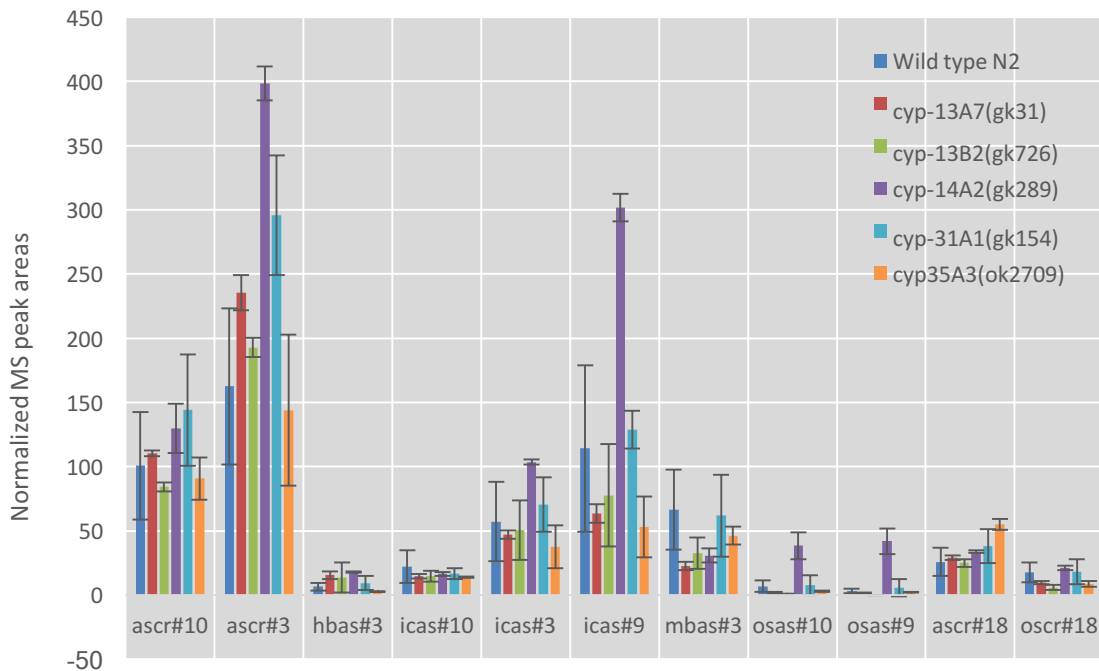


**Figure B.3: The *cyp* Gene Family.** The *cyp* family encodes for cytochrome P450 enzymes that can act as monooxygenases. Peaks are normalized to worm pellet mass. Averages and standard deviations are based on two biological replicates.

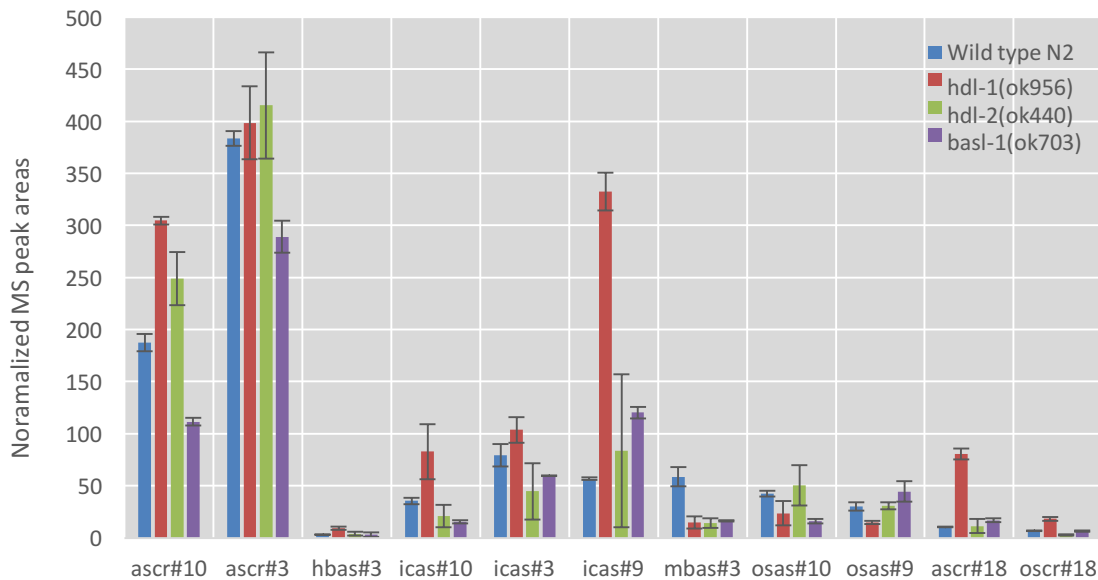


**Figure B.4: Decarboxylases.** In some bacteria and plants, decarboxylases have been shown to play a role in the biosynthesis of indole-3-carboxylic acid. Peaks are normalized to worm pellet mass. Averages and standard deviations are based on two biological replicates.

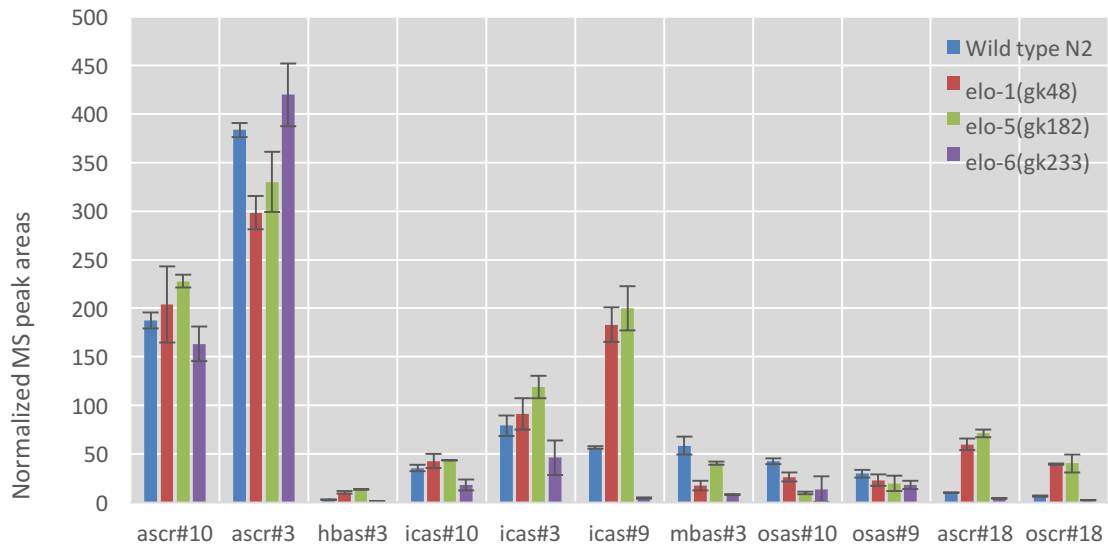


**Figure B.5: The *elo* Gene Family.** The *elo* genes encode fatty acid elongases. Peaks are normalized to worm pellet mass. Averages and standard deviations are based on two biological replicates.

## B.4 References

1. von Reuss, S. H.; Bose, N.; Srinivasan, J.; Yim, J. J.; Judkins, J. C.; Sternberg, P. W.; Schroeder, F. C., Comparative metabolomics reveals biogenesis of ascarosides, a modular library of small-molecule signals in *C. elegans*. *J Am Chem Soc* **2012**, *134* (3), 1817-24.
2. Butcher, R. A.; Ragains, J. R.; Li, W.; Ruvkun, G.; Clardy, J.; Mak, H. Y., Biosynthesis of the *Caenorhabditis elegans* dauer pheromone. *Proc Natl Acad Sci U S A* **2009**, *106* (6), 1875-9.
3. Joo, H. J.; Kim, K. Y.; Yim, Y. H.; Jin, Y. X.; Kim, H.; Kim, M. Y.; Paik, Y. K., Contribution of the peroxisomal *acox* gene to the dynamic balance of daumone production in *Caenorhabditis elegans*. *J Biol Chem* **2010**, *285* (38), 29319-25.
4. Joo, H. J.; Yim, Y. H.; Jeong, P. Y.; Jin, Y. X.; Lee, J. E.; Kim, H.; Jeong, S. K.; Chitwood, D. J.; Paik, Y. K., *Caenorhabditis elegans* utilizes dauer pheromone biosynthesis to dispose of toxic peroxisomal fatty acids for cellular homeostasis. *Biochem J* **2009**, *422* (1), 61-71.
5. Srinivasan, J.; von Reuss, S. H.; Bose, N.; Zaslaver, A.; Mahanti, P.; Ho, M. C.; O'Doherty, O. G.; Edison, A. S.; Sternberg, P. W.; Schroeder, F. C., A modular library of small molecule signals regulates social behaviors in *Caenorhabditis elegans*. *PLoS Biol* **2012**, *10* (1), e1001237.
6. Won, C.; Shen, X.; Mashiguchi, K.; Zheng, Z.; Dai, X.; Cheng, Y.; Kasahara, H.; Kamiya, Y.; Chory, J.; Zhao, Y., Conversion of tryptophan to indole-3-acetic acid

by TRYPTOPHAN AMINOTRANSFERASES OF ARABIDOPSIS and YUCCAs in Arabidopsis. *Proc Natl Acad Sci U S A* **2011**, *108* (45), 18518-23.

7. Mashiguchi, K.; Tanaka, K.; Sakai, T.; Sugawara, S.; Kawaide, H.; Natsume, M.; Hanada, A.; Yaeno, T.; Shirasu, K.; Yao, H.; McSteen, P.; Zhao, Y.; Hayashi, K.; Kamiya, Y.; Kasahara, H., The main auxin biosynthesis pathway in Arabidopsis. *Proc Natl Acad Sci U S A* **2011**, *108* (45), 18512-7.
8. Tivendale, N. D.; Davies, N. W.; Molesworth, P. P.; Davidson, S. E.; Smith, J. A.; Lowe, E. K.; Reid, J. B.; Ross, J. J., Reassessing the role of N-hydroxytryptamine in auxin biosynthesis. *Plant Physiol* **2010**, *154* (4), 1957-65.

## Appendix C

## STRAINS, PLASMIDS, AND PRIMERS

Table C.1: Strains

Strain	Genotype	Source
N2	wild type, Bristol	CGC
RB859	<i>daf-22(ok693)</i>	CGC
PS7211	<i>daf-22(ok693); syIs456[Pvha-6::GFP::DAF-22]</i>	A. Akagi
PS7212	<i>daf-22(ok693); syIs457[Pmyo-3::GFP::DAF-22]</i>	A. Akagi
PS7213	<i>daf-22(ok693); syIs458[Pdpy-7::GFP::DAF-22]</i>	A. Akagi
FX06781	<i>acs-7(tm6781)</i>	O. Panda
PS7396	<i>acs-7(tm6781); syIs459[Pacs-7::ACS-7::GFP]</i>	A. Akagi
PS7447	<i>unc-119(ed3); syEx1592[Pacs-7::ACS-7::GFP; Pvha-6::mcherrySKL; unc-119(+)]</i>	A. Akagi
GH10	<i>glo-1(zu437)</i>	D. Gems
RB811	<i>glo-4(ok623)</i>	CGC
RB662	<i>apb-2(ok429)</i>	CGC
GH378	<i>pgp-2(kx48)</i>	CGC

**Sources:**

Caenorhabditis Genetics Center (CGC, Minnesota)

Allison Akagi (A. Akagi, California Institute of Technology, California)

Oishika Panda (O. Panda, Cornell University, New York)

**Table C.2: Plasmids**

Name	Contents	Source
pAEA1	<i>Pvha-6::GFP::daf-22::unc-54 3'UTR</i>	A. Akagi
pAEA3	<i>Pdpy-7::GFP::daf-22::unc-54 3'UTR</i>	A. Akagi
pAEA4	<i>Pmyo-3::GFP::daf-22::unc-54 3'UTR</i>	A. Akagi
pAEA10	<i>Pacs-7::acs-7::GFP::unc-54 3'UTR</i>	A. Akagi
pAEA15	<i>Pvha-6::mCherrySKL::unc-54 3'UTR</i>	A. Akagi
HYM433	<i>Pvha-6::GFP::daf-22::unc-54 3'UTR</i>	H.Y. Mak
pU57	ACS-7 coding sequence with C-terminal His-tag	H. Le
pPH92	PSM GFP	Bargmann Lab
pPH93	PSM mCherry	Bargmann Lab
unnamed	<i>Pmyo-3::dsRed</i>	Sternberg Lab
pDP#MM051	<i>unc-119</i> rescue construct	D. Pilgrim
pRB1017	gRNA expression cassette	Fire Lab
pJA58	<i>dpy-10</i> gRNA plasmid	J. Arribere
#46168	<i>Peft-3::cas9-SV40_NLS::tbb-2 3'UTR</i>	Addgene

**Sources:**

Allison Akagi (A. Akagi, California Institute of Technology, California)  
 Ho Yi Mak (H.Y. Mak, Hong Kong University of Science and Technology, Hong Kong)  
 Henry Le (H. Le, Cornell University, New York)  
 Cornelia Bargmann Lab (Bargmann Lab, The Rockefeller University, New York)  
 Paul Sternberg Lab (Sternberg Lab, California Institute of Technology, California)  
 David Pilgrim (D. Pilgrim, University of Alberta, Edmonton, Canada)  
 Andy Fire Lab (Fire Lab, Stanford University, California)  
 Joshua Arribere (J. Arribere, Stanford University, California)  
 Addgene (Massachusetts)

**Table C.3. Primers**

<b>Name</b>	<b>Purpose</b>	<b>Sequence</b>
oAA001	Construction of pAEA5 (gRNA sequence)	TCTTGGACGCAACCGGTGCACGAG
oAA 002	Construction of pAEA5 (gRNA sequence)	AAACCTCGTGCACCGGTTGCGTCC
oAA 003	Construction of pAEA6 (gRNA sequence)	TCTTGGGAGGATCTACGGAGAACT
oAA 004	Construction of pAEA6 (gRNA sequence)	AAACAGTTCTCCGTAGATCCTCCC
oAA 005	Construction of pAEA7 (gRNA sequence)	TCTTGCGATTCCGAAGCTTCCGTC
oAA 006	Construction of pAEA7 (gRNA sequence)	AAACCGATTCCGAAGCTTCCGTCC
oAA 007	Construction of pAEA8 (gRNA sequence)	TCTTGCGATTCCGAAGCTTCCGTCGGGG
oAA 008	Construction of pAEA8 (gRNA sequence)	AAACCCCGACGGAAGCTTCGGAATCGC
oAA 009	<i>acs-10</i> CRISPR knockout genotyping	GTTGCCAGTTCTACTAGTCAACGAAATG
oAA 010	<i>acs-10</i> CRISPR knockout genotyping	GAATGACATTGGATCGAGAAAGGGTGTC

Name	Purpose	Sequence
oAA 011	Construction of pAEA4 ( <i>myo-3</i> promoter)	CGACTCACTATAGGGCGAATTGGGTACCGG CTATAATAAGTTCTTGAATAAAAATAATTTTC CC
oAA 012	Construction of pAEA4 ( <i>myo-3</i> promoter)	GTTCTTCTCCTTTACTCATGGCGCGCCTCTA GATGGATCTAGTGGTCGTG
oAA 013	Construction of pAEA3 ( <i>dpy-7</i> promoter)	CTCACTATAGGGCGAATTGGGTACCTCATT CCACGATTTCTCGCAACACATC
oAA 014	Construction of pAEA3 ( <i>dpy-7</i> promoter)	CTCCTTTACTCATGGCGCGCCTTATCTGGA ACAAAATGTAAGAATATTCTTAAAAATTG
oAA 015	Construction of pAEA1 ( <i>unc-54</i> 3'UTR)	CTGCACAGTCCAAGATTTGAAGGCCTGGCC GCTGTCATCAGAGTAAG
oAA 016	Construction of pAEA1 ( <i>unc-54</i> 3'UTR)	CAGGAATTCGATATCAAGCTTATCGATGTA CGGCCGACTAGTAGGAAAC
oAA 017	Construction of pAEA1 ( <i>GFP::daf-22</i> )	CTACCAAACCCATAAAAAGGGCGCGCCA TGAGTAAAGGAG AAGAAC
oAA 018	Construction of pAEA1 ( <i>GFP::daf-22</i> )	CTTACTCTGATGACAGCGGCCAGGCCTTCA AATCTTGGACTGTGC
oAA 019	Construction of pAEA1 ( <i>vha-6</i> promoter)	GACTCACTATAGGGCGAATTGGGTACCCTC AACGTTGCCAGTGATGAATC
oAA 020	Construction of pAEA1 ( <i>vha-6</i> promoter)	GTTCTTCTCCTTTACTCATGGCGCGCCCTTT TTATGGGTTTTGGTAGGTTTTAG

Name	Purpose	Sequence
oAA 065	Construction of pAEA10 ( <i>acs-7</i> promoter)	GATTACGCCAAGCTTGCATGCGGCCGGCCT GCCACATCAAAAAGATTCGCTCAAC
oAA 066	Construction of pAEA10 ( <i>acs-7</i> promoter)	CTTTGGCCAATCCCGGGGATCCGGCGCGCC TTCTGAAAATGTTGTGATCGAAAGG
oAA 067	Construction of pAEA10 ( <i>acs-7</i> cDNA)	CATTTTCAGGAGGACCCTTGGATGATATTTT ACGGTGAACAACCTTGAG
oAA 068	Construction of pAEA10 ( <i>acs-7</i> cDNA)	CTCCTTTACTCATTTTTTTCTACCGGCAATTA GCCTTTTTTGCATCC
oAA 077	pAEA10 sequencing	CCAAGAGAAAGATCCTGATAATGTTG
oAA 078	pAEA10 sequencing	CGA TGA ATA GGG TAA GAA TAC AAT ATC
oAA 079	pAEA10 sequencing	GGAGAACTTTGGATTAAGGGTCCT
oAA 080	pAEA10 sequencing	GGT AAG TTT TCC GTA TGT TGC ATC
oAA 093	Construction of pAEA15 (mCherrySKL)	CAAAACCCATAAAAAGGATCCCCGGGATGG TGAGCAAGGGCGAGGAG
oAA 094	Construction of pAEA15 (mCherry SKL)	GCCGATGCGGCTAAGATCTGGTACCTTAGA GCTTAGACTTGTACAGCTCGTCCATGCCGC
oAA 095	pAEA15 sequencing	GTGTGGAATTGTGAGCGGATAAC
oAA 096	pAEA15 sequencing	CCTTGGTCACCTTCAGCTTGG
oAA 097	pAEA15 sequencing	GTCTTCGGTTTTTCAGTCTTTAGTTC
oAA 098	pAEA15 sequencing	GAG AAA GAG CAT GTA GGG ATG TTG

Name	Purpose	Sequence
oHW36f	<i>acs-10</i> CRISPR deletion repair	CACTTGAACTTCAATACGGCAAGATGAGAA TGACTGGAAACCGTACCGCATGCGGTGCCT ATGGTAGCGGAGCTTCACATGGCTTCAGAC CAACAGCCTAT